

## **Influence of basement heterogeneity on the architecture of low subsidence rate Paleozoic intracratonic basins (Ahnet and Mouydir basins, Central Sahara)**

Paul Perron, Michel Guiraud, Emmanuelle Vennin, Eric Portier, Isabelle Moretti, Moussa Konaté

Solid Earth

MS NO.: se-2018-50

We would like to thank all the referees: Dr Jobst Wendt, Dr Réda Samy Zazoun and Dr Fabio Lottaroli for their constructive and helpful reviews that we believe have undoubtedly improved our manuscript. We also thanks Dr Alex Peace for his “short comment”. We have incorporate our responses into the original reviews (highlighted in red), before appending a tracked changes document showing the changes made to the manuscript.

### Color legend in manuscript:

~~Green~~ + Green = moved sentences

~~Red~~ = deleted sentences

Red = added sentences

## **Reviewer 1: Réda, Samy Zazoun**

### **I-Text**

**1- Lines 100-101; 106 to 110; 113; 115 to 116; 118 to 120.....:** Put references from oldest to most recent.

-“We are using the publication style of Solid Earth where references are classified alphabetically.”

**2- Line 253:** is composed of fluvatile Cambrian. The whole sedimentary series described in the literature is composed of fluvatile to Braid-deltaic plain Cambrian, not only fluvatile (eg. Brahmaputra River analogue), with a transitional facies from continental to shallow marine (Sabaou et al., 2009, p160).

-“We have modified and added reference (line 308-311).”

**3- Line 254:**..... glacial Ordovician. Upper Ordovician glaciogenic deposits....

-“We have modified (line 311).”

**4- Line 255:**..... argillaceous deep marine Silurian...argillaceous deep marine Silurian deposits....

-“We have modified (line 313).”

**5- Line 255:** Missing the last reference for the Silurian (Djouder et al., 2018).

Djouder, H., Lüning, S., Da Siva, A-C., Abdellah, H., Boulvain, F. (2018), Silurian deltaic progradation, Tassili n’Ajjer plateau, south-eastern Algeria: Sedimentology, ichnology and

sequence stratigraphy. *Journal of African Earth Sciences*, Volume 142, June 2018, Pages 170-192

-“We have added reference (line 313-314).”

**6- Line 266:** the term Algerian platform don't exist, you speak probably about the Algerian part of Saharan platform

-“We have modified (line 324).”

**7- Line 300 and Figure 2:** In the Illizi basin, these facies are mainly recorded in the Cambrian Ajjers Formation

In the Illizi Basin, and Saharan platform, the Ajjers Formation and/or the equivalent formation are dated: Upper Cambrian? to Ordovician (Tremadoc to Caradoc)(Fabre, 2005 ; Vecoli, 2000 ; Vecoli & Playford, 1997; Vecoli et al., 1995 ;Vecoli et al.,1999).

-“We have modified and added references (line 358-360).”

### **References for the datation:**

Vecoli, M., 2000. Palaeoenvironmental interpretation of microphytoplankton diversity trends in the Cambrian–Ordovician of the northern Saharan Platform. *Palaeogeography, Palaeoclimatology, Palaeoecology* 160, 329–346.

Vecoli, M., Playford, G., 1997. Stratigraphically significant acritarchs in uppermost Cambrian to basal Ordovician strata of Northwest Algeria. *Grana* 36, 17–28.

Vecoli, M., Albani, R., Ghomari, A., Massa, D., Tongiorgi, M., 1995. Précisions sur la limite Cambrien–Ordovicien au Sahara Algérien (secteur de Hassi-R'mel). *Comptes Rendus de l'Académie des Sciences, Paris* 320 (IIa), 515–522.

Vecoli, M., Tongiorgi, M., Abdesselam-Rouighi, F.F., Benzarti, R., Massa, D., 1999. Palynostratigraphy of Upper Cambrian–Upper Ordovician intracratonic clastic sequences, North Africa. *Bollettino della Società Paleontologica Italiana* 38 (2–3), 331–341.

Vecoli, M., Videt, B., Paris, F., 2008. First biostratigraphic (palynological) dating of Middle and Late Cambrian strata in the subsurface of northwestern Algeria, North Africa: implications for regional stratigraphy. *Review of Palaeobotany and Palynology* 149 (1–2), 57–62.

**8-** There was confusion about the subdivision used. Often, it is extracted from English papers. It is best to keep the original nomenclature in French, as it was established by geologists (BRPA, 1964; in Beuf et al., 1971), in fact: (Beuf et al., 1971, Tab-1, p.158; Bennacef et al., 1971; Fabre, 2005).

-“We have modified in the text and in Fig. 2 keeping the original French nomenclature (see Fig. Fig. 3 and line 360-361, 395-396, 409, 433-434, 442, 470-473, 493, 518).”

From de base to the top, we observe:

A- The Ajjers Formation

It's divided from the bottom to the top:

In the Tassilis-N-Ajjers (Outcrops)

- Les Grès/Conglomérats d' El Moungar (Unit I)
- Les Grès de Tin Taradjelli (Unit II)
- La Vire du Mouflon (Unit III-1)
- La Banquette (Unit III-2)

In the Illizi basin (Subsurface equivalents)

- (Unit II) : R3+R2+Ra +Ri
- (Unit III-1) : La Zone des Alternances + Les Argiles d'El Gassi + les Grès d'El Atchane
- (Unit III-2) : Les Quartzites de Hamra

B- The In Tahouite Formation (Unité III-3) (outcrops)

(Unit III-3) : Les Grès de Ouargla + Argiles d'Azzel + Grès de Oued Saret (subsurface)

C- The Tamadjert Formation (Unit IV) (outcrops)

Ajjers Formation + In Tahouite Formation represent the Sequence 1 (Preglacial-deposits)

Tamadjert Formation (Outcrops) and the equivalent in the subsurface (Unit-IV) is the sequence 2 (syn-glacial deposits)

Also for The Siluro-Devonian, keep the original nomenclature in French (Text and Fig.2):

Tigillites Talus: Talus à Tigillites (Lines 348 ; 371)

-“We have modified in the text and in Fig. 2 (see above).”

Passage Zone: Zone de passage (Lines 379, 427)

-“We have modified in the text and in Fig. 2 (see above).”

Middle Bar: Barre Moyenne (Lines 301, 335)

-“We have modified in the text and in Fig. 2 (see above).”

Sidewalks: Trottoirs

-“We have modified in the text and in Fig. 2 (see above).”

Upper Bar: Barre Supérieure (Lines 301, 335).....etc.

-“We have modified in the text and in Fig. 2 (see above).”

### **References for The Ajjers Formation:**

Bennacef, A., Beuf, S., Biju-Duval, B., De Charpal, O., Gariel, O., Rognon, P., 1971. Example of cratonic sedimentation: Lower Palaeozoic of Algerian Sahara. The American Association of Petroleum Geologists Bulletin 55 (12), 2225–2245.

Beuf, S., Biju-Duval, B., de Charpal, D., Rognon, R., Bennacef, A., 1971. Les grès du Paléozoïque inférieur au Sahara. Sedimentation et discontinuité: évolution structurale d'un craton. Institut Français Pétrole, Collection Sciences Techniques P&role 18, 464~.

Sabaou, N., Aït Salem, H., Zazoun, R.S., 2009. Chemostratigraphy, tectonic setting and provenance of the Cambro-Ordovician clastic deposits of the subsurface Algerian Sahara. Journal of African Earth Sciences 55 (3–4), 158–174.

Zazoun, R.S., Mahdjoub, Y., 2011. Strain analysis of Late Ordovician tectonic events in the In-Tahouite and Tamadjert Formations (Tassili-n-Ajjers area, Algeria). *J. Afr. Earth Sci.* 60, 63–78.

**9- Line 489:** as Hirnantian glacial valleys ....as Hirnantian glacial-Palæovalleys

-“We have modified (line 562-563).”

**10- Line 534:** Hoggar shield ? sometimes, you speak about Tuareg shield (TS)...Hoggar is the massif and the Tuareg is the shield.

-“We have modified (line 200).”

**11- Line 526 :** Missing reference: Hercynian Tectonic Event

According to Zazoun (2001).....The basement fabric features exerted a very strong control on the structural evolution during the Hercynian deformation (See also Haddoum et al., 2001).

-“We have modified and added references (line 613-615).”

### **References for The Hercynian Tectonic Event**

Haddoum, H., Guiraud, R., Moussine-Pouchkine, A., 2001. Hercynian compressional deformations of the Ahnet-Mouydir Basin, Algerian Saharan platform: far-field stress effects of the Late Paleozoic orogeny. *Terra Nova* 13, 220–226.

Zazoun, R, S. 2001. La tectogenèse hercynienne dans la partie occidentale du bassin de l’Ahnet et la région de Bled El-Mass, Sahara Algérien: un continuum de déformation *Journal of African Earth Sciences* Vo.32, N°4, 869-887.

**12- Lines 671:** Abdesselam-Roughi, F ; Abdesselam-Rouighi, F.F

-“We have modified.”

**13- Line 902:** Fabre, J. 2005. Géologie du sahara occidental et central. Musée Royal de l’Afrique Centrale-Belgique.Tervuren African Geoscience Collection Vol.108. ISBN 90-75894-66-x ; ISSN : 1780-8551, 610 p.

-“We have modified.”

**14- Line 980:** Hassan Kemandji, A.M or Kemandji, A.M.H., ?

-“We have modified.”

**15- For the terranes notion please see the last publication about this topic :**

Sonia Brahimi, Jean-Paul Liégeois, Jean-François Ghienne, Marc Munsch, Amar Bourmatte. 2018. The Tuareg shield terranes revisited and extended towards the northern Gondwana margin: Magnetic and gravimetric constraints. *Earth-Science Reviews*, doi:10.1016/j.earscirev.2018.07.002 (Accepted manuscript)

-“It is a very interesting publication sent at the same time, globally coherent with our observations. We have added to our citations (line 649-650).”

### 16- Lines 64 and 1313

Missing : Intra-Arenig unconformity cited by (Fabre 2005, pp 169) in the North Africa, Eschard et al., (2010) and Kracha thesis, (2011) in the Ahnet Basin and Beuf et al., (1968-1971) in the Tassilli-N-Ajers and Eschard et al. (2006) in the Berkine Basin.

*“Erosion occurred in many places during an intra-Arenig unconformity” (Eschard et al., 2010)  
“ Une discordance de faible amplitude, mais dont l’extension intéressera tout le Maghreb depuis l’Anti-Atlas occidental jusqu’à la Libye marque la fin...de ce premier cycle Ordovicien » c’est-à-dire Tremadoc et Arenig inférieur....(Fabre, 2005)*

*« De même, les « Argiles de Tiferouine » transgressent progressivement sur la série de Bled El Mass, et sont limitées à la base par une discordance angulaire conglomératique, qui pourrait bien correspondre à la discordance Intra-Arenig, mise en évidence dans de nombreuses régions sahariennes (Beuf et al., 1968; 1971; Eschard et al., 2006)..... » in Kracha., 2011, pages 73-86-100*

*« Le passage des « Quartzites de Hamra » vers les « Grès de Ouargla » se fait de manière progressive, et l’on assiste par la suite à la troncature des termes sommitaux de cette formation sous la discordance Intra-Arenig qui annonce l’arrivée brutale des « Argiles d’Azzel-Tiferouine ». Les « Grès d’Oued Saret » sont peu préservés sous les ravinements glaciaires de l’Unité IV (et/ou la discordance Taconique) (Kracha, 2011)..... Pages 113 et 121.*

*-“We have added these references and modified Fig. 2 integrating this unconformity (see Fig. 3 and line 76)”*

### **References for the Intra-Arenig unconformity**

Beuf. S., Biju-Duval. B., Mauvier, A., Legrand Ph. (1968). Nouvelles observations sur le “Cambro-Ordovicien” du Bled El Mass (Sahara central), Publ. Serv. Géol. Algérie, Bulletin n° 38, p.39-51.

Beuf. S., Biju-Duval. B., De Charpal. O., Rognon. P., Gariel. O., et Bennacef, A. (1971). Les grès du Palaeozoïque inférieur du Sahara. Publication Institute Français du Pétrole, Collection Science et Technologie du Pétrole, Paris, No. 18. 484 p.

Eschard.R, Hellat.C, Malla.M, Bénamane.K, Betioui.H, Callot.J.P, Carpentier.B, Chelcheb.S, Couprie.E, Dahi.M, Delmarre.S, Desaubliaux.G, Deschamps.G, Euzen.T, Hachemi.L, Hannoun.R, Jacolin.J.E, Lassal.A, Leblond.C, Levêque.I, Lorant.F, Mokhtari.N, Lorin.T, Rabary.G, Rudkiewicz.J.L, Wattine.A. (2006). Berkine Gas project. Evaluation of the Gas potential in the Berkine basin (Algeria). Rap. Conf. Ifp.

Eschard. R, Braik.F, Bekkouche.D, Ben Rahuma.M, Desaubliaux.G Deschamps.R et Proust. J. N. (2010). Paleohighs: their influence on the North African Paleozoic petroleum systems. Geological Magazine, 147 (1), 28-41.

Kracha, N. 2011. Relations entre sédimentologie, fracturation naturelle et diagenèse d’un réservoir à faible perméabilité : application aux réservoirs de l’Ordovicien, Bassin de l’Ahnet, Sahara Central, Algérie. Thèse de Doctorat, Université des sciences et Technologies de Lille. 458p, Thèse non publiée.

**17-** It would be desirable to speak also about the work of Boote et al (1998). These authors define the notion of “The Gondwana Super-cycle” between the infra-Cambrian (Panafrican) Unconformity and the Hercynian Unconformity. This Super-cycle has been divided in 02 Super-cycles: a Lower Gondwana Super-cycle and an Upper Gondwana Super-cycle. This nomenclature which is defined at the scale of north Africa also applies in South America (Souza Cruz et al., 2000) and Saudi Arabia (Sharland et al., 2000, Davidson et al. 2001), even if a slight diachrony may exist between these areas.

1- Lower Gondwana Super-cycle (Infra-Cambrian Unconformity to Caledonian Unconformity): is a major second order transgressive-regressive megacycle, in the sens of Vail et al. (1977)

2- Upper Gondwana Super-cycle (from the Caledonian Unconformity to the Hercynian Unconformity)

(in: The Lower Paleozoic sedimentation of the Algerian Saharan craton, Tassili N’Ajjer outcrops. Field Guide Book, February 20-25, 2003. AAPG symposium, Algiers 18-20 February 2003, 103p).

-“We have chosen to present in Fig. 2 column (7) the 2<sup>nd</sup> order transgressive-regressive cycle highlighted by Carr, (2002), and Eschard et al., (2005) (see Fig. 3).”

### **References for “The Gondwana Super-cycle”**

Davidson, L., Bestwetherick, S., Craig, J., Eales, M., Fisher, A., Himmali, A., Jho, J., Mejrab, B. and Smart, J. 2000. The structure, stratigraphy and petroleum geology of the Murzuk basin, southwest Libya. In Geological exploration in Murzuq basin, (in: Eds M.A. Sola and D.Worsley), Elsevier, 295-320.

Sharland, P.R., Archer, R., Casey, D.M., Davies, R.B., Hall, S.H., Heward, A.P., Horbury, A.D. and Simmons, M.D., 2001. Arabian Plate Sequence Stratigraphy. Georabia, Special Publications, 2, 371p, 2 plates.

Souza Cruz, C.E., Miranda, A. P., and Oller, J. 2000. Facies analysis and depositional systems of Late Silurian-Devonian subandean basin, southern Bolivia and Northern Argentina. In: Memorias del Congreso Geologico Boliviano, La Paz, 14-18 Noviembre 2000, 85-90.

### **18- Thermal History of Ahnet and Sbaa Basins (Histoire Thermique)**

**(See Akkouche Thesis) : you will find below the conclusions of Mr. Akkouche about the Fission track study of Ahnet and Sbaâ**

Akkouche, M. 2007, Application de la datation par traces de fission à l’analyse de la thermicité de bassins à potentialités pétrolières. Exemple de la cuvette de Sbaâ et du bassin de l’Ahnet-Nord (plate-forme saharienne occidentale, Algérie). Thèse de Doctorat, Université de Bordeaux 1, 297p.

You can download the thesis at the link below : [www.iaea.org/inis/collection/NCLCollectionStore/\\_Public/41/021/41021844.pdf](http://www.iaea.org/inis/collection/NCLCollectionStore/_Public/41/021/41021844.pdf)

### **Histoire Thermique du bassin de l’Ahnet**

Les traces de fission témoignent d’épisodes thermiques et d’érosion différents suivant les domaines du bassin avec une tendance générale à l’effacement des traces du Nord vers le Sud. Au Nord du bassin de l’Ahnet (MRS-1 et MSL-1), les âges obtenus dans les formations de

l'Ordovicien et de la base du Silurien sont de 50 Ma environ. Ils témoignent d'une phase thermique post-varisque qui a affecté la colonne paléozoïque. On peut estimer que les températures atteintes au cours de cet épisode thermique, probablement >100°C, sont également à mettre en relation avec l'épisode thermique d'extension régionale d'âge triasico-jurassique. Cet événement thermique pourrait également être à l'origine de l'effacement total des traces pré-existantes du niveau dévonien du forage MSR-1 qui présente, à 505 m sous la discordance varisque, un âge TF de 100 Ma. Plus au Sud, les âges respectifs de 37 Ma et 26 Ma obtenus à des profondeurs de 1030 m (forage MKRN-1) et 1532 m (forage BH-5), suggèrent une altération thermique cénozoïque des traces de fission plus intense que celle mise en évidence dans le Nord du bassin. Cette caractéristique pourrait refléter une érosion récente plus importante, mais également l'action éventuelle de gradients géothermiques plus élevés

### **Histoire Thermique de la cuvette de Sbaâ basin (See Akkouche Thesis)**

La plupart des résultats obtenus sur les échantillons prélevés dans les forages de la cuvette de Sbaâ est compatible avec ceux obtenus par les chercheurs de la Société GEOTRACK sur le forage OTRA-1, situé à 50 kilomètres du forage ODZ 1-bis. Dans le forage ODZ-1bis, les résultats suggèrent une histoire thermique marquée par trois événements de refroidissement. Le plus ancien se situe entre 200 et 300 Ma. Le second aurait un âge proche de 170-210 Ma et le plus récent entre 30 et 50 Ma. Ces âges témoigneraient successivement des événements de refroidissement carbonifère (fin de l'orogénèse varisque), jurassique (détumescence thermique post-rifting atlantique) et éocène (bombement du Hoggar). Un seul échantillon présente un résultat surprenant. Il s'agit de l'échantillon n°644 (forage ODZ-1bis) qui donne un âge de 472±11 Ma, prélevé dans un horizon détritique du Tournaisien. Onze des 12 apatites de cet échantillon présentent des traces de fission fossiles pré-datant nettement le Carbonifère. En d'autres termes, l'épisode varisque n'a jamais atteint un seuil thermique suffisant pour effacer ces traces au niveau de la bordure septentrionale de la cuvette de Sbaâ. Ce constat suggère que la cuvette de Sbaâ est un des domaines de la plate forme saharienne occidentale les moins affectées par les événements thermiques post-varisques. De toute évidence, à partir de la fin du Carbonifère, voire du Permien, la cuvette de Sbaâ est structurée et demeurera dans un climat structural relativement superficiel.

-“We are aware of post-Hercynian tectono-thermal events, however it wasn't the object of our study. We have focused the paper on the Palaeozoic.”

### **II-Figures**

#### **1- Figure 2 :**

- Column 4 : Mouydir not Mouyrdir -“corrected”
- Column 6 (Tassili) : In Tahouite Formation is the Unit III-3, not The Unit III-2 -“corrected”
- Tin Taradjelli Sandstones is the Unit II -“added”
- Column 6: Orsine Formation not Orsine -“corrected”
- Tin Meras Formation not Tin Meras -“corrected”
- Illrene Formation not Illrene -“corrected”
- El Moungar Conglomerat is the Unit I -“added”
- The intra-Arenig unconformity is missing
- “see Fig. 3.”

### **III- Conclusions : (See Referee comments above)**

- Several references have been omitted (Ajers Formation, Silurian, Hercynian tectonic Event, Terranes...): see bibliography attached for each remark.
- Very minor corrections are required.
- The intra-Arenig unconformity was not mentioned.

- Figure 2 is to be corrected.
- Put references from oldest to most recent.
- Some typographic mistakes about the names of the authors.
- Ovoid the translation of the nomenclature in English language.

## **Reviewer 2: Jobst Wendt**

### **Preliminary remarks:**

Though I have been working on the Paleozoic of the Algerian Sahara for many years (1987-2006) I am only familiar with the Devonian and Carboniferous, but not with the older formations and the crystalline basement. Therefore, I can only judge these aspects of the above manuscript. Likewise, I feel not competent enough to consider some tectonic reconstructions. I hope that the other reviewer(s) are able to review these aspects of the manuscript with a better competence.

The manuscript is an overview of the bio- and lithostratigraphic, sedimentologic, paleogeographic and paleotectonic evolution of the Ahnet-Mouydir area in southern Algeria based on field data from previous authors, well log analysis, satellite images and geophysical data. As such it is a good summary of the evolution of a marginal basin-and ridge system which farther north in central Algeria has yielded enormous oil and gas reservoirs.

### **Detailed critical remarks:**

Title: The research areas covers a much larger area (including also the Reggane, Basin, Illizi Basin, Hoggar Shield) than expressed in the title. This should be made clear in the title.

-“We have added this remarks to the title even if the study is essentially focusing the Ahnet-Mouydir basins (line 2).”

Line 20: Pan-African orogeny. Strictly spoken this was around 600 MA, but including earlier phases it was 900-520 MA. What do you mean exactly?

- “We have corrected (line 46). Indeed, the Pan-African orogeny result from the accretion, then collision of different terranes during different phases. This polyphased event has constrained the structural framework of the Saharan Platform.”

Line 35: “Devonian compression”. I consider this as a mere speculation. According to all previously gathered data the Devonian was a period of tectonic quiescence accompanied by slight extension.

-“We refer to the (a) Siluro-Devonian (also called Caledonian) and the (b) Mid to Late Devonian events. We bring in our paper new evidences in favour of these tectonic events through seismic lines (Fig. 7) and satellite images (Fig. 6C, D, E, F). Besides, they are already mentioned in the literature:

(a) In the Saharan platform, the Caledonian tectonic event, is mainly mentioned as uplifting of some trends, large-scale folding or blocktilting (e.g. Gargaff arch, Tihemboka arch, Ahara high, Amguid El Biod), associated with breaks in the series and frequent angular unconformities below Early Devonian formations (Beuf et al., 1971; Boote et al., 1998; Boudjema, 1987; Carruba et al., 2014; Coward and Ries, 2003; Echikh, 1998; Eschard et al., 2010; Frizon de Lamotte et al., 2013; Ghienne et al., 2013; Gindre et al., 2012; Legrand, 1967b, 1967a). During this compressive event, large wavelength folds and paleohighs were accentuated, affecting sedimentation and facies distribution in the sedimentary basins (Eschard et al., 2010; Galeazzi

et al., 2010). Locally, paleohighs may have provided detrital material (Eschard et al., 2010; Galeazzi et al., 2010). Evidence of the Caledonian event is documented, in the southwestern and southern flank of the Ghadames Basin, the Lower Devonian Tadrart formation is seen to directly overlie the Upper Silurian basal Acacus series with a progressive truncation of the Acacus (Upper Silurian) units from NE to SW on this unconformity (Echikh, 1998). In the Illizi basin, only the lowermost part of Acacus Formation is preserved (Echikh, 1998). Besides, seismic data may show folding of the Silurian section below flat-lying Devonian deposits (Echikh, 1998). Well described indications of Caledonian unconformity are also highlighted in the Murzuq basin (Ghienne et al., 2013) and Al Kufrah basin (Gindre et al., 2012). Massive sand injection associated with igneous intrusion triggered by basin-scale uplift are also described in the Murzuq basin (Moreau et al., 2012). These structural features imply NW-SE shortening, probably of moderate intensity, though much weaker than the Hercynian one (Guiraud et al., 2005). Elsewhere, in the Drâa basin, in the NW Libya and over the Al Kabir trend, there is also no sign of this event in Lower Devonian series (Echikh, 1998; Ouanaimi and Lazreq, 2008).

Moreover, a widespread near top Emsian unconformity probably triggered by regional tectonic activity has been identified in the Illizi basin (Abdessalam-Rouighi, 2003; Boudjema, 1987; Boumendjel et al., 1988; Brice and Latrèche, 1998; Moreau-Benoit et al., 1993), in the Ahnet-Mouydir basin (Wendt et al., 2006), in the Libyan Ghadames and Al Kufra basins (Bellini and Massa, 1980). It is associated to basaltic volcanism and intrusive activity in the Ahnet basin (?) and Anti-Atlas (Belka, 1998; Wendt et al., 1997)

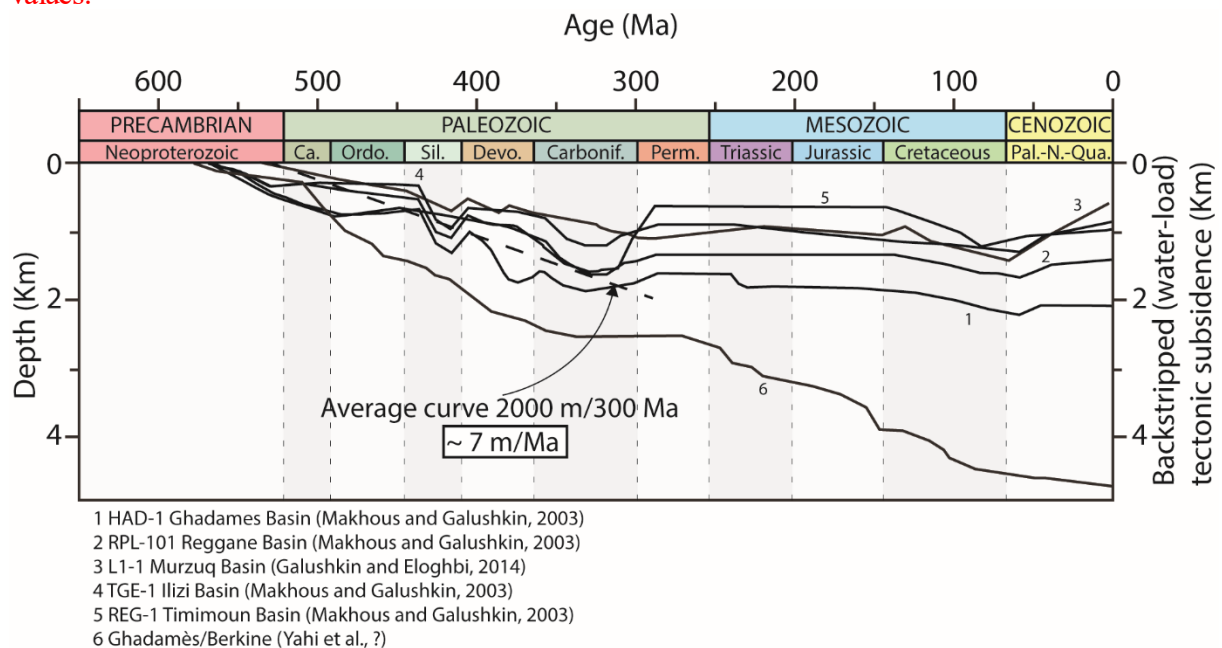
Many authors have correlated the Late Silurian to Early Devonian tectonism as the maximum collisional deformation of the Caledonian Orogeny (see references below). However, this event clearly relates to collisions involving far away continents and terranes where Gondwana was located thousands of kilometres to the south and separated from the collisional zone by a major ocean during this time (Craig et al., 2006; Mckerrow et al., 2000; Stampfli and Borel, 2002). Tectonic events in North Africa during post-Infracambrian-pre-Hercynian times were therefore independent of the Caledonian Orogeny. Time-descriptive terms may be preferred instead (Craig et al., 2006). This denomination is thus controversial. The origin of this intra-plate stress could be linked to far field stresses, knowing that, in continental craton compression stresses can be transmitted through distances of up to 1600 km from a collision front (Ziegler et al., 1995). The origin of Late Silurian to Early Devonian intra-plate stress in North Africa is currently unclear but is possibly associated either with a phase of rifting along the Gondwana margin (Boote et al., 1998) or with initial closure of the Iapetus Ocean (Fekirine and Abdallah, 1998). Frizon de Lamotte et al., 2013 didn't interpret it as a far effect of the Variscan orogeny, contrary to Fabre, 2005 who associated to the beginning of it.

(b) The Middle to Late Devonian is the time for two contrasting large-scale tectonic processes: the onset of the Variscan Orogeny along the Gondwana-Laurussia margin on the one hand and the development of magmatism, rifting and domal basement uplift within these continents on the other hand (Frizon de Lamotte et al., 2013). The collision between Gondwana and Laurasia that ultimately produced the Hercynian Orogeny possibly first affected North Africa during the mid-Devonian, creating extension/transension pull-apart basins (Craig et al., 2006). This Devonian deformation has reactivated megashear zone systems coeval with semi-regional uplift of the Ghadames and Illizi basins and of the adjacent Tihemboka, Ahara, Gargaf and Brak-Bin Ghanimah arches in the mid-Eifelian and at the end of the mid-Devonian (Late Givetian) and with the related development of the Frasnian Unconformity (Craig et al., 2006). Evidence of extensional structures and/or tectonic activity during the Late Devonian, as proved by the major thickness variations of these series are documented in the Anti-Atlas (Baïdier et al., 2008; Michard et al., 2008; Wendt, 1985), in the northern Africa and Arabia platform (Frizon de

Lamotte et al., 2013) and in the Ahnet basin (Wendt et al., 2006). This event corresponds to a major collapse and even “disintegration” of the north-western Gondwana margin prior to the Variscan Orogeny (Wendt, 1985). While, the activity of the palaeohighs (e.g. Ahara, Gargaff and Tihemboka High) almost ceased during the Frasnian times, with marine shales onlapping different elements of the Palaeozoic succession below and sealing most of the palaeohighs (Eschard et al., 2010).”

Line 52: 7 m/MA. Give reference.

-“We have calculated it:  $200\text{m}/300\text{Ma} \approx 7\text{m}/\text{Ma}$  (cf. figure below). It is not very precise but it is in the order of magnitude. Holt et al., (2010) indicate 22.2m/Myr (Ghadames) and 10.1 m/Myr (Al Kufrah) for the highest rates. Sloss, (1988) show 20-30 m/Myr to 3-4 m/Myr values.”



Line 61: 16 million km<sup>2</sup>. Impossible! The entire Sahara occupies about 9 million km<sup>2</sup>.

-“We have modified this value (line 73).”

Line 121 ff. and 133: It is not clear if the authors have ever been in the field; equivalent data seem to be based on previous published sources only. This should be made clear unequivocally.

-“This study is written in the frame of a PhD and there wasn’t fieldtrip during this time. However, some of the authors have been on the field and have many years of experience of the area throughout the oil industry (NEPTUNE former ENGIE/GDFsuez) or throughout academic. We have better specified the new data (especially satellite images, seismic lines and well-logs) which have been used in this study. We have integrated a figure presenting the method and original work (cf. fig. 4 in manuscript in supply).”

Line 141: Please separate both calibration of well-logs by palynomorphs (which are poorly reliable biostratigraphic markers) and field sections by conodonts (which give by far the best time resolution), goniatites and brachiopods. Both biostratigraphic subdivisions can be only roughly be correlated.

-“We have modified and we are more careful with the data set (line 168-174). Indeed, we aware about the poor resolution of palynomorphs calibration. Unfortunately, it is the only data available in wells.”

Line 144 (and later): “Synsedimentary extensional and compressional markers”: This means during the Devonian and Carboniferous. On which evidence these important tectonic events are based? Apparently not on field data. During about 9 months of personal field work I followed typical marker levels (e.g. the upper Eifelian/Givetian limestone ridge) for tens of kilometers (walking from ridge into basin deposits), but I have never seen something like that. The observation of doubtless Hercynian faults does not automatically allow the conclusion that they are rejuvenated earlier structures.

-“In our area, evidences of tectono-sedimentary structures (i.e. thickness variations, lateral facies variations, current directions variations) showing activation and reactivations of arches were already highlighted in the literature by field studies:

-In the Arak-Foum Belrem arch see (a), (b) and (c) below from (Beuf et al., 1971, 1968b) during the Ajjers deposition (i.e. Upper Cambrian Lower Ordovician).

-In the Bled El mass area of the Azzel Matti arch see e below from (Beuf et al., 1968a; Eschard et al., 2010) during the Ajjers deposition (i.e. Upper Cambrian Lower Ordovician).

-In the Tanezrouft area of the Azzel Matti arch see d below from (Beuf et al., 1971) during the Ajjers deposition (i.e. Upper Cambrian Lower Ordovician).

Then, during the Caledonian (i.e. Siluro Devonian), these structures are also known in the field:

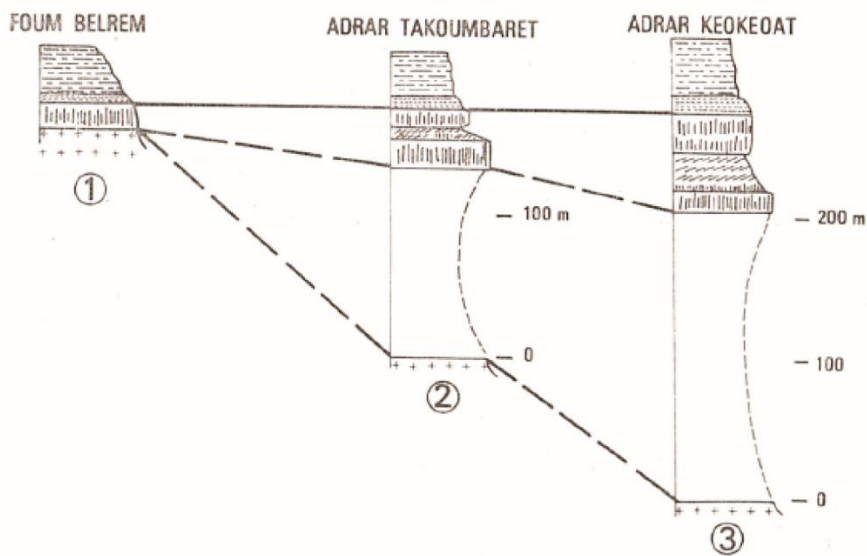
-In the Assedjrad area on the Azzel Matti arch see (h) below from (Beuf et al., 1971).

-In the Arak-Foum Belrem arch see (g) below from (Legrand, 1967a), see (h) below from (Beuf et al., 1971) and see also in (Biju-Duval et al., 1968).

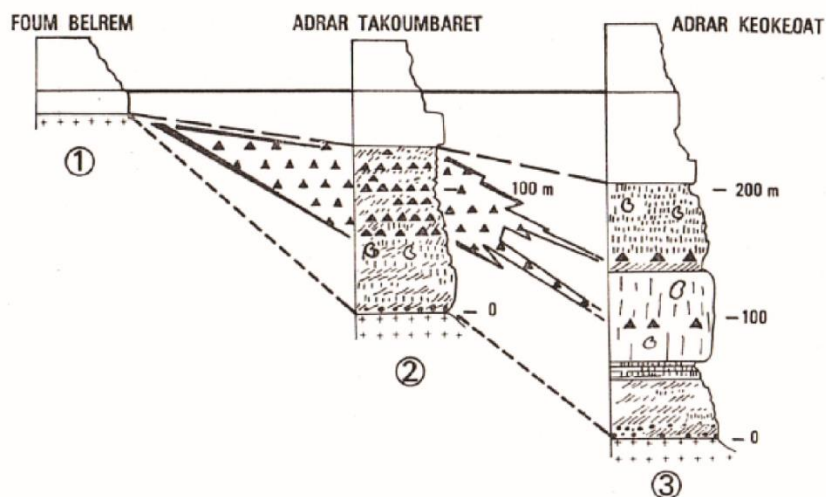
-In the Idjerane axis see (f) below from (Legrand, 1967a).

These latter are evidences of the early activity of the arches leading to the individualization of the different basins since the Cambro-Ordovician time. Then, the arches were reactivated during the Caledonian (i.e. Siluro-Devonian). Here, we don't cite other arches (i.e. Tihemboka, Ahara, Amguid El Biod, Gargaf, Dor El Gussa-Murizidié...) of the Saharan Platform where these syn-sedimentary structures are also described (Borocco and Nyssen, 1959; Carruba et al., 2014; Chaumeau et al., 1961; Chavand and Claracq, 1960; Collomb, 1962; Dubois and Mazelet, 1964; Eschard et al., 2010; Fabre, 2005; Frizon de Lamotte et al., 2013; Ghienne et al., 2013; Massa, 1988)”.

From this literature, we bring new evidences of syn-sedimentary tectonic reactivating successively arches structures during Paleozoic by using new unpublished data (from 3D Google Earth satellite images and seismic lines).



(a) Variation of Ajjers series on the Arak-Foum Belrem Arch (Beuf et al., 1968b).



(b) Syn-tectonic conglomerates in Ajjers series (i.e. Cambro-Ordovician) on the Arak-Foum Belrem Arch (Beuf et al., 1968b).

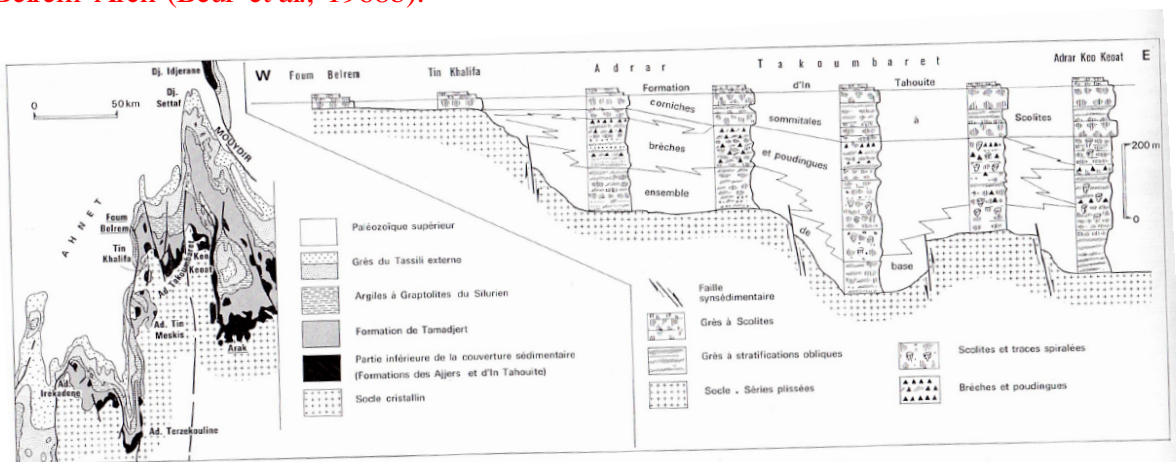


FIG. 301. — Réductions de série et variations sédimentaires dans la formation des Ajjers (partie nord-orientale du môle de Foum Belrem).

(c) Syn-tectonic conglomerates in Ajjers series (i.e. Cambro-Ordovician) on the Arak-Foum Belrem Arch (see fig. 301, p. 366) (Beuf et al., 1971).

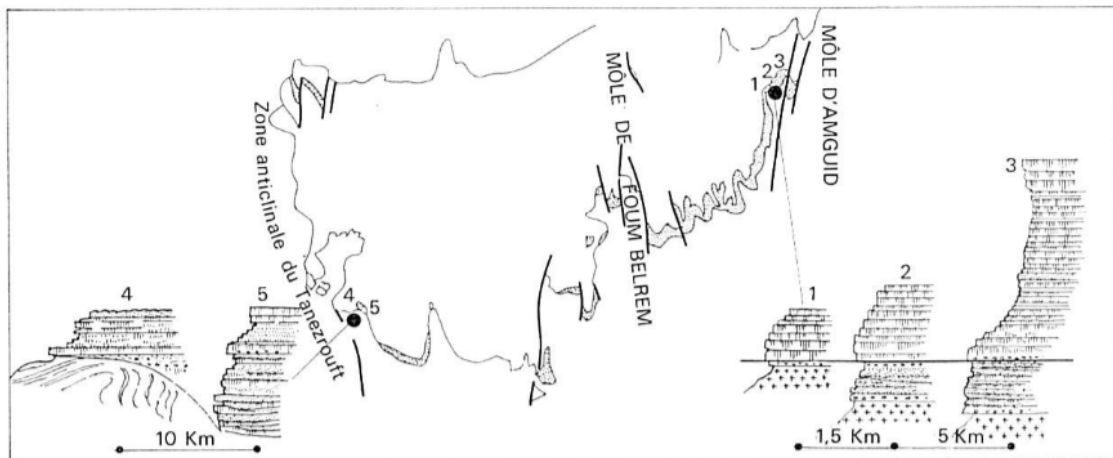
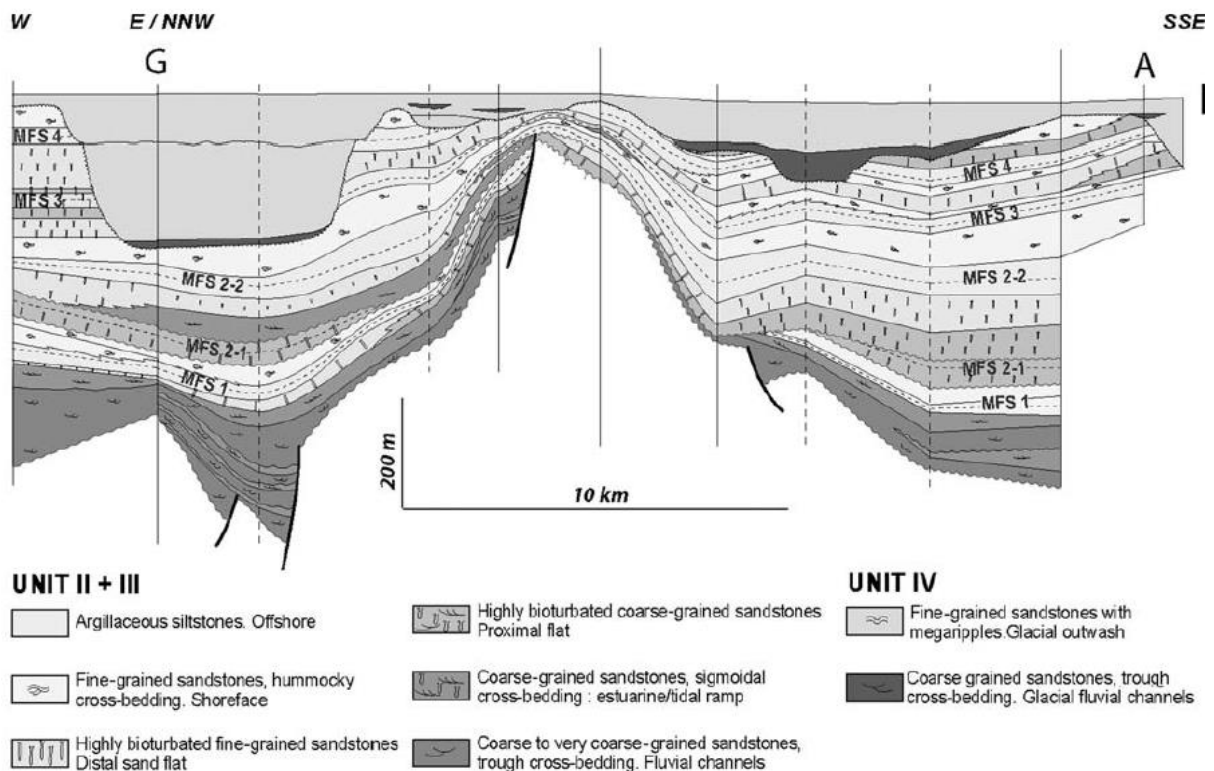
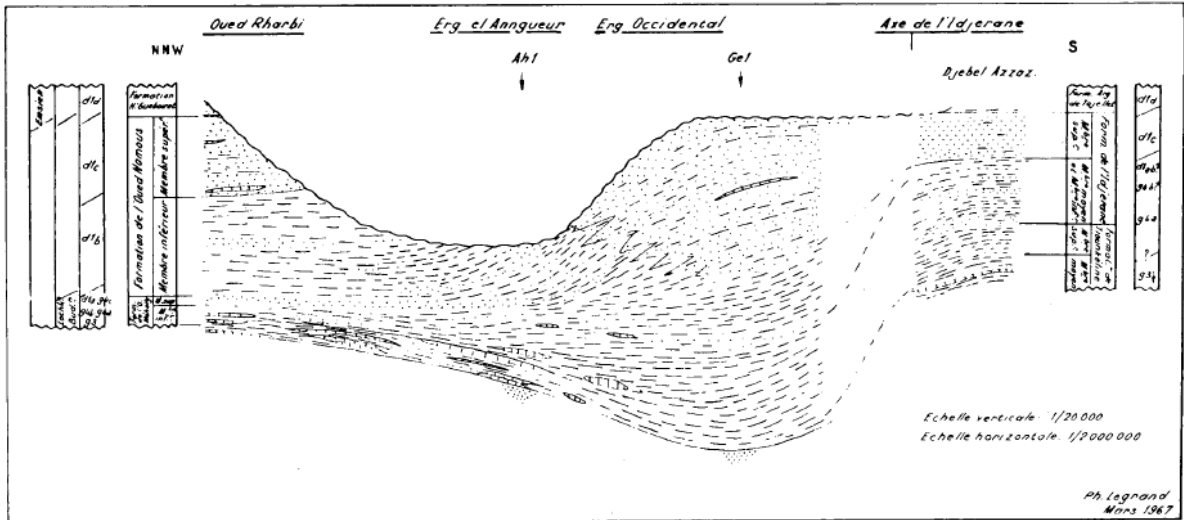


FIG. 331. — Influences de la tectonique synsédimentaire sur le dépôt de la formation des Ajjers (môle d'Amguid et bordure du Tanezrouft).

(d) Influence of syn-sedimentary tectonic in Ajjers series on the Azzel Matti Arch and Amguid El Biod Arch (Beuf et al., 1971).

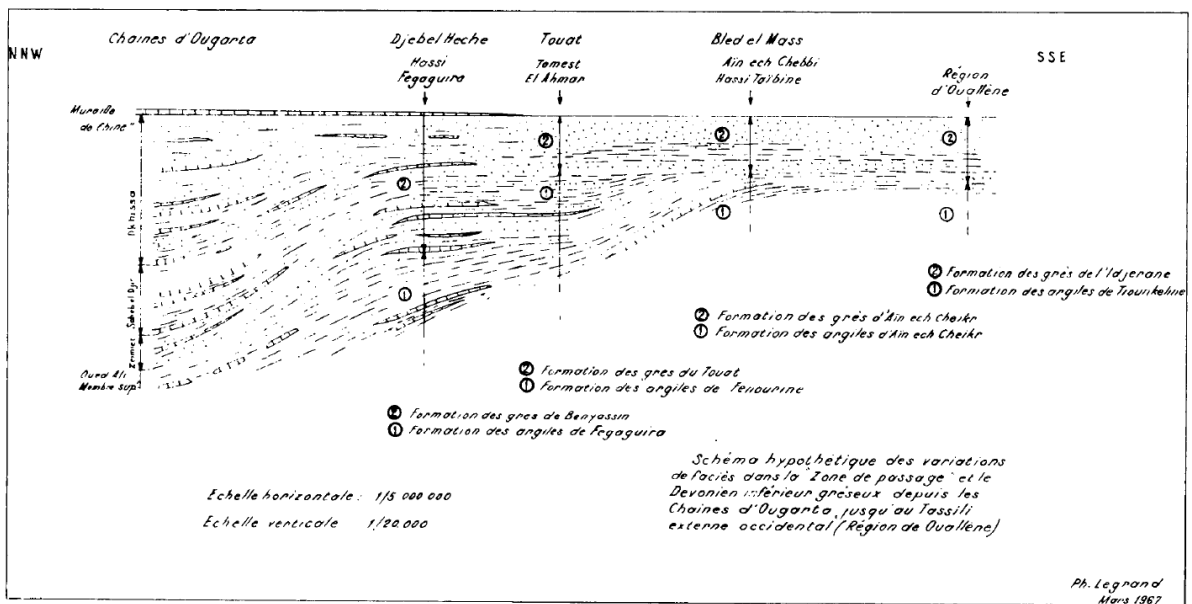


(e) NNW-SSE cross section on the Azzel Matti Arch (Ahnet Basin) showing variation of thickness, wedges strata in the Cambro-Ordovician series (Fig. 15) (Eschard et al., 2010).



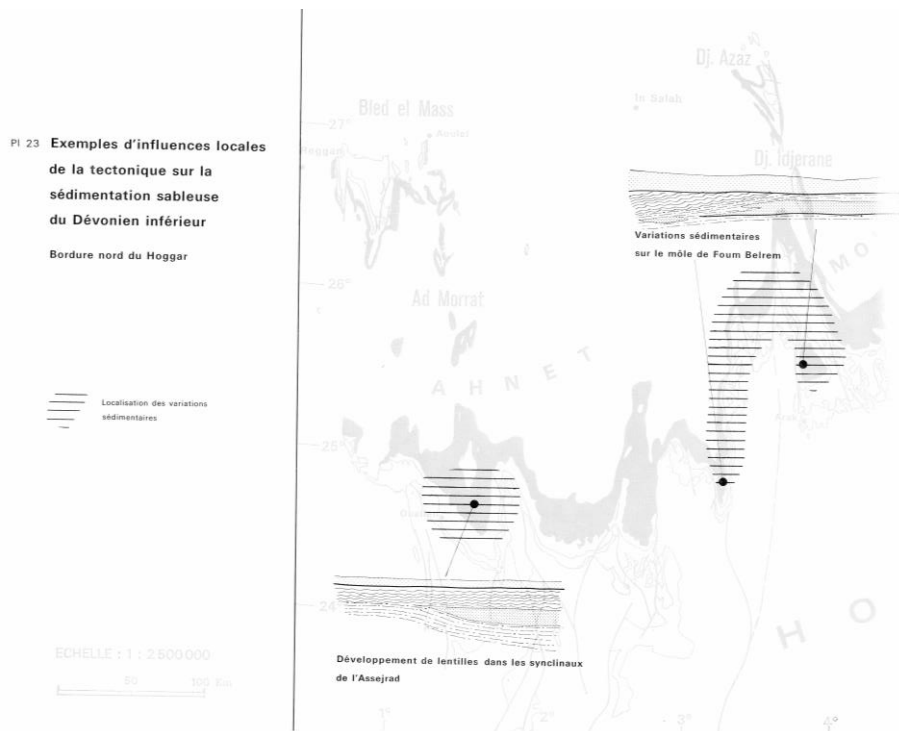
Pl. 3a. "ZONE DE PASSAGE" ET DEVONIAN INFÉRIEUR GRESEUX. A travers la région de l'Erg occidental, la région de l'Oued et de l'Erg el Anqueur jusqu'aux affleurements du Djebel Azzaz.

(f) Thickness and facies variations of Siluro-Devonian formations on the Idjerane axis (i.e. Arak-Foum belrem arch) (Legrand, 1967a).



Pl. 4. Schéma hypothétique des variations de faciès dans la "Zone de Passage" et le Dévonien inférieur gréseux depuis les Chânes d'Ougarta jusqu'au Tassili externe occidental (Région de Ouallène).

(g) Thickness and facies variations of Siluro-Devonian formations in the Bled El Mass area (i.e. Azzel Matti arch) (Legrand, 1967a).



(h) Example of local influence of tectonic in Lower Devonian series (Beuf et al., 1971).

Line 146: Outcrop sections O1- O12 cannot be detected in Figs 9 and 10. Are they personal field data? Position of well logs W1-W21 can only very roughly be located from Fig. 3A. Given the importance of these data (which apparently have never been published previously) it is absolutely necessary to indicate individual coordinates (best as an appendix) for both.

-“We have integrated supplementary data to the paper (cf. fig. 4, 11 and 13), even if there weren’t indispensable for the comprehension of the paper (showing some redundancy). They allow a better understanding. This has changed the order of the figures. O1-O12 are presented in fig. 11, they are based and modified from Wendt et al., (2006), (2009).”

Line 152: add: major “depositional” unconformities, in order to avoid confusion with angular unconformities.

-“We have modified (line 184).”

Lines 153-154: The top Pragian unconformity is diachronous (comprises also the lowermost Emsian in the Reggane Basin and on the Azel Matti ridge). Top Givetian and top mid-Frasnian are no unconformities over the entire study area. Top Quaternary is an unconformity worldwide, therefore omit. Or do you mean base Quaternary? But this would be trivial. In this list you have omitted the most important depositional unconformity, the transgression of the lower Eifelian (costatus-Zone).

-“The calibration of the seismic lines to wells is not really precise (due to differential resolution between the two) that’s why we added “Near top” for each horizons. Due to faulting or calibration issues, choose seismic horizons that are extendable is often not easy. Some of the horizon are not unconformities sensu stricto but just well-identifiable and extendable.

-The horizon named near top Pragian doesn’t represent the top Pragian but a mid lower Devonian reflector horizon that is easily extendable (i.e. near top Pragian horizon).

-Top Quaternary was corrected to near base Quaternary.

-The transgression of the Lower Eifelian was difficultly extendable to the entire area due to lack of well-calibration and faulting between hanging-wall/footwall (furthermore, the seismic reflectors aren't "bright"), so was dismissed."

Line 156: geological map is 1: 200.000, not 1:20.000.

-“We have modified (line 189).”

Line 171: circular or oval shape of basins. This is pure imagination. Basins and ridges are capped by erosion in the south and by overlying Jurassic or Cretaceous in the north. Thus the second dimension of the paleogeographic units is unknown.

-“The observations of Fig. 1 resulting from Pre-Mesozoic subcrop geological maps of the Saharan Platform (Boote et al., 1998; Galeazzi et al., 2010) show this circular and oval shaped feature. They are bordered by the different arches (cf. Fig. 1 from Eschard et al., 2010 below). For example, it is well-represented by the Reggane or the Mouydir basins (cf. below Plate 1 from Galeazzi et al., 2010).”

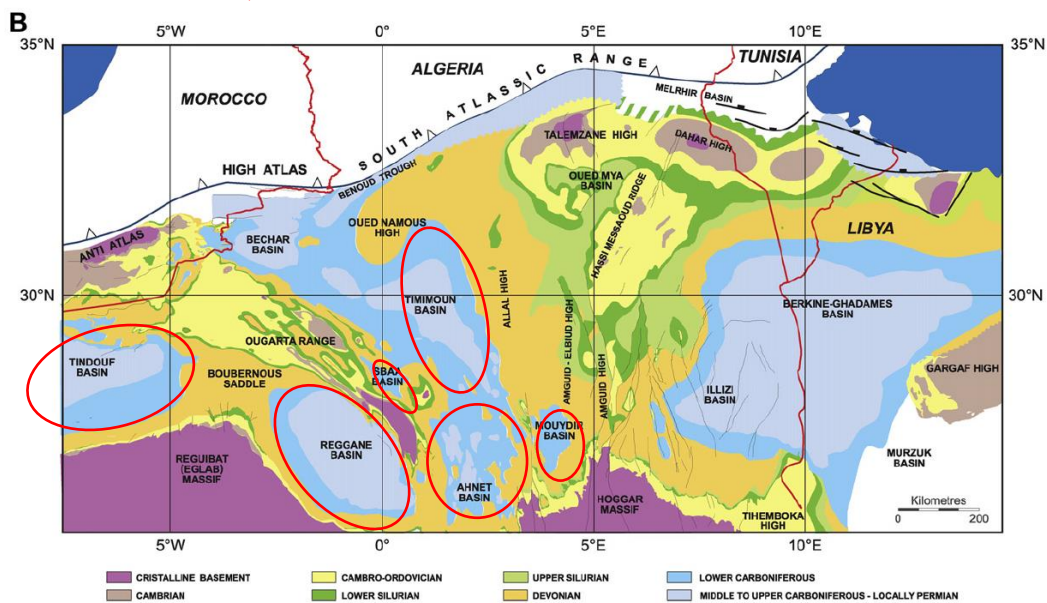


**Plate 1.** (A) Enhanced satellite image of the Maghreb region (NW Africa), showing the main tectonic domains of the area and the location of the study area (NW Africa). The Berkine–Ghadames and Illizi basins are Palaeozoic intracratonic depressions developed within the Saharan Platform. The Pan-African Tilemsi Suture separates the Eglab and Hoggar massifs. N-S oriented basement faults formed during the Pan-African Orogeny and strongly influenced the structural grain of the Berkine–Ghadames and Illizi basins. The Amguid fault and its continuation into the Amguid–El Biod fault trend bounds both basins to the west. (B) Pre-Mesozoic subcrop map of the Saharan Platform, showing the main Late Palaeozoic (mostly ‘Hercynian’)–Early Mesozoic tectonic elements.

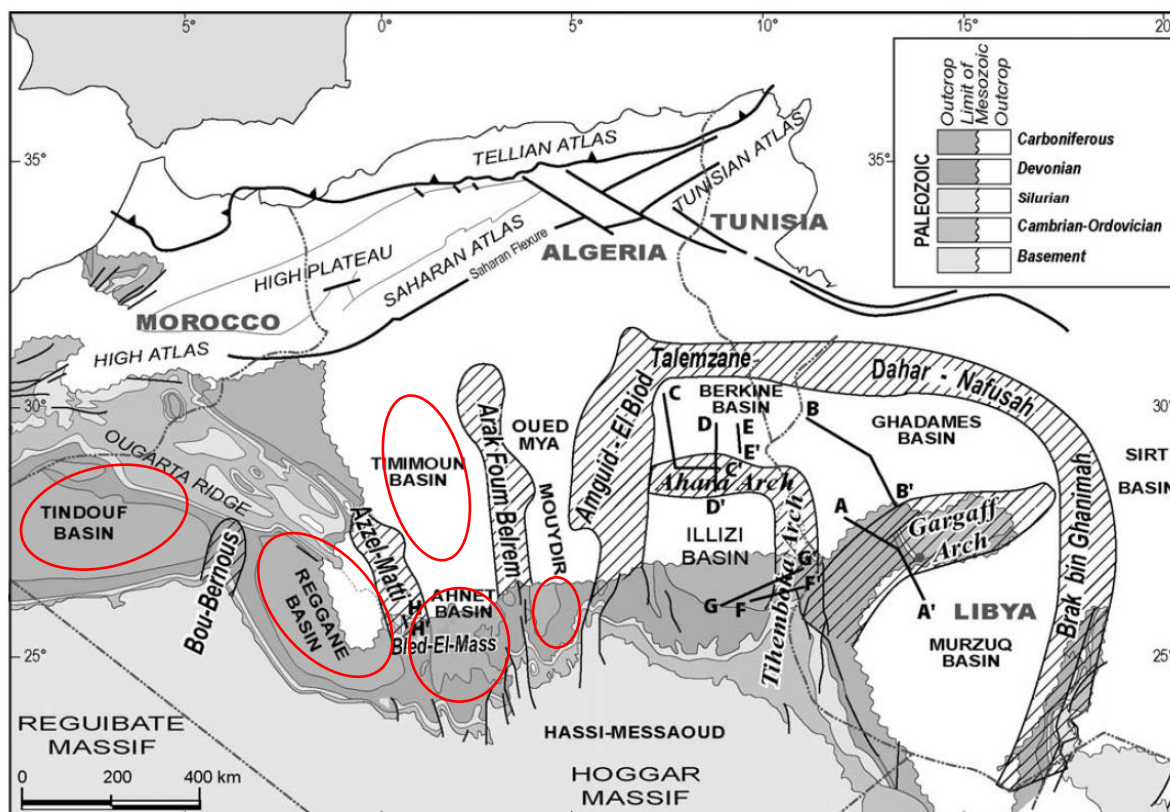


Fig. 1. Structural map showing the distribution of the main highs and basins across the Saharan Platform (partially redrawn from Boote *et al.* 1998). The hatched areas correspond to the main highs described in the text.

Line 174: major faults are all Hercynian. Eventual pre-Hercynian faults are inferred, but have never been documented in the field, thus are mere speculation.

-“Previous work from Beuf *et al.* monograph essentially based on field studies has documented the formation and maintain of arches-basins shape through the Paleozoic (see previously). It is documented elsewhere on the Saharan Platform.”

Line 178: “long” instead of “length”.

-“We have modified (line 226).”

After line 178: Generally, at this point there is a paragraph entitled “Previous work”, but this is missing here.

-“Previous works are already well summarized in Wendt *et al.*, (2006) and since there weren’t major studies on the area. However, we can add a little summary if it is needed.”

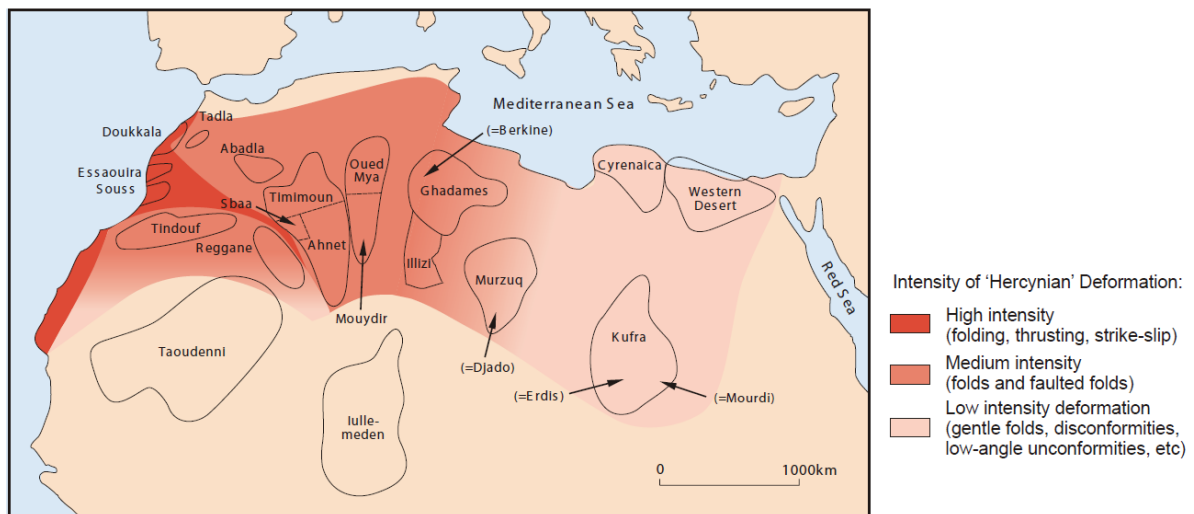
Line 179: this chapter should be re-written avoiding speculations, even if they would fit well into a hypothetical and inferred depositional image. Regarding eventual “synsedimentary extensional markers” see above.

-“see explanation Line 174 above.”

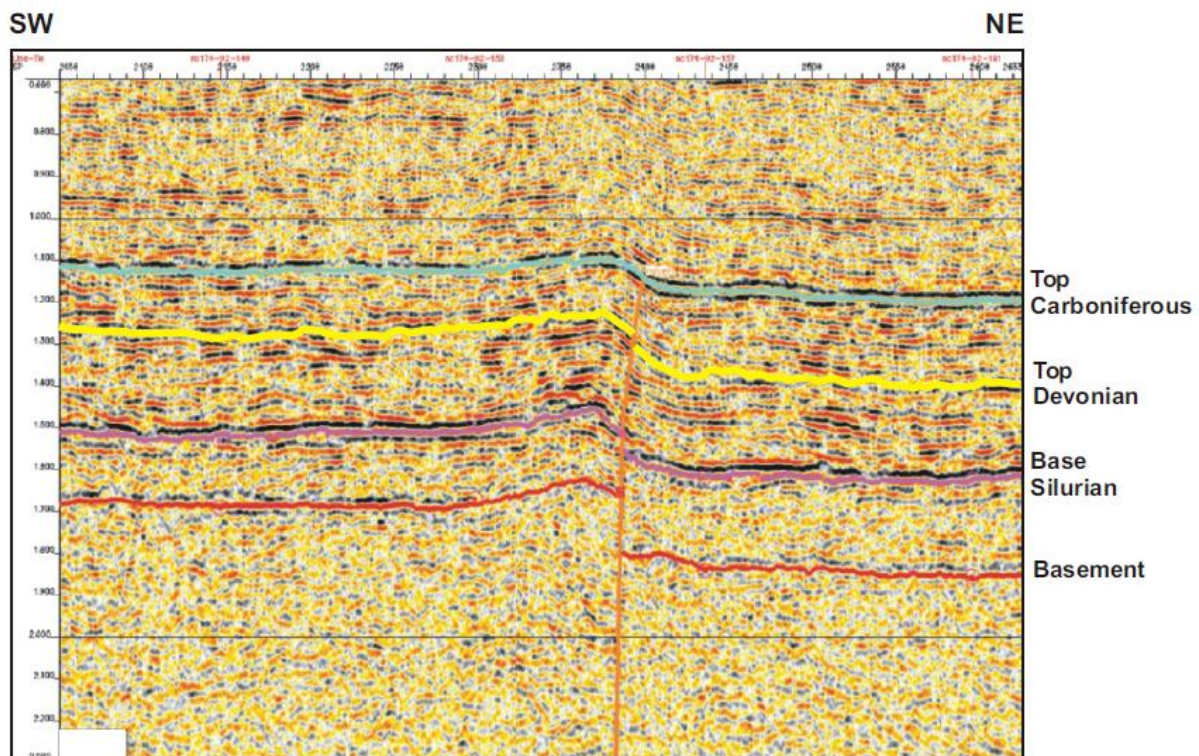
Line 191: Hercynian folding is restricted to the Reggane, Ahnet and western Mouydir Basins, but decreases markedly towards the east (eastern Mouydir and Illizi Basins) where Paleozoic strata are completely flat-lying.

-“Indeed, the strain deformation of the Hercynian is decreasing eastwards (see fig. a below). Nevertheless, there still exist folding as far as Murzuq basin (even farther) visible in seismic

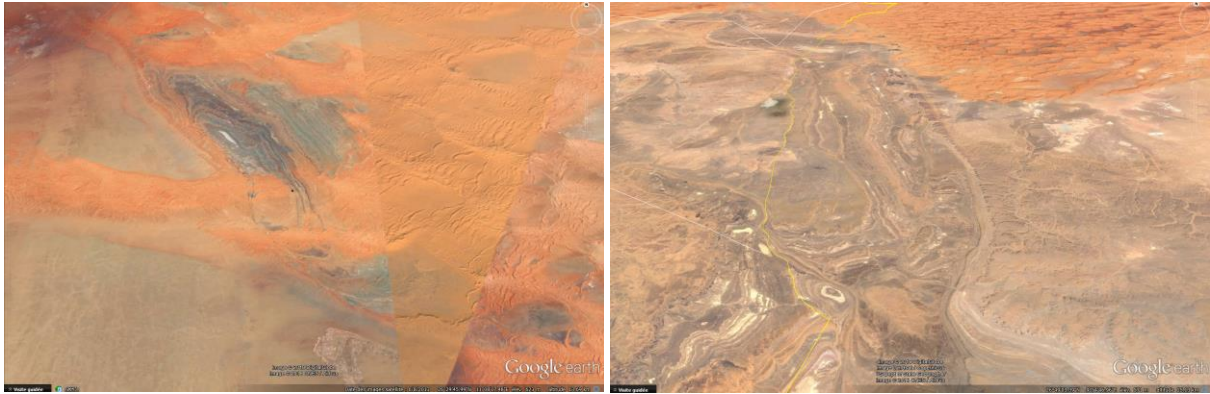
(see b below) or satellite images (see c below). These structures are often difficult to observe eastwards because of sand dunes or Mesozoic series.”



(a) Intensity of Hercynian deformation on the Saharan Platform modified from (Craig et al., 2006)



(b) Seismic sections through selected structures in the Murzuq Basin, southwest Libya showing evidence of abrupt thickening of Cambro-Ordovician and Late Devonian to Carboniferous sequences across steeply-dipping faults (Craig et al., 2006).



(c) Fold on the Tihemboka arch (right), Atchan arch (left) visible on Google Earth images (Murzuq basin).

Lines 205-207: synsedimentary horst and graben structures – see above (lines 174 and below).  
 What is a “synsedimentary forced fold”? A slump?

-“Forced folds were defined by Stearns, (1978) as ‘folds in which the final overall shape and trend are dominated by the shape of some forcing member below’. There are also referred to as extensional fault-propagation folds, form in response to the upward propagation of normal faults (i.e. developed above tips of propagating faults) (e.g. Withjack et al., 1990). Growth strata, onlaps and thickness variation upon have permitted to date the deformation (see a below). See also abundant literature on the subject (e.g. Gawthorpe and Hardy, 2002; Hardy and McClay, 1999; Kane et al., 2010; Lewis et al., 2015). The kinematic is extensional in these cases. In our study, this structural style is coherent with the accommodation of deformation by basement block movement. The Silurian shales have the role of decoupling between Cambro-Ordovician sandstones and Devonian series.”

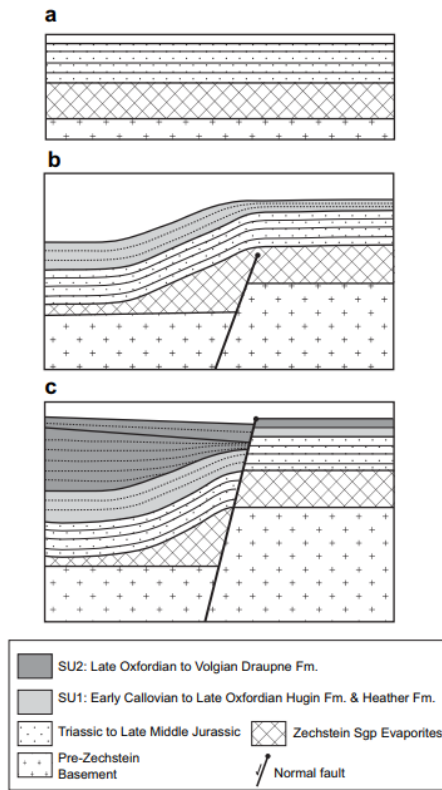


**Fig. 13.** Synoptic model illustrating the influence of extensional forced-fold development on syn-rift stratigraphic architecture (a) Geometry of basement, Zechstein Supergroup and pre-rift strata prior to fault propagation – units are assumed to be isochronous. (b) Early Callovian to Late Oxfordian (SU1). Upward fault propagation is inhibited by the presence of the salt, resulting in forced folding (*sensu* Withjack et al., 2002) of pre-rift cover strata and thinning of SU1 sediments towards the developing fold. (c) Late Oxfordian to Volgian (SU2). Early SU2 sediments onlap the upper surface of SU1 and continue to thin towards the fault until after the fault has breached the salt layer and overlying cover strata. This results in displacement at-surface and the migration of the depocentre towards the fault. Note that stage (c) is only applicable to the central and southern parts of the Sleipner Basin.

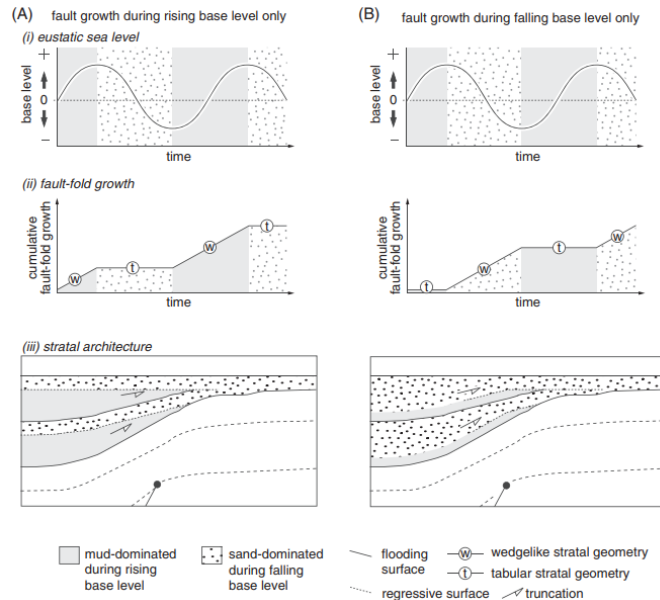


**Figure 17.** A schematic model illustrating how forced folding and eustasy combine to control the stratal architecture of early synrift deposits on the flanks of extensional forced folds. Two end-member scenarios, which both depict shallow marine shoreface sandstone deposition during falling base level (forced regression) only, are illustrated: (1) fault propagation and forced fold amplification during rising base level only, fold amplification and hanging-wall deepening during rising base level results in basinward thickening of mudstone-dominated bodies. Shoreface sand bodies are deposited during times of tectonic quiescence thus are uniform in thickness, and truncate underlying mudstones and amalgamate toward the fold crest, and (2) fault growth during falling base level only, fold amplification and hanging-wall subsidence during falling base level results in basinward thickening of sandstone-dominated bodies. Mudstone-dominated units are deposited during times of tectonic quiescence thus are uniform in thickness, being truncated toward and thinning onto the fold crest. The regressive surfaces of marine erosion that bound the bases of individual sand bodies may be sharp near the fold crest and pass basinward into a correlative conformity.

(a) Left from (Kane et al., 2010), and right from (Lewis et al., 2015).

Line 247: From Google Earth images it is possible to recognize faults, but it is impossible to determine their age. Please explain why the faults figures in Figs 4 and 6 are Silurian-Devonian and Middle to Late Devonian age.

-“The age is based on stratigraphic markers identified from georeferenced geological maps (Bennacef et al., 1974; Bensalah et al., 1971) which were veneering on 3D Google Earth images (i.e. associated with a digital elevation model DEM) (see Figs. below).

The high quality of the new satellite images permits also the differentiation between shale and sandstones levels (when knowing the stratigraphic succession of the area it is a help too).

It is sure that it does not replace a field mission but it allows to have an overview on very large objects. Kmz format (i.e. Google Earth format) of geological maps can be added to supplementary data. Or these figures can be added to the paper?!

The timing of faults activity (in seismic or in satellite images) is done by identifying sedimentary structures such as divergent onlaps (growth strata), thickness variation and truncatures in the hanging wall synclines of forced folds (cf. above).

For example:

-In figure 5A, the sinuous morphologies of the faults indicate syndepositional fault propagation. So, the age of faults is given by stratigraphic layer impacted (i.e. *oTj* here Tamadjert fm. i.e. Unit IV).

-In figure 5B, age of faults are given by their control on channelized sandstone body systems which are dated late Hirnantian (Girard et al., 2012). Besides, in figure 6A, divergent onlaps (DO1) in In Tahouite series (*oTh* i.e. Unit III) located in the hanging-wall syncline of fault F2 permit to date the (re)activation of fault during the Ordovician. Then, F2 is reactivated during the Silurian (fig. 6B i.e. DO2 in *sIm* series).

-In figure 6C, divergent onlaps (DO2) in Asedjrad series (*sdAs1, dAs2*) located in the hanging-wall syncline of fault F5 permit to date the (re)activation of fault during the Siluro-Devonian.

-In figure 6E, divergent onlaps (DO3) in Givetian to Mehden Yahia series (*d2b, d3a, d3b*) located in the hanging-wall syncline of fault F2 permit to date the (re)activation of fault during the Middle to Late Devonian.

-In figure 7, divergent onlaps (DO0 to DO3), thickness variations in hanging walls or and footwalls are evidence of faults reactivations.”

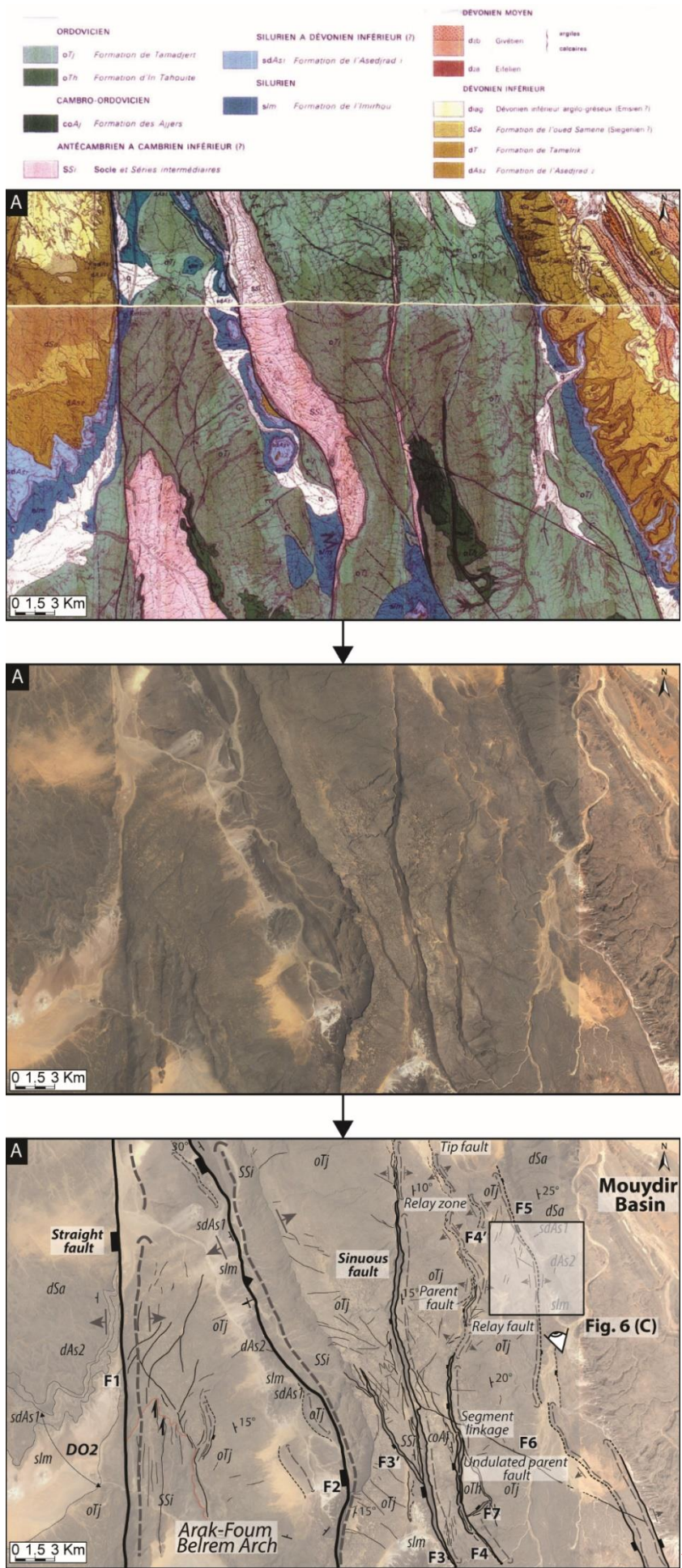


Fig. 5A (previous Fig. 4A) 22

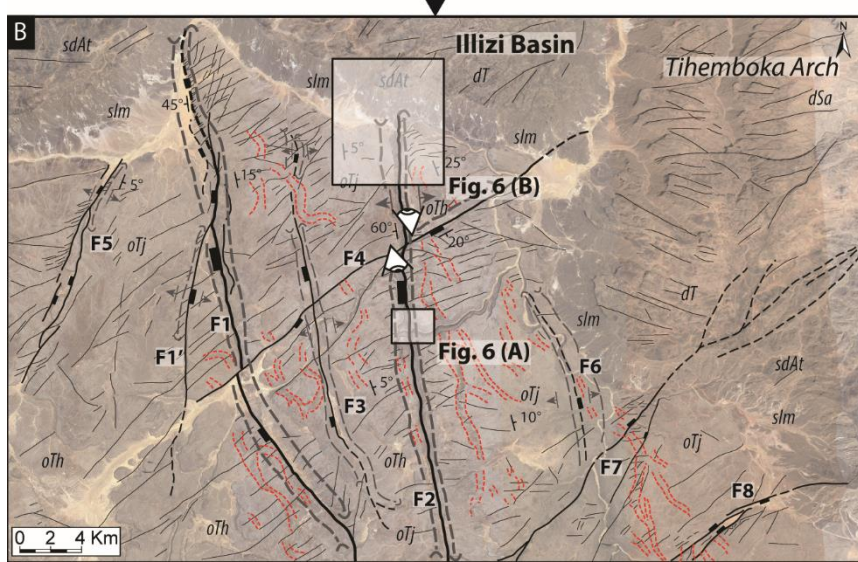
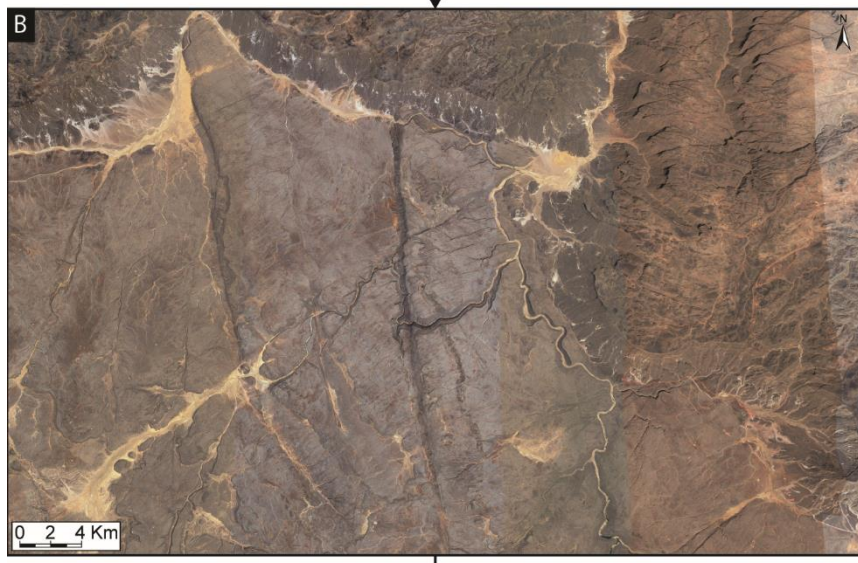
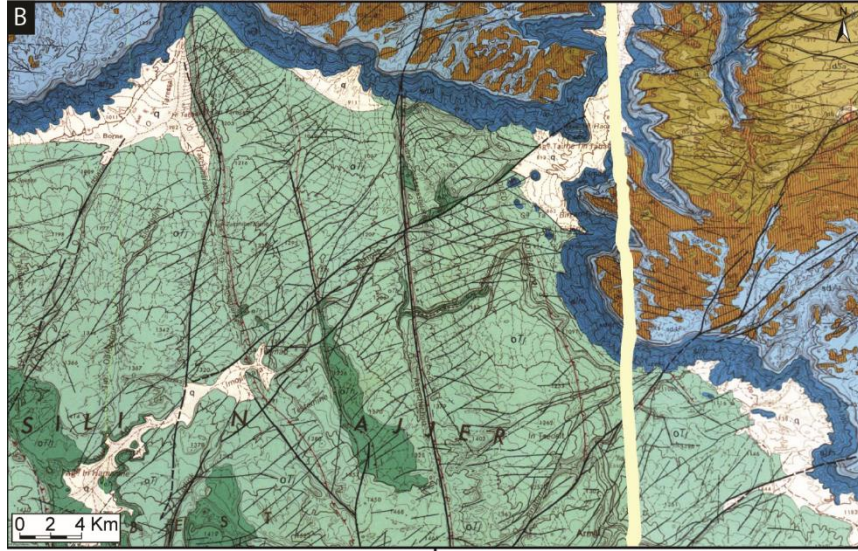
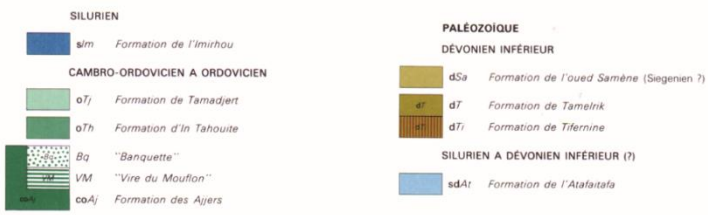


Fig. 5B (previous Fig. 4B)

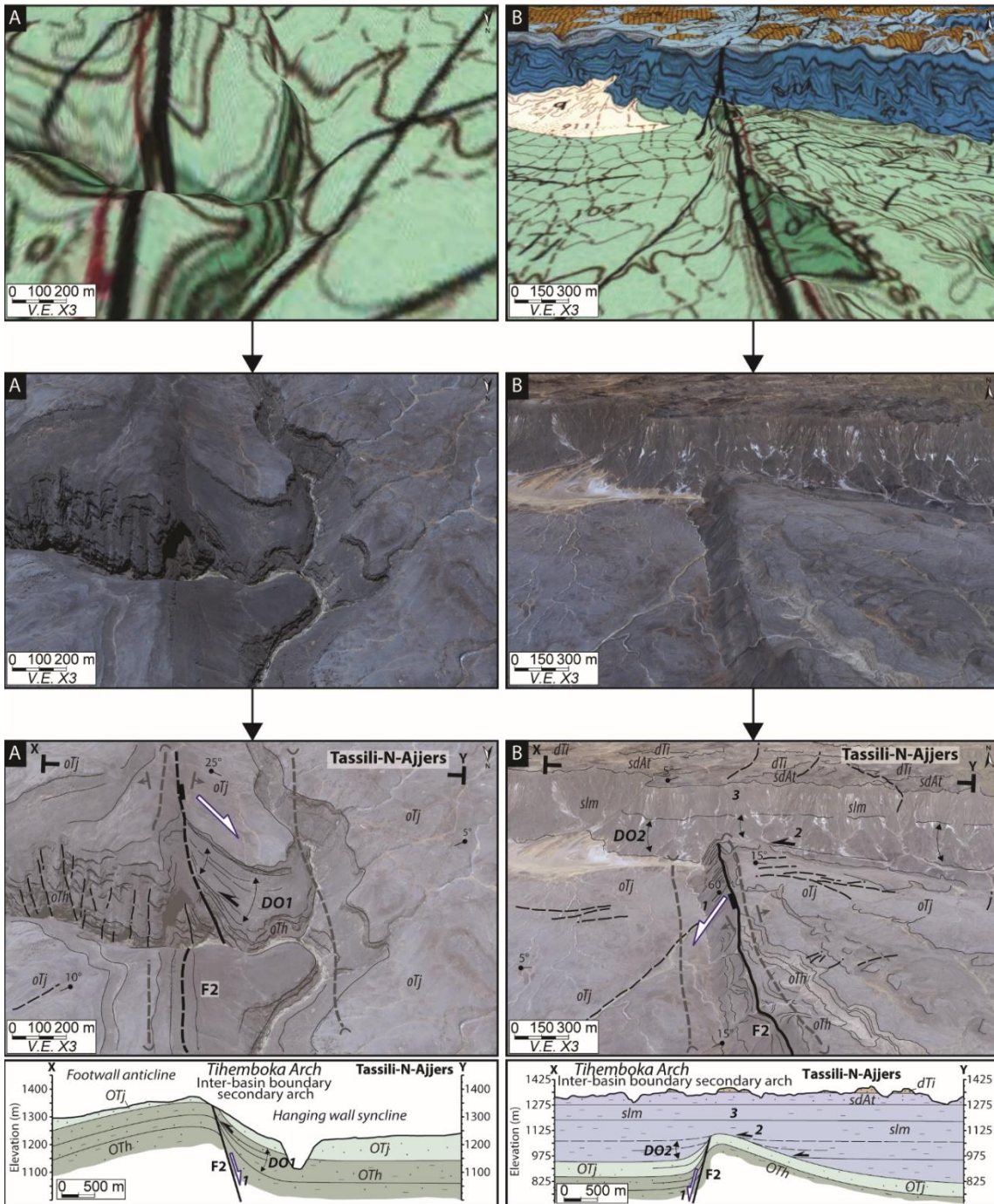


Fig. 6A and B (previous Fig. 5A and B)

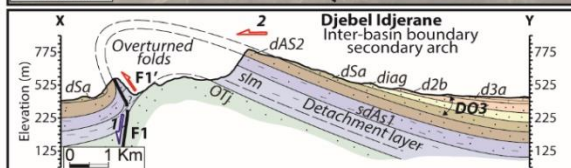
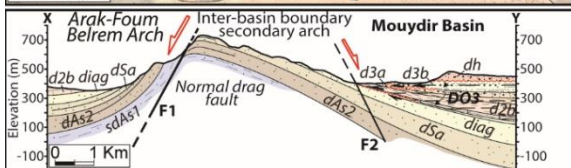
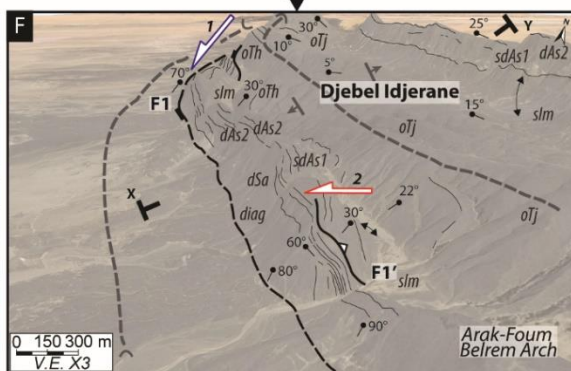
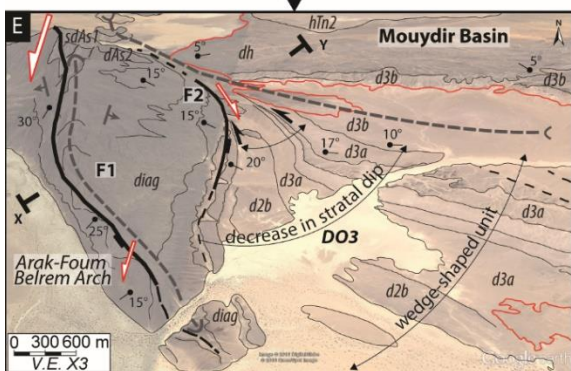
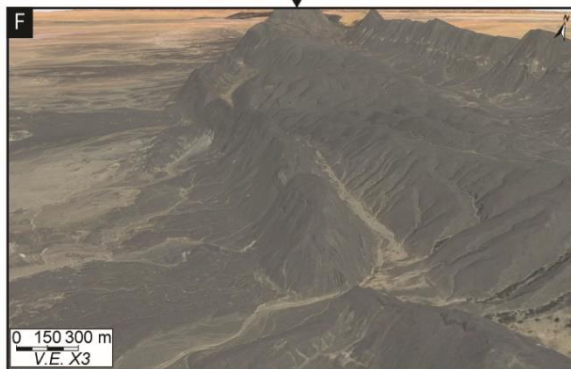
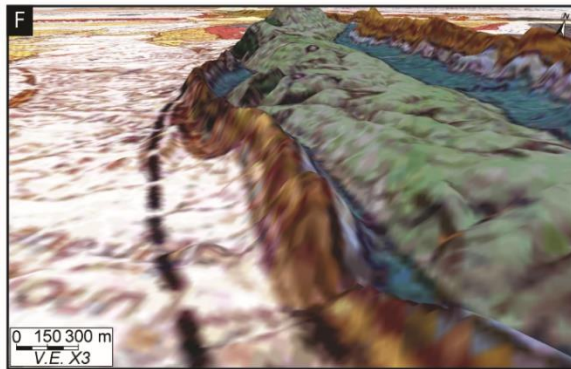
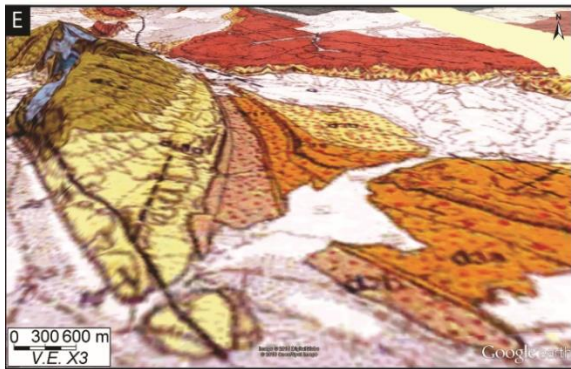
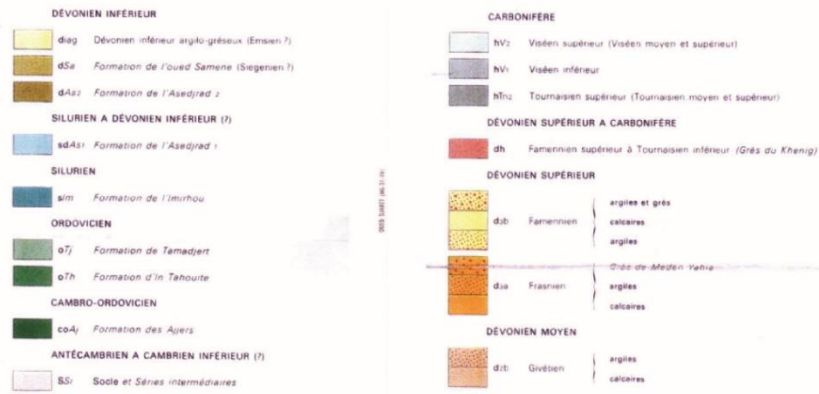


Fig. 6E and F (previous Fig. 5E and F)

- SILURIEN A DEVONNIEN INFÉRIEUR (1)
- sdAs1 Formation de l'Asedrad 1
- SILURIEN
- slm Formation de l'Imrhou
- ORDOVICIEN
- oT1 Formation de Tamadert
- oT2 Formation d'In Tahoute
- CAMBRO-ORDOVICIEN
- coA1 Formation des Aijers
- ANTÉCAMBRIEN A CAMBRIEN INFÉRIEUR (1)
- SS1 Socle et Séries intermédiaires

- DEVONNIEN MOYEN
- d1b Gréivien argiles calcaires
- d1a Efelien
- DEVONNIEN INFÉRIEUR
- diag Devonien inférieur argilo gréseux (Emsien 1)
- dSa Formation de l'oued Samene (Siegenien 1)
- dT Formation de Tametrik
- dAs2 Formation de l'Asedrad 2

- DEVONNIEN MOYEN
- d2b Gréivien argiles calcaires
- d2a Efelien
- DEVONNIEN INFÉRIEUR
- d1ag Devonien inférieur argilo gréseux (Emsien 1)
- dSa Formation de l'oued Samene (Siegenien 1)
- dAs2 Formation de l'Asedrad 2
- SILURIEN A DEVONNIEN INFÉRIEUR (1)
- sdAs1 Formation de l'Asedrad 1
- SILURIEN
- slm Formation de l'Imrhou
- ORDOVICIEN
- oT1 Formation de Tamadert
- CAMBRO-ORDOVICIEN
- coA1 Formation des Aijers
- ANTÉCAMBRIEN A CAMBRIEN INFÉRIEUR (1)
- SS1 Socle et Séries intermédiaires
- CARBONIFÈRE
- hN1 Namurien inférieur (Namurien A)
- hV1 Vieux supérieur (Vieux moyen et supérieur)
- hV2 Vieux inférieur
- N121 Tournaisien supérieur (Tournaisien moyen et supérieur)
- DEVONNIEN SUPÉRIEUR A CARBONIFÈRE
- d3b Famennien supérieur à Tournaisien inférieur (Gres de Kheng)
- DEVONNIEN SUPÉRIEUR
- d3a Famennien argiles et grès
- d3b Famennien argiles
- SS2 Socle de Maden Yaha
- d3a Famennien argiles calcaires

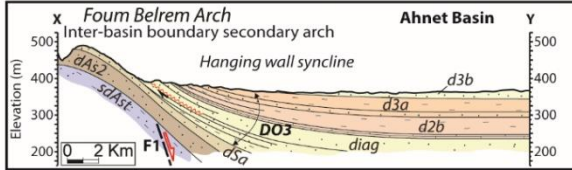
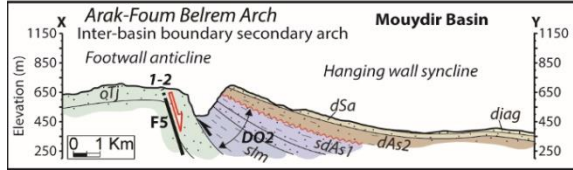
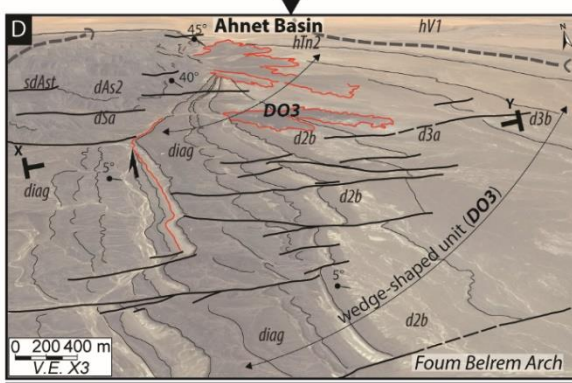
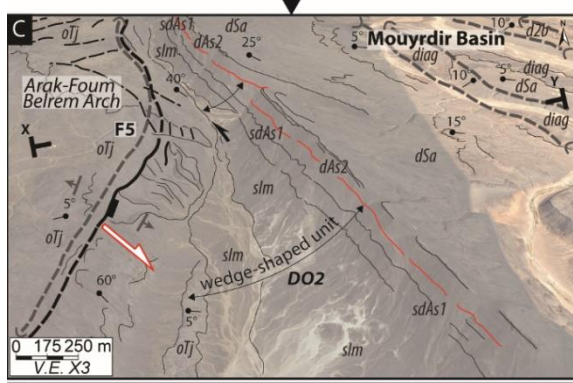
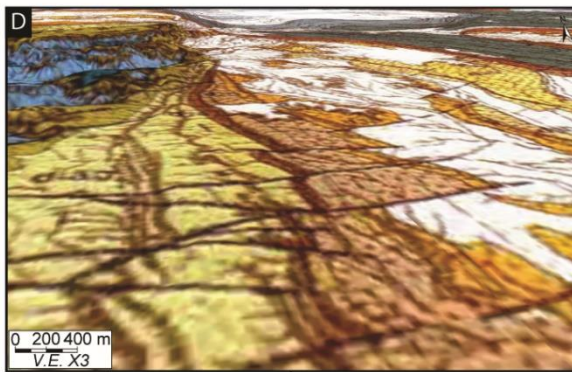
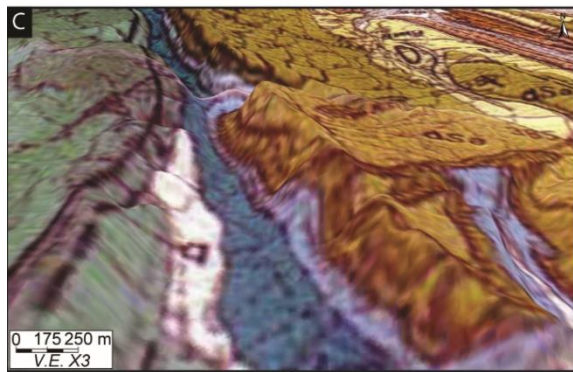


Fig. 6C and D (previous Fig. 5C and D)

Line 261: “Nine facies associations” cannot be detected in Figs 9 and 10. Do you mean the depositional environments? (these are 5). I also could not find the “supplementary data”.

-“We have modified (line 319). We have integrated supplementary data to the paper (cf. fig. 4, 11 and 13).”

Line 291: There is no clear horizontal (gAPI) scale in Fig. 8. Thus it is impossible to check the numbers.

-“We have done a bigger lettering (see Fig. 9).”

Line 298: values range to 120, not 200 in Fig. 8D.

-“modified (line 298).”

Lines 329-330: 30-60 gAPI are low, not high.

-“modified (line 389).”

Line 346: 25-60 gAPI are low, not high.

-“modified (line 407).”

Line 366: stromatoporoids, tabulate and rugose corals are not mentioned on Tab. 1.

-“modified (see Table 1).”

Line 378: same as above.\*

-“modified (line 440).”

Line 382-83: same as above.

-“modified (line 445).”

Line 395: HCS probably stands for hummocky cross stratification. If this should be the case, these structures indicate a shallow marine environment, not deep marine. The same interpretation refers to “influence of storms”, i.e. shallow, not deep.

-“We have modified (line 459-463) and proposed that it corresponds to deeper than shoreface deposits. AF5a is interpreted as upper offshore (i.e. a kind of offshore transition). The occurrence of HCS and wavy-bedded structures, as well as the fossil traces indicate that this facies association recorded deposition in a marine environment between the fair-weather (MFWB) and the storm-wave base (MSWB) under the influence of storm wave’s oscillatory currents (Dott and Bourgeois, 1982; Reading, 2002). No influence of waves has been recorded and the storm-induced deposits are embedded in fine grain sediment (mud dominated).

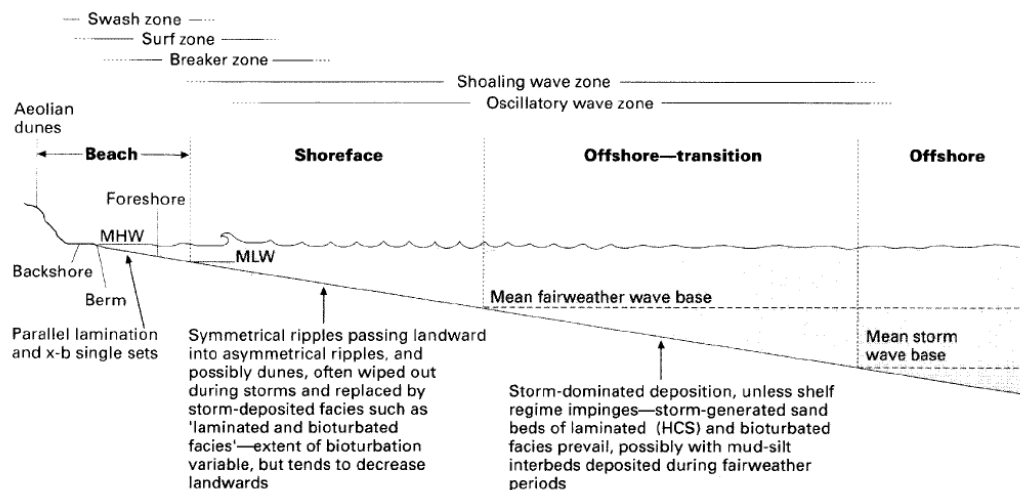


Figure 6.6 Generalized shoreline profile showing subenvironments, processes and facies.

From (Reading and Collinson, 2009) p. 160.

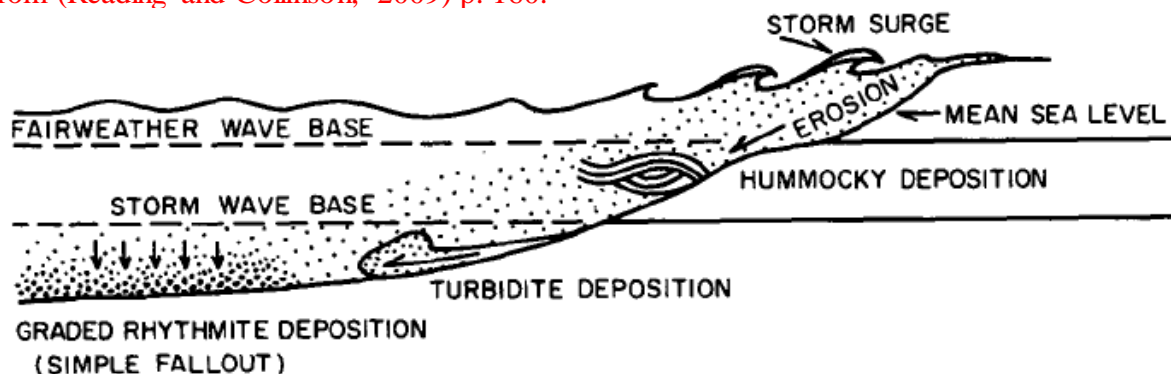
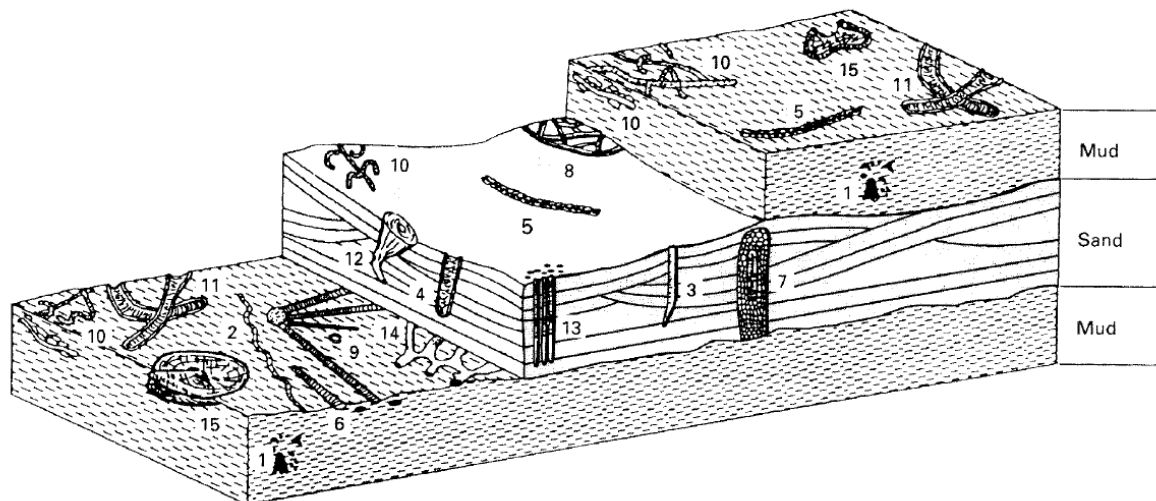


Figure 22. Diagram showing inferred storm origin of hummocky stratification and graded sand laminae on shelves. Storm surge erodes sand at shore; hummocky stratification is deposited and preserved in stormy seas between fair-weather and storm-wave bases; graded laminae may be deposited and preserved at greater depths by simple settling from suspension and/or from turbidity currents. (Modified from Walker, 1979, Fig. 15, and Dott and Bourgeois, 1980, Fig. 3.)

From (Dott and Bourgeois, 1982).

Line 396: The ichnofauna of AF5a does not necessarily indicate a deep marine environment, but could also be much more shallow, as indicated by the “influence of storms”.

-“We agree that *Zoophycus* by itself can be interpreted as formed in shallow environments but also in deeper offshore setting (MacEachern et al., 2007; Vinn and Toom, 2015). In the literature, even if *Zoophycus* can be found in broad environmental systems, it occurs preferentially in deeper environments especially in slope area (Seilacher, 1967).



**Figure 7.41** Typical trace fossil assemblages within offshore storm (hummocky cross-stratified) sand layers and their bounding mud units. 1, *Chondrites*; 2, *Cochlichnus*; 3, *Cylindrichnus*; 4, *Diplocraterion*; 5, *Gyrochorte*; 6, *Muensteria*; 7, *Ophiomorpha*;

8, *Palaeophycus*; 9, *Phoebichnus*; 10, *Planolites*; 11, *Rbizocorallium*; 12, *Roselia*; 13, *Skolithus*; 14, *Thalassinoides*; 15, *Zoophycus* (from Ekdale, Bromley & Pemberton, 1984).

From (Reading, 2002) p. 264.

Line 406: The Grès de Mehden (not “Meden) Yahia and the Temertasset (not “Terमतasset) shales were deposited during a regressive phase and should be discussed in one of the preceding paragraphs.

-“We have modified and added to paragraph 5.2 the regressive trend (line 520-522). However, it is written ‘Meden’ in geological maps (Bennacef et al., 1974; Bensalah et al., 1971) see above. Indeed, the transition from shales to sandstones correspond to a regressive trend (as proposed Wendt et al., 2006) but this paragraph only deal with the Argiles de Mehden Yahia shales interpreted as deeper environment the pattern corresponds to a MFS.”

Line 410: not “Paleozoic” but “Devonian”. Fig. 7 shows almost exclusively Devonian.

-“modified (line 476).”

Line 421: The major flooding surface is not MFS5 but MFS4 (Eifelian transgression).

-“We have added this comments (line 505-507). However, the MFS5 correspond to the transition of an important changes in geodynamic context but do not significate that it is an important MFS at the scale of the Devonian record. Besides, it is easily identified and extendable horizon because of a gamma ray peak. So, we have decided to horizontalized on it. Besides, outcrops (O1 – O9) from Wendt et al., (2006) are horizontalized on top Givetian.”

Line 423: same error. Moreover, you have omitted the gap in the Emsian.

-“This gap is included in the pattern from D1 to D5 and is discussed in paragraph 6 (F) (line 585-591). Upper Emsian emergence is characterized by truncatures from satellites images (see fig. 6D and 6E) and well cross section (erosion and pinch out of upper Emsian to Eifelian series) (see fig. 10, 12 and 13).”

Lines 433-436: This is highly exaggerated. The facies variations between the Ahnet Basin and the adjacent ridges are very weak.

-“modified (line 500). We have moderated our purpose.”

Line 442: MFS5 is not a major flooding surface. The corresponding black shales are diachronous (earliest ones in the Givetian, latest ones in the upper Frasnian), and their occurrence depends mainly on paleogeographic factors. It is true that there is an evident gap between the Givetian and the Frasnian, but this occurs only on the ridges, not in the basins, and it is caused by non-deposition, not by transgression.

-“The apparition of hot shales is observed during early Frasnian. This layer has been chosen as correlation layer as it was observed by GR in all the study core section and due to our biostratigraphical scale. These hot shales correspond to a flooding at the basin scale.”

Line 451: not a maximum flooding but regression (see above).

-“D6 to D9 encompass the whole Frasnian to Famennian sedimentary succession interrupted by several sequence boundary and recording T-R trends (as shown in fig. 8).”

Line 514: an “early Eifelian” hiatus does not exist. Or do you mean the partitus Zone which in fact has not been documented? But I did not check the other references which appear to depend on palynomorph stratigraphy which, compared to conodont stratigraphy, is much less reliable.

-“corrected.”

Line 660: Which are the “Three different periods of tectonic compressional pulses”? I am aware only of one, the Hercynian.

-“The Caledonian (i.e. Siluro-Devonian), Middle to Late Devonian and Pre-Hercynian events identified both in this study and in the literature see below.”

Lines 668-1266: References: The reference list occupies almost the same space as the preceding text and should be drastically reduced, at least to one half. In order to avoid the impression that the article is nothing but a general review paper. Only articles referring to the study area should be included in the reference list. Unfortunately, the latter in its present length shows many incomplete citations (missing volume, missing pages, missing dots in abbreviations, missing editor, missing town (for books), missing capitalizing, wrong spelling), such as in lines 673, 676, 681, 685, 690, 696, 699, 740, 743, 745, 755, 762, 764, 765, 777, 814, 828, 830, 844, 863, 873, 893, 900, 902, 938, 957, 963, 979, 982, 1001, 1003, 1013, 1018, 1033, 1037, 1041, 1075, 1081, 1082, 1095, 1099, 1112, 1124, 1129, 1158, 1160, 1162, 1169, 1176, 1181, 1185, 1186, 1195, 1221, 1222, 1226, 1244, 1253, 1255, 1257, 1260. This list, however, is not complete. I did not check, if every reference in the text does also appear in the reference list and vice versa. This can be done much more accurately by a simple computer program (which I do not have). On the other hand, important local works are not cited.

-“We have modified references by using ZOTERO software and limited them in the text.”

### **Remarks to figures:**

Fig. 1: line 1275: 1: 200.000.

-“modified (line 1411).”

Line 1281: where are the supplementary data?

Map and reference of Monod (1931-1932) are missing.

“We have integrated supplementary data to the paper (cf. fig. 4, 11 and 13). Expect error on our part, we didn't use map from Monod.”

Fig. 2: Illizi Fm. Is missing in the Illizi column.

-“It is present in the Tassili column (see Fig. 3).”

Fig. 3: give exact coordinates for wells (W1- W21) and for outcrops (O1 – O9). What are the latter? Own data or previously published ones? Why there is no cross section along the O1-O9 line?

-“Coordinates of wells (W1- W21) are confidential they are put in a banalized format. O1-O9 outcrops data came from Wendt et al., (2006). However, you didn’t had access to supplementary data. They are added to the paper (see fig. 11 and 13).”

Fig. 7: larger lettering is required. (I had to use a 3x magnifier to read it). What are the tiny arrows in the left gamma-ray-column?

-“We have done a bigger lettering. The tiny arrows were giving the trend of the gamma ray but they are not indispensable for understanding. They were deleted (see Fig. 8).”

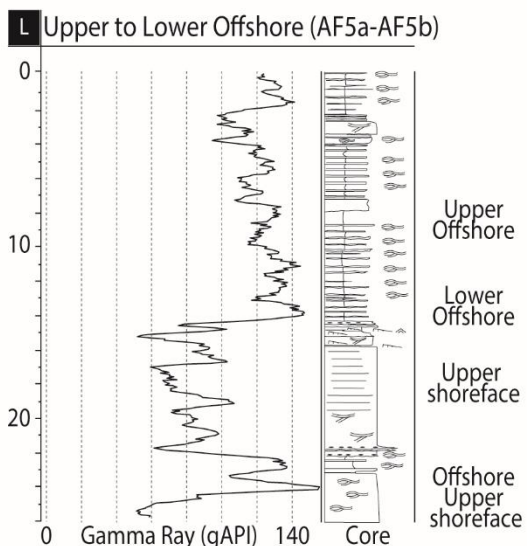
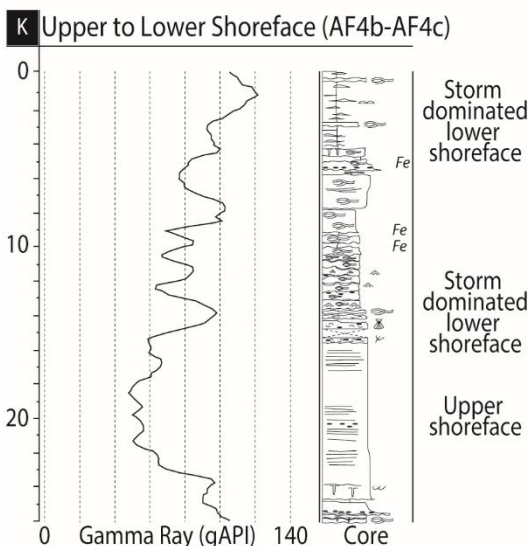
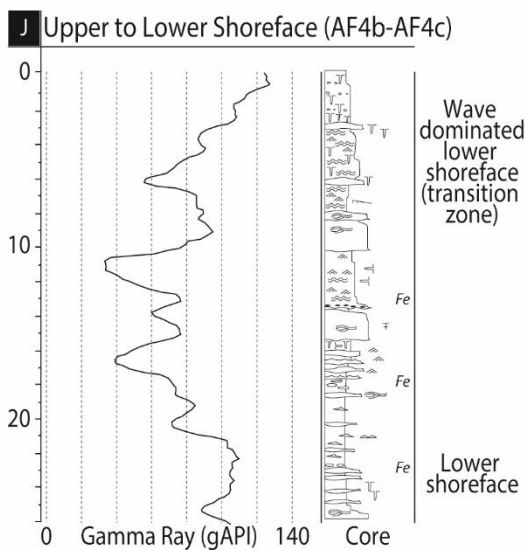
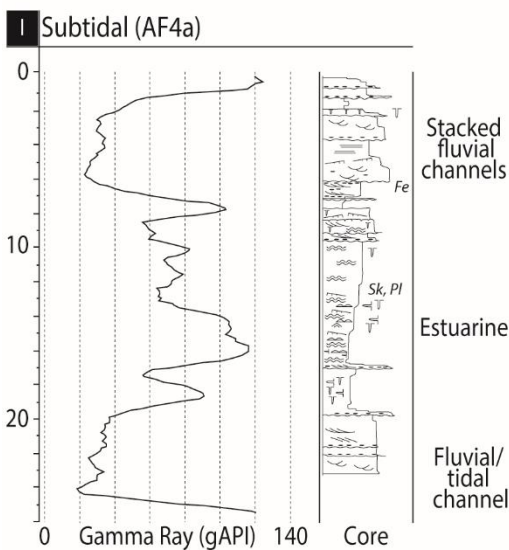
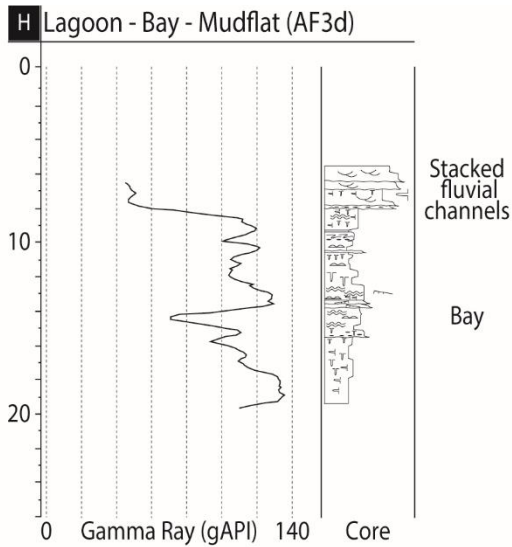
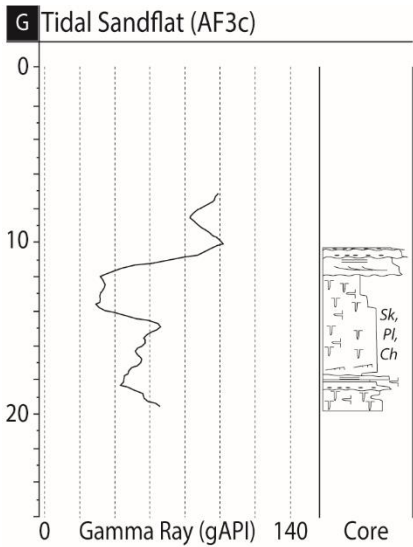
Tab. 1: Please add a column with the equivalent individual formation names. In the present form this table is rather theoretical and shows no relation to the Devonian depositional areas.

-“added (see Table 1).”

Fig. 8: Because of its tiny lettering this figure is almost unreadable. Stages and formation names should be added for each sub-figure. The accompanying sections are unreadable. I could not check the source because the equivalent reference is incomplete. In the present form this figure appears rather useless. Gamma-ray-curves often do not correspond to their interpretation in the text (see above). It would make a certain sense, if there were a comparison with equivalent well logs in each sub-figure, but it would better to omit this figure completely.

-“We have done a bigger lettering cf. fig. 9 (size minimum 7). We can divide this figure by 2 to magnify for a better visibility (cf. Fig. a and b below).”





Sedimentary structures			Fossils & Faunal activity		
Planar bedding	Hummocky cross bedding	Load & escape structures	FG Firm ground	Bivalves	
Wave-ripple bedding	Swaley cross bedding	Slump	ScS Scoured surface	Fossil debris	
Convolute bedding	Cross bedding	Mud & pellets/clasts/drapes	Syn Syneresis crack	Bryozoans	
Flaser bedding	Wave ripple bedding	Mud cracks	Finning upwards	Crinoids	
Bi-directional bedding	Combined flow ripples			Ichnofacies	
Trough cross stratification	Planar cross low angle stratification			Bioturbations	
Asymmetrical ripples	Lenticular stratification & ripples				
Sigmoidal cross bedding	Flat lens				
			Fe Iron		
			Si Silica		
			Py Pyrite		

(b)

Fig. 9: Needs larger lettering! In Fig. 2 the Emsian is a gap (which is correct), but in Fig. 9 this stage is represented by strata, which is an obvious contradiction.

-“We have done a bigger lettering. In Fig. 10, 12 and 13 upper Emsian series are truncated. An evidence of hiatus. On this representation format we cannot show the presence of hiatus (It is not a chronostratigraphic representation).”

Fig. 10: same as Fig. 9.

-“see above.”

Fig. 11: “K” is missing on A and B. (line 1486).

-“modified (line 1658-1659).”

Fig. 12: larger lettering, the smallest ones are illegible.

-“We have enlarged the lettering (size minimum 7). However, enlarged the figure cannot be done without separating in two the figure. So, we have separated in two the figure (see Fig. 15 and 16).”

### **Conclusion:**

As a whole the paper is well written, rather concise and accompanied by good illustrations (apart from the above remarks). It is an example of a modern interpretation of a basin and ridge paleogeography using all available techniques. An important contribution is the representation of well data which are difficult to obtain by non-oil geologists. Nevertheless, it cannot be overlooked that as a whole the paper appears to be based almost exclusively on pre-existing data. The personal contribution to the subject is difficult to distinguish. Thus, in several aspects and conclusions the interpretations of the data are not or only poorly compatible with well-established field data. Some of them are highly speculative. It should also be made clear that the depositional units (basins and ridges) are nothing else than the southern prolongation of the same (but more accentuated) ones farther north. It should also be clearly expressed that the basin-and-ridge paleotopography in the Ahnet and Mouydir is of relatively short duration (early Eifelian to early Famennian). The depositional pattern of the late Famennian and the Carboniferous is totally different from the Devonian one. A Devonian sea-level curve would be highly desirable. Absolutely necessary are several block diagrams to show the basin-and-ridge configuration at various stages. I recommend publication of the manuscript after major revision, but I would be glad to receive the revised manuscript once more before its final acceptance.

-“We have added a method figure (fig. 4) and better specified the original work in the method part. In our paper, we argue that the basement structures (at a lithospheric scale) are alternately reactivated (i.e. uplifted basement=>forced folds) during the Paleozoic. The basin-and-ridge feature was preserved since the Cambrian until the Carboniferous (as seen before) due to tectonic pulses (syn-sedimentary) and to the inherited basement features (i.e. mega shear zones and terranes rheologies). This particular zonation of the terranes (Archean, Paleoproterozoic, Proterozoic...) has constrained the basin-and-ridge architecture. However, we agree with the fact that the arches were consecutively levelled and flooded (i.e. eustatic control) during some major transgression periods. A similar block diagrams showing the evolution of basin-and-ridge configuration is published (Eschard et al., 2010), even if there are some minor differences.”

### Cited References:

- Abdesselam-Rouighi, F.-F.: Biostratigraphie des spores, acritarches et chitinozoaires du Dévonien moyen et supérieur du bassin d'Illizi (Algérie), *Bull. Serv. Géologique Algérie*, 14(2), 97–117, 2003.
- Baidder, L., Raddi, Y., Tahiri, M. and Michard, A.: Devonian extension of the Pan-African crust north of the West African craton, and its bearing on the Variscan foreland deformation: evidence from eastern Anti-Atlas (Morocco), *Geol. Soc. Lond. Spec. Publ.*, 297(1), 453–465, doi:10.1144/SP297.21, 2008.
- Belka, Z.: Early Devonian Kess-Kess carbonate mud mounds of the eastern Anti-Atlas (Morocco), and their relation to submarine hydrothermal venting, *J. Sediment. Res.*, 68(3), 368–377, 1998.
- Bellini, E. and Massa, D.: A stratigraphic contribution to the Palaeozoic of the southern basins of Libya, *Geol. Libya*, 1, 3–56, 1980.
- Bennacef, A., Attar, A., Froukhi, R., Beuf, S., Philippe, G., Schmerber, G. and Vermeire, J. C.: Cartes Géologiques d'Iherir-Dider (NG-32-IX), Iherir (NG-32-X), Illizi (NG-32-XV), Aharhar (NG-32-VIII), Oued Samène (NG-32-XIV), Erg Tihodaine (NG-32-VII), Tin Alkoum (NG-32-V), Djanet (NG-32-IV), Ta-N-Mellet (NG-32-XIII), Ta-N-Elak (NG-32-XIX), Fort Tarat (NG-32-XVI), Tilmas El Mra (NG-31-XXIV), Ers Oum El Lil (NG-31-XXII), Amguid (NG-31-XVIII), 1/200000 Sonatrach-Ministère de l'Industrie et des Mines, Algérie, 1974.
- Bensalah, A., Beuf, S., Gabriel, O., Philippe, G., Lacot, R., Paris, A., Basseto, D., Conrad, J. and Moussine-Pouchkine, A.: Cartes Géologiques de Khanguet El Hadid (NG-31-XVII), Aïn Tidjoubar (NG-31-XVI), Oued Djaret (NG-31-XV), Aoulef El Arab (NG-31-XIV), Reggane (NG-31-XIII), Ifetessene (NG-31-IX), Arak (NG-31-X et NG-31-IV), Meredoua (NG-31-XIII), Tanezrouft (NG-31-VII et NG-31-I), In Heguis (NG-31-IX), Tin Senasset (NG-31-III), Ouallene (NG-31-II) 1/200000 Sonatrach-Ministère de l'Industrie et des Mines, Algérie, 1971.
- Beuf, S., Biju-Duval, B., Mauvier, A. and Legrand, P.: Nouvelles observations sur le 'Cambro-Ordovicien' du Bled El Mass (Sahara central), *Publ. Serv. Géologique Algér. Bull.*, 38, 39–51, 1968a.
- Beuf, S., Biju-Duval, B., De Charpal, O., Gariel, O., Bennacef, A., Black, R., Arene, J., Boissonnas, J., Chachau, F., Guérangé, B. and others: Une conséquence directe de la structure du bouclier Africain: L'ébauche des bassins de l'Ahnet et du Mouydir au Paléozoïque inférieur, *Publ. Serv. Géologique L'Algérie Nouv. Sér. Bull.*, 38, 105–34, 1968b.
- Beuf, S., Biju-Duval, B., de Charpal, O., Rognon, P., Gabriel, O. and Bennacef, A.: Les grès du Paléozoïque inférieur au Sahara: Sédimentation et discontinuités évolution structurale d'un craton, *Technip., Paris.*, 1971.
- Biju-Duval, B., de Charpal, O., Beuf, S. and Bennacef, A.: Lithostratigraphie du Dévonien inférieur dans l'Ahnet et le Mouydir (Sahara Central), *Bull Serv Géologique Algérie*, (38), 83–104, 1968.
- Boote, D. R. D., Clark-Lowes, D. D. and Traut, M. W.: Palaeozoic petroleum systems of North Africa, *Geol. Soc. Lond. Spec. Publ.*, 132(1), 7–68, doi:10.1144/GSL.SP.1998.132.01.02, 1998.

- Borocco, J. and Nyssen, R.: Nouvelles observations sur les "gres inférieurs" cambro-ordoviciens du Tassili interne (Nord-Hoggar), *Bull. Société Géologique Fr.*, S7-I(2), 197–206, doi:10.2113/gssgfbull.S7-I.2.197, 1959.
- Boudjema, A.: Evolution structurale du bassin pétrolier " triasique" du Sahara nord oriental (Algérie), Doctoral dissertation, Paris 11, France., 1987.
- Boumendjel, K., Loboziak, S., Paris, F., Steemans, P. and Streef, M.: Biostratigraphie des Miospores et des Chitinozoaires du Silurien supérieur et du Dévonien dans le bassin d'Illizi (S.E. du Sahara algérien), *Geobios*, 21(3), 329–357, doi:10.1016/S0016-6995(88)80057-3, 1988.
- Brice, D. and Latrèche, S.: Brachiopodes du bassin d'Illizi (Sahara algérien oriental) près de la limite Givétien-Frasnien, *Geobios*, 31(4), 437–454, doi:10.1016/S0016-6995(98)80116-2, 1998.
- Carruba, S., Perotti, C., Rinaldi, M., Bresciani, I. and Bertozzi, G.: Intraplate deformation of the Al Qarqaf Arch and the southern sector of the Ghadames Basin (SW Libya), *J. Afr. Earth Sci.*, 97, 19–39, doi:10.1016/j.jafrearsci.2014.05.001, 2014.
- Chaumeau, J., Legrand, P. and Renaud, A.: Contribution à l'étude du Couvinien dans le bassin de Fort-de-Polignac (Sahara), *Bull. Société Géologique Fr.*, S7-III(5), 449–456, doi:10.2113/gssgfbull.S7-III.5.449, 1961.
- Chavand, J. C. and Claracq, P.: La disparition du Tassili externe à l'E de Fort-Polignac (Sahara central), *CR Soc Géol Fr*, 1959, 172–174, 1960.
- Collomb, G. R.: Étude géologique du Jebel Fezzan et de sa bordure paléozoïque, *Compagnie française des pétroles.*, 1962.
- Coward, M. P. and Ries, A. C.: Tectonic development of North African basins, *Geol. Soc. Lond. Spec. Publ.*, 207(1), 61–83, doi:10.1144/GSL.SP.2003.207.4, 2003.
- Craig, J., Rizzi, C., Thusu, B., Lüning, S., Asbali, A. I., Keeley, M. L., Bell, J. F., Durham, M. J., Eales, M. H., Beswetherick, S. and Bishop, C.: Structural Styles and Prospectivity in the Precambrian and Palaeozoic Hydrocarbon Systems of North Africa, 2006.
- Dott, R. H. and Bourgeois, J.: Hummocky stratification: Significance of its variable bedding sequences, *Geol. Soc. Am. Bull.*, 93(8), 663, doi:10.1130/0016-7606(1982)93<663:HSSOIV>2.0.CO;2, 1982.
- Dubois, P. and Mazelet, P.: Stratigraphie du Silurien du Tassili N'Ajjer, *Bull. Société Géologique Fr.*, S7-VI(4), 586–591, doi:10.2113/gssgfbull.S7-VI.4.586, 1964.
- Echikh, K.: Geology and hydrocarbon occurrences in the Ghadames basin, Algeria, Tunisia, Libya, *Geol. Soc. Lond. Spec. Publ.*, 132(1), 109–129, 1998.
- Eschard, R., Braïk, F., Bekkouche, D., Rahuma, M. B., Desaubliaux, G., Deschamps, R. and Proust, J. N.: Palaeohighs: their influence on the North African Palaeozoic petroleum systems, *Pet. Geol. Mature Basins New Front. 7th Pet. Geol. Conf.*, 707–724, 2010.
- Fabre, J.: Géologie du Sahara occidental et central, *Musée royal de l'Afrique centrale.*, 2005.

Fekirine, B. and Abdallah, H.: Palaeozoic lithofacies correlatives and sequence stratigraphy of the Saharan Platform, Algeria, *Geol. Soc. Lond. Spec. Publ.*, 132(1), 97–108, doi:10.1144/GSL.SP.1998.132.01.05, 1998.

Frizon de Lamotte, D., Tavakoli-Shirazi, S., Leturmy, P., Averbuch, O., Mouchot, N., Raulin, C., Leparmentier, F., Blanpied, C. and Ringenbach, J.-C.: Evidence for Late Devonian vertical movements and extensional deformation in northern Africa and Arabia: Integration in the geodynamics of the Devonian world: Devonian evolution Northern Gondwana, *Tectonics*, 32(2), 107–122, doi:10.1002/tect.20007, 2013.

Galeazzi, S., Point, O., Haddadi, N., Mather, J. and Druesne, D.: Regional geology and petroleum systems of the Illizi–Berkine area of the Algerian Saharan Platform: An overview, *Mar. Pet. Geol.*, 27(1), 143–178, doi:10.1016/j.marpetgeo.2008.10.002, 2010.

Gawthorpe, R. and Hardy, S.: Extensional fault-propagation folding and base-level change as controls on growth-strata geometries, *Sediment. Geol.*, 146(1–2), 47–56, doi:10.1016/S0037-0738(01)00165-8, 2002.

Ghienne, J.-F., Moreau, J., Degermann, L. and Rubino, J.-L.: Lower Palaeozoic unconformities in an intracratonic platform setting: glacial erosion versus tectonics in the eastern Murzuq Basin (southern Libya), *Int. J. Earth Sci.*, 102(2), 455–482, doi:10.1007/s00531-012-0815-y, 2013.

Gindre, L., Le Heron, D. and Bjørnseth, H. M.: High resolution facies analysis and sequence stratigraphy of the Siluro-Devonian succession of Al Kufrah basin (SE Libya), *J. Afr. Earth Sci.*, 76, 8–26, doi:10.1016/j.jafrearsci.2012.08.002, 2012.

Girard, F., Ghienne, J.-F. and Rubino, J.-L.: Channelized sandstone bodies (‘cordons’) in the Tassili N’Ajjjer (Algeria & Libya): snapshots of a Late Ordovician proglacial outwash plain, *Geol. Soc. Lond. Spec. Publ.*, 368(1), 355–379, doi:10.1144/SP368.3, 2012.

Guiraud, R., Bosworth, W., Thierry, J. and Delplanque, A.: Phanerozoic geological evolution of Northern and Central Africa: An overview, *J. Afr. Earth Sci.*, 43(1–3), 83–143, doi:10.1016/j.jafrearsci.2005.07.017, 2005.

Hardy, S. and McClay, K.: Kinematic modelling of extensional fault-propagation folding, *J. Struct. Geol.*, 21(7), 695–702, doi:10.1016/S0191-8141(99)00072-3, 1999.

Holt, P. J., Allen, M. B., van Hunen, J. and Bjørnseth, H. M.: Lithospheric cooling and thickening as a basin forming mechanism, *Tectonophysics*, 495(3–4), 184–194, doi:10.1016/j.tecto.2010.09.014, 2010.

Kane, K. E., Jackson, C. A.-L. and Larsen, E.: Normal fault growth and fault-related folding in a salt-influenced rift basin: South Viking Graben, offshore Norway, *J. Struct. Geol.*, 32(4), 490–506, doi:10.1016/j.jsg.2010.02.005, 2010.

Legrand, P.: Le Devonien du Sahara Algerien, *Can. Soc. Pet. Geol.*, 1, 245–284, 1967a.

Legrand, P.: Nouvelles connaissances acquises sur la limite des systèmes Silurien et Dévonien au Sahara algérien, *Bull. Bur. Rech. Géologiques Minières*, 33, 119–37, 1967b.

Lewis, M. M., Jackson, C. A.-L., Gawthorpe, R. L. and Whipp, P. S.: Early synrift reservoir development on the flanks of extensional forced folds: A seismic-scale outcrop analog from the

Hadahid fault system, Suez rift, Egypt, *AAPG Bull.*, 99(06), 985–1012, doi:10.1306/12011414036, 2015.

MacEachern, J. A., Pemberton, S. G., Gingras, M. K. and Bann, K. L.: CHAPTER 4 - The Ichnofacies Paradigm: A Fifty-Year Retrospective, in *Trace Fossils*, edited by W. Miller, pp. 52–77, Elsevier, Amsterdam., 2007.

Massa, D.: Paléozoïque de Libye occidentale : stratigraphie et paléogéographie, Doctoral dissertation, Université de Nice, France., 1988.

Mckerrow, W. S., Niocaill, C. M. and Dewey, J. F.: The Caledonian Orogeny redefined, *J. Geol. Soc.*, 157(6), 1149–1154, doi:10.1144/jgs.157.6.1149, 2000.

Michard, A., Hoepffner, C., Soulimani, A. and Baidder, L.: The Variscan Belt, *Earth Sci.*, 2008.

Moreau, J., Ghienne, J. F. and Hurst, A.: Kilometre-scale sand injectites in the intracratonic Murzuq Basin (South-west Libya): an igneous trigger?: Sand injectites in the Murzuq Basin: an igneous trigger?, *Sedimentology*, 59(4), 1321–1344, doi:10.1111/j.1365-3091.2011.01308.x, 2012.

Moreau-Benoit, A., Coquel, R. and Latreche, S.: Étude palynologique du dévoniendu bassin d’illizi (Sahara oriental algérien). Approche biostratigraphique, *Geobios*, 26(1), 3–31, doi:10.1016/S0016-6995(93)80002-9, 1993.

Ouanaimi, H. and Lazreq, N.: The ‘Rich’ group of the Drâa Basin (Lower Devonian, Anti-Atlas, Morocco): an integrated sedimentary and tectonic approach, *Geol. Soc. Lond. Spec. Publ.*, 297(1), 467–482, doi:10.1144/SP297.22, 2008.

Reading, H. G. and Collinson, J. D.: Clastic coasts, in *Sedimentary environments: processes, facies, and stratigraphy*, pp. 154–231, John Wiley & Sons, Oxford ; Cambridge, Mass., 2009.

Seilacher, A.: Bathymetry of trace fossils, *Mar. Geol.*, 5(5), 413–428, doi:10.1016/0025-3227(67)90051-5, 1967.

Sloss, L. L.: *Sedimentary Cover—North American Craton: U.S.*, Geological Society of America., 1988.

Stampfli, G. M. and Borel, G. D.: A plate tectonic model for the Paleozoic and Mesozoic constrained by dynamic plate boundaries and restored synthetic oceanic isochrons, *Earth Planet. Sci. Lett.*, 196(1), 17–33, 2002.

Stearns, D. W.: Faulting and forced folding in the Rocky Mountains foreland, Laramide Fold. Assoc. Basement Block Faulting West. U. S. Geol. Soc. Am. Mem., 151, 1–37, 1978.

Vinn, O. and Toom, U.: The trace fossil *Zoophycos* from the Silurian of Estonia, *Est. J. Earth Sci.*, 64(4), 284, 2015.

Wendt, J.: Disintegration of the continental margin of northwestern Gondwana: Late Devonian of the eastern Anti-Atlas (Morocco), *Geology*, 13(11), 815–818, 1985.

Wendt, J., Belka, Z., Kaufmann, B., Kostrewa, R. and Hayer, J.: The world's most spectacular carbonate mud mounds (Middle Devonian, Algerian Sahara), *J. Sediment. Res.*, 67(3), 424–436, doi:10.1306/D426858B-2B26-11D7-8648000102C1865D, 1997.

Wendt, J., Kaufmann, B., Belka, Z., Klug, C. and Lubeseder, S.: Sedimentary evolution of a Palaeozoic basin and ridge system: the Middle and Upper Devonian of the Ahnet and Mouydir (Algerian Sahara), *Geol. Mag.*, 143(3), 269–299, doi:10.1017/S0016756806001737, 2006.

Wendt, J., Kaufmann, B. and Belka, Z.: Devonian stratigraphy and depositional environments in the southern Illizi Basin (Algerian Sahara), *J. Afr. Earth Sci.*, 54(3–4), 85–96, doi:10.1016/j.jafrearsci.2009.03.006, 2009.

Withjack, M. O., Olson, J. and Peterson, E.: Experimental models of extensional forced folds, *AAPG Bull.*, 74(7), 1038–1054, 1990.

Ziegler, P. A., Cloetingh, S. and van Wees, J.-D.: Dynamics of intra-plate compressional deformation: the Alpine foreland and other examples, *Tectonophysics*, 252(1), 7–59, doi:10.1016/0040-1951(95)00102-6, 1995.

### **Reviewer 3: Fabio Lottaroli**

Beside the technical and scientific value of the paper I have collected some observations on the structure of the article. How data are presented and how much is clear which is the original work performed with respect of what has been re-digested from previous published work. On this respect there is to me some room of improvement. The reader needs a bit of help in being directed towards the key messages. As it is structured now I found it a little difficult, too much relevant observations in “brackets”, too frequently reader is requested to look at more than one figures with reference to the same concept, jumping ahead and back-word. I would suggest some degree of simplification. At the end, even if is important to mark how big has been the effort of to give spatial relevance to info already published (e.g geochronology, etc: : :) the important thing is to convey the new and original message of the work. I Have never seen in my life Figures Captions as these. Captions represents basically another article. The relevance of illustrations must be stated in the article text. The Figure needs clear legends, but captions, if possible must be concise.

**Abstract Row 17 – 40:** It is lacking reference to your original work and the results of it. What make this paper one of original scientific content? Which is the new aspects of your approach with respect to what (a lot) have been already published on North Africa Paleozoic? Shorten the introductive remarks on Paleozoic Basins and expand the above.

-“We have reformulated the abstract axing on our work approach and results line 17-52).”

**Introduction R47\_** No need to cite specific Figure of Heine for a general remark like this, work citation is enough

-“We have modified (line 59).”

R48\_ Non-conventional exploration has revived interest: : : : explain why and where

-“It is not the purpose of the paper.”



**5.1 Facies association:** : : : R268. Explain how the present study add knowledge to what stated above in defining the facies associations. Which are the new data? Which is the news with respect to the works cited?

-“We have better specified the new data (especially satellite images, seismic lines and well-logs) which have been used in this study. We have integrated a figure presenting the method (cf. fig. 4 in manuscript). Well correlation and stratigraphy sequence interpretation need depositional environment electrofacies analysis. However, they come from previous work not always published. So, in order to go further, they were compiled and synthetized.”

R454 6. An association: : ..refer the title to an observation not to a conclusion: : ..eg: subsidence and tectonic history

-“We have added (line 525).”

R532. Same as above

-“We have modified (line 620).”

R546: : list of thermos orogenic events is complex, brackets inside brackets, cite name or age

-“We have modified (line 209-215). The age of different events are in the legend of fig. 1.”

## Figures

Fig.1 . Too full. Very difficult to read. I would simplify the Paleozoic series legend it is impossible to identify on Map different grades of colours within Cambrian or Carboniferous.

-“The legend is based on published geological maps. So, it is difficult to simply (loose of resolution). However, we have simplified the legend of the figure.”

Too much writings in the AOI (fig3A) too small figure and too dense posting of the Geochronology data to appreciate their relationships with terrains

-“We have corrected and added (see fig. 2 previous fig. 3).”

Fig.3. W=well and O=Outcrops not in the legend.

-“We have added (line 1435-1436).”

Reference to location of sections Fig 5 & 6 difficult to read in Map.

-“We have increased the thickness of cadres and lines localizing the figures for a better visibility (cf. fig. 1 and 2).”

Capital letters of arches and basins confusing with letters that make reference to following figures.

-“Typography was homogenized (arches vs basins) between different figures.”

Fig.4. I do not understand which is the extent of this area with respect to the previous Map (Fig.3A). The small writings (eg: Otj: : : : ) are completely unreadable, remove it or enlarge.

Fig.5. Same comment made above for the small writings in Figures. I do not understand the need to differentiate map and section with A, A’

-“We have simplified the numeration (i.e. avoiding A-A’) and captions of figures. Captions are much concise. We have also resized lettering (Otj...) (see Fig. 5 and 6).”

Fig.7. symbols on core description section are too small to be understand.

-“We have enlarged the lettering. However, enlarged the figure cannot be done without separating in multiple part the figure (see Fig. 8).”

Fig11. K cited in legend but not in Figure  
-“modified (line 1658-1659).”

Fig.12. A,B & C are too small, it should be enlarged. D &E are necessary?

-“We have enlarged the lettering and separated the figure in two (cf. Figs. 15 and 16 in revised manuscript). The D & E show the structural pattern of shear zones (i.e. SC sigmoidal geometries) which have constrained the tectonic framework of the Saharan platform. It is a typical structural style inherited in the area.”

## **Short comment 1: Alex Peace**

Perron et al. describe a study into the role of inherited structures in intracratonic basins in the Central Sahara using a combination of seismic interpretation, various GIS analyses, stratigraphy and geochronology. In my opinion the background information is adequate (just requiring a few minor amendments), the analyses appear to have been appropriately conducted and the discussion and conclusions appear to suitably draw upon the results. In addition, the figures are generally of high quality and should be commended. However, at times some sections seem longer than required and there is potentially some repetition of information. The study is of current relevance with a number of recent papers also addressing similar topics, including a paper in *Solid Earth* (Phillips et al., 2018). Thus, *Solid Earth* seems like a suitable place for publication.

I would therefore like to recommend publication if the relatively minor points suggested here and in the other comments are appropriately addressed. These minor points should not be too arduous, but I think that they will improve the manuscript. I hope you find these suggestions useful and I look forward to seeing a final version of the paper. If you would like clarification of any of my suggestions feel free to contact me.

First, I felt that it was not clear from the abstract what the purpose, aims and main findings of the study were. The reason for this appears to be that much of the abstract (and introduction to some extent) is devoted to regional background information. Although such information is obviously important I suggest more clearly outlining the main findings and study aims in the abstract. In addition, I think the introduction would benefit from a short but general overview of structural inheritance, including information from geological settings from beyond the present study to demonstrate the significance of such processes. Moreover, particularly in the abstract but also in the introduction, it is not always clear what is a finding of this study and what information is from previous work. I suggest Perron et al. clarify these sections with this in mind. Related to the previous point is that the introduction contains a lot of material that would likely be better placed in the subsequent dedicated ‘Geological setting’ section. An example of this is the material in lines 59-75. I think that moving such information into the geological setting and using the introduction to better set up the aims and rationale would be better.

In addition to the previous points I think that the ‘Data and methods’ section requires additional information to be of more use to readers. For example ‘Geographic Information System analysis (GIS)’ (Line 124) is very ambiguous as this could mean any one of a number of approaches. Also minimal details are provided regarding the seismic data or the methods deployed in its interpretation. I suggest that Perron et al. consider adding additional technical information regarding their data sets and the analyses used. Some of these details are provided later in various sections but I think they would be better placed here in the dedicated section.

The descriptions of results in sections 4-6 are generally very good. In particular, good use of the figures is made in the text. However, I found that in section 7 there is an abundance of

material that might be better placed in the ‘Geological Setting’ or the ‘Data and Methods’ sections. Some examples of this are noted below but I suggest Perron et al. reconsider the location of some of the material in this section.

Other minor points include:

-Line 32 – This line is quite awkward. Suggest rewording.

-“We have reformulated the abstract.”

-Line 35 – Replace ‘activated’ with ‘reactivated’?

-“We have modified (line 39).”

-Lines 59-60 – I don’t quite understand this sentence.

-“We wanted to explain that features of worldwide intracratonic basin are identified in the Sharan Platform.”

-Line 89 – Figure 3 appears to be called before figure 2.

-“We have changed the order of figures (see Figs. 2 and 3).”

-Lines 89-93 – This opening paragraph of the geological setting feels like it needs references.

-“This is basic geographic localisation.”

-Lines 130-132 – This reads more like results. Consider moving it.

-“Well-exposed area is the reason why we choose to use satellite images for tectonic interpretation.”

-Line 145 – Suggest providing more details of the seismic data.

-“What kind?”

-Line 171 – ‘oval’ has been mentioned quite a few times before this. Is it really necessary to mention it this often?

-“We have deleted repetition (line 106).”

-Line 258 – Suggest clarifying why the Devonian deposits are sensitive to such processes.

-Lines 534-538 – This paragraph reads more like geological setting.

-“We have placed it in geological settings paragraph (line 121-127).”

-Lines 539-549 – This description of the analyses would be better placed in the ‘Data and methods’ section.

-“We have placed it in data and methods paragraph (line 200-215).”

-Lines 551-554 – The geological setting section might be more appropriate for this information.

-“We have placed it in data and methods paragraph (line 121-127).”

**Influence of basement heterogeneity on the architecture of low subsidence rate Paleozoic intracratonic basins (Reggane, Ahnet, Mouydir and Illizi basins, Hoggar massif)**

Paul Perron<sup>1</sup>, Michel Guiraud<sup>1</sup>, Emmanuelle Vennin<sup>1</sup>, Isabelle Moretti<sup>2</sup>, Éric Portier<sup>3</sup>, Laetitia Le Pourhiet<sup>4</sup>, Moussa Konaté<sup>5</sup>

<sup>1</sup>Université de Bourgogne Franche-Comté, Centre des Sciences de la Terre, UMR CNRS 6282 Biogéosciences, 6 Bd Gabriel, 21000 Dijon, France.

<sup>2</sup>ENGIE, Département Exploration & Production, 1, place Samuel de Champlain, Faubourg de l'Arche, 92930 Paris La Défense, France.

<sup>3</sup>NEPTUNE Energy International S.A., 9-11 Allée de l'Arche – Tour EGEE – 92400 Courbevoie, France.

<sup>4</sup>Sorbonne Université, CNRS-INSU, Institut des Sciences de la Terre Paris, ISTeP UMR 7193, F-75005 Paris, France.

<sup>5</sup>Département de Géologie, Université Abdou Moumouni de Niamey, BP :10662, Niamey, Niger.

Corresponding author: paul.perron@u-bourgogne.fr, paul.perron@hotmail.fr

**Abstract**

The Paleozoic intracratonic North African Platform is characterized by an association of arches (ridges, domes, swells or paleo-highs) and low subsidence rate syncline basins of different wavelengths (75–620 km). In the Reggane, Ahnet, and Mouydir and Illizi basins are successively delimited from east to west by the Amguid El Biod, Arak-Foum Belrem, and Azzel Matti arches, ~~bounded by inherited Precambrian sub-vertical fault systems which were repeatedly reactivated or inverted during the Paleozoic.~~ Major unconformities are related to several tectonic events such as the Cambrian-Ordovician extension, Ordovician-Silurian

~~glacial rebound, Silurian–Devonian “Caledonian” extension/compression, late Devonian extension/compression, and “Hercynian” compression.~~ Through the analysis of new unpublished geological data (i.e. satellite images, well-logs, seismic lines), the deposits associated with these arches and syncline basins exhibit thickness variations and facies changes ranging from continental to marine environments. The arches are characterized by thin amalgamated deposits with condensed and erosional surfaces, whereas the syncline basins exhibit thicker and well-preserved successions. In addition, the vertical facies succession evolves from thin Silurian to Givetian deposits into thick Upper Devonian sediments. Synsedimentary structures and major unconformities are related to several tectonic events such as the Cambrian–Ordovician extension, Ordovician–Silurian glacial rebound, Silurian–Devonian “Caledonian” extension/compression, late Devonian extension/compression, and “Hercynian” compression. ~~Synsedimentary deformations are evidenced by wedges, truncations, and divergent onlaps.~~ Locally, deformation is characterized by near-vertical planar normal faults responsible for horst and graben structuring associated with folding during the Cambrian–Ordovician–Silurian period. These structures may have been inverted or reactivated during the Devonian (i.e. Caledonian, Mid-Late Devonian) compression and the Carboniferous (i.e. pre-Hercynian to Hercynian).

Additionally, basement characterization from geological and geophysics data (aeromagnetic and gravity maps), shows an interesting age-dependent zonation of the terranes which are bounded by mega shear zones with the arches-basins framework. The “old” terranes are situated under arches while the “young” terranes are located under the basins depocenter. This structural framework results from the accretion of Archean and Proterozoic terranes inherited from during the Pan-African former orogeny (e.g. Pan-African orogeny (750–580 900–520 Ma).

So, the sedimentary infilling pattern and the nature of deformation result from the slow Paleozoic repeatedly reactivation of Precambrian terranes bounded by sub-vertical lithospheric

fault ~~zones~~ systems. Alternating periods of tectonic quiescence and low-rate subsidence acceleration associated with extension and local inversion tectonics correspond to a succession of Paleozoic geodynamic events (i.e. far-field orogenic belt, glaciation).

Keywords: intracratonic basin, Paleozoic, arches, low-rate subsidence, tectonic heritage, terranes, Central Sahara

## 1 Introduction

Paleozoic deposits fill numerous intracratonic basins, which may also be referred to as “cratonic basins”, “interior cratonic basins”, or “intracontinental sags”. Intracratonic basins are widespread around the world (~~see Fig. 6~~ from Heine et al., 2008) and exploration for non-conventional petroleum has revived interest in them. They are located in “stable” lithospheric areas and share several common features (Allen and Armitage, 2011): ~~such as~~ Their geometries are (i.e. large circular, elliptical, saucer-shaped to oval), Their stratigraphy is (i.e. filled with continental to shallow-water sediments), ~~Their low subsidence rate of sedimentation (an average of 7 m/Myr), there is low (5 to 50 m/Ma) and long-term subsidence~~ (sometimes more than 540 Myr), ~~and~~ Their structural framework shows (reactivation of structures and emergence of arches also referred to in the literature as “ridges”, “paleo-highs”, “domes”, and “swells”). Multiple hypotheses and models have been proposed to explain how these slowly subsiding, long-lived intracratonic basins formed and evolved (see Allen and Armitage, 2011 and references therein or Hartley and Allen, 1994). However, their tectonic and sedimentary architectures are often poorly constrained.

The main specificities of intracratonic basins are found on the Paleozoic North Saharan Platform. The sedimentary infilling during c. 250 Myr is relatively thin (i.e. around a few hundred to a few thousand meters), of great lateral extent (i.e. ~~16~~ 9 million km<sup>2</sup>), and is

separated by major regional unconformities (Beuf et al., 1968a, 1971; Carr, 2002; Eschard et al., 2005, 2010; Fabre, 1988, 2005; Fekirine and Abdallah, 1998; Guiraud et al., 2005; [Kracha, 2011](#); Legrand, 2003a). Depositional environments were mainly continental to shallow-marine and homogeneous. Very slow and subtle lateral variations occurred over time (Beuf et al., 1971; Carr, 2002; Fabre, 1988; Guiraud et al., 2005; Legrand, 2003a). The Paleozoic North Saharan Platform is arranged (Fig. 1) into an association of long-lived broad synclines (i.e. basins [or sub-basins](#)) and anticlines (i.e. arches ~~swells, domes, highs, or ridges~~) of different wavelengths ( $\lambda$ : 75–620 km). Burov and Cloetingh (2009) report deformation wavelengths of the order of 200–600 km when the whole lithosphere is involved and of 50–100 km when the crust is decoupled from the lithospheric mantle. This insight suggests that the inherited basement fabric influences [intracratonic](#) basin architecture at a large scale. [Besides, pre-existing structures, such as shear zones and terrane suture zones, are present throughout the lithosphere, affecting the geometry and evolution of upper-crustal structural framework forming during later tectonic events \(Peace et al., 2018; Phillips et al., 2018\). Intracratonic basins are affected by basement involved faults which are often reactivated in response to tectonic pulses \(Beuf et al., 1971; Boote et al., 1998; Eschard et al., 2010; Fabre, 1988; Frizon de Lamotte et al., 2013; Galeazzi et al., 2010; Guiraud et al., 2005; Wendt et al., 2006\).](#)

In this study of the [Reggane](#), Ahnet, ~~and~~ Mouydir [and Illizi](#) basins, a multidisciplinary workflow involving various tools (e.g. seismic profiles, satellite images) and techniques (e.g. photo-geology, seismic interpretation, well correlation, geophysics, geochronology) has enabled us to (1) make a tectono-sedimentary analysis, (2) determine the spatial arrangement of depositional environments calibrated by biostratigraphic zonation, (3) characterize basin geometry, and (4) ascertain the inherited architecture of the basement and its tectonic evolution. We propose a conceptual coupled model explaining the architecture of the intracratonic basins of the North Saharan Platform. This model highlights the role of basement heritage heterogeneities in an

accreted mobile belt and their influence on the structure and evolution of intracratonic basins. It is a first step towards a better understanding of the factors and mechanisms that drive intracratonic basins.

## **2 Geological setting: The Paleozoic North Saharan Platform and the Reggane, Ahnet, and Mouydir and Illizi basins**

The Reggane, Ahnet, ~~and~~ Mouydir and Illizi basins (Figs 1 and 3 2) are located in south-western Algeria, north-west of the Hoggar massif (Ahaggar). They are ~~N-S oval~~ depressions filled by Paleozoic deposits. The basins are bounded to the south by the Hoggar massif (Tuareg Shield), ~~to the west by the Azzel Matti arch, to the east by the Amguid El Biod arch~~ and they are separated ~~from together~~ by the Azzel Matti, the Arak-Foum Belrem the Amguid El Biod arches.

Figure 2 3 synthesizes the lithostratigraphy, the large-scale sequence stratigraphic framework delimited by ~~five~~ six main regional unconformities (A to F), and the tectonic events proposed in the literature (cf. references under Fig. 2 3) affecting the Paleozoic North Saharan Platform.

During the Paleozoic, the Reggane, Ahnet, ~~and~~ Mouydir and Illizi basins were part of a set of the super-continent Gondwana (Fig. 1). This super-continent resulted from the collision of the West African Craton (WAC) and the East Saharan Craton (ESC), sandwiching the Tuareg Shield (TS) mobile belt during the Pan-African orogeny (Craig et al., 2008; Guiraud et al., 2005; Trompette, 2000). This orogenic cycle followed by the chain's collapse (c. 1000–525 Ma) was also marked by phases of oceanization and continentalization (c. 900–600 Ma) giving rise to the heterogeneous terranes in the accreted mobile belt (Trompette, 2000). The Hoggar shield massif is composed of several accreted, sutured, and amalgamated terranes of various ages and compositions resulting from multiple phases of geodynamic events (Bertrand and Caby, 1978; Black et al., 1994; Caby, 2003; Liégeois et al., 2003). Twenty-three well preserved terranes in the Hoggar were identified and grouped into Archean, Paleoproterozoic, and

Mesoproterozoic–Neoproterozoic juvenile Pan-African terranes (see legend in Fig. 1). In the West African Craton, the Reguibat shield is composed of Archean terrains in the west and of Paleoproterozoic terranes in the east (Peucat et al., 2003, 2005).

Then, there is evidence of a complex and polyphased history throughout the Paleozoic (Fig. 2 3), with alternating periods of quiescence and tectonic activity, individualizing and rejuvenating ancient NS, NE–SW, or NW–SE structures in arch and basin configurations (Badalini et al., 2002; ~~Benmacef et al., 1971; Beuf et al., 1968b, 1971;~~ Boote et al., 1998; Boudjema, 1987; ~~Chavand and Clareaq, 1960;~~ Coward and Ries, 2003; Craig et al., 2008; ~~Eschard et al., 2005, 2010; Fabre, 1988, 2005; Frizon de Lamotte et al., 2013;~~ Guiraud et al., 2005; Logan and Duddy, 1998; Lüning, 2005; ~~Wendt et al., 2006~~). The Paleozoic successions of the North Saharan Platform are predominantly composed of siliciclastic detrital sediments (Beuf et al., 1971; Eschard et al., 2005). They form the largest area of detrital sediments ever found on continental crust (Burke et al., 2003), dipping gently NNW (Beuf et al., 1971, 1969; Fabre, 1988, 2005; Fröhlich et al., 2010; Gariel et al., 1968; Le Heron et al., 2009). Carbonate deposits are observed from the Mid–Late Devonian to the Carboniferous (Wendt, 1985, 1988, 1995; Wendt et al., 1993, 1997, 2006, 2009a; Wendt and Kaufmann, 1998). From south to north, the facies progressively evolve from continental fluvial to shallow marine (i.e. upper to lower shoreface) and then to offshore facies (Beuf et al., 1971; Carr, 2002; Eschard et al., 2005, 2010; Fabre, 1988, 2005; Fekirine and Abdallah, 1998; ~~Guiraud et al., 2005;~~ Legrand, 1967a).

### **3 Data and methods**

A multidisciplinary approach has been used in this study integrating new data (i.e. satellite images, seismic lines and well-logs data) in particular from the Reggane, Ahnet, Mouydir, Illizi basins and Hoggar massif (~~see supplementary data 1 Fig. 4~~):

~~–Geographic Information System analysis (GIS);~~

~~–The basins and the main geological structures were identified from Landsat satellite images;~~

~~–Seismic section interpretation;~~

~~–Sedimentological and well-log analysis;~~

~~–Biostratigraphy and sequence stratigraphy;~~

~~–Geochronology and geophysical data.~~

The Paleozoic series of the Ahnet and Mouydir basins are well-exposed over an area of approximately 170,000 km<sup>2</sup> and are well observed in satellite images (Google Earth and Landsat from USGS). Furthermore, a significant geological database (i.e. wells, seismic records, ~~field-trips~~, geological reports) has been compiled in the course of petroleum exploration since the 1950s. The sedimentological dataset is based on the integration and analysis of cores, outcrops, well-logs, and of lithological and biostratigraphic data. They were synthesized from internal SONATRACH (Dokka, 1999), IFP-SONATRACH consortium reports (Eschard et al., 1999), and published articles (Beuf et al., 1971; Biju-Duval et al., 1968; Wendt et al., 2006). Facies described from cores and outcrops of these studies were grouped into facies associations corresponding to the main depositional environments observed on the Saharan Platform (Table 1). Characteristic gamma-ray patterns (electrofacies) are proposed to illustrate the different facies associations. The gamma-ray (GR) peaks are commonly interpreted as the maximum flooding surfaces (MFS) (e.g. Catuneanu et al., 2009; Galloway, 1989; Milton et al., 1990; Serra and Serra, 2003). Time calibration of well-logs ~~and outcrops~~ is based on palynomorphs (essentially Chitinozoans and spores) and outcrops on conodonts, goniatites, and brachiopods (Wendt et al., 2006). Palynological data of wells (W1, W7, W12, W19 and W20) from internal unpublished data (Abdesselam-Rouighi, 1991; Azzoune, 1999; Hassan, 1984; Khier, 1974) are based on biozonations from Magloire, (1967) and Boumendjel et al., (1988). Well W18 is supported by palynological data and biozonations from Hassan Kermadjji et al., (2008).

Synsedimentary extensional and compressional markers are characterized in this structural framework based on the analyses of satellite images (Figs 4 5 and 5 6), seismic profiles (Fig. 6 7), 21 wells (W1 to W21), and 12 outcrop cross-sections (O1 to O12). Wells and outcrop sections are arranged into three E–W sections (Figs 9 10, 10 11 and ~~supplementary data 2 12~~) and one N–S section (~~supplementary data 3~~ Fig. 13). Satellite images (Figs 4 5 and 5 6) and seismic profiles (Fig. 6 7) are located at key areas (i.e. near arches) illustrating the relevant structures (Fig. 3 2). The calibration of the key stratigraphic horizon on seismic profiles (Figs ~~7 9 and 10~~) was settled by sonic well-log data using PETREL and OPENDTECT software. Nine key horizons easily extendable at the regional scale are identified and essentially correspond to major depositional unconformities: near top Infra-Cambrian, near top Ordovician, near top Silurian, near top Pragian, near top Givetian, near top mid-Frasnian, near top Famennian, ~~top~~ near base Quaternary and ~~top~~ near Hercynian unconformities (Figs ~~7 9 and 10~~). The stratigraphic layers are identified by the integration of satellite images (Google Earth and Landsat USGS: <https://earthexplorer.usgs.gov/>), digital elevation model (DEM) and the 1:200,000 geological maps of Algeria (Bennacef et al., 1974; Bensalah et al., 1971).

Subsidence analysis characterizes the vertical displacements of a given sedimentary depositional surface by tracking its subsidence and uplift history (Van Hinte, 1978). The resulting curve details the total subsidence history for a given stratigraphic column (Allen and Allen, 2005; Van Hinte, 1978). Backstripping is also used to restore the initial thicknesses of a sedimentary column (Allen and Allen, 2005; Angevine et al., 1990). Lithologies and paleobathymetries have been defined using facies analysis or literature data. Porosity and the compaction proxy are based on experimental data from (Sclater and Christie, 1980). In this study, subsidence analyses were performed on sections using OSXBackstrip software performing 1D Airy backstripping (after Allen and Allen, 2005; Watts, 2001); available at: <http://www.ux.uis.no/neslor/work/programs.html>).

The 800 km<sup>2</sup> outcrop of basement rocks of the Hoggar ~~shield~~ ~~massif~~ provides an exceptional case ~~study~~ of an exhumed mobile belt composed of accreted terranes of different ages. To reconstruct the nature of the basement, a terrane map (Fig. 15 and 16) was put together by integrating geophysical data (aeromagnetic anomaly map: <https://www.geomag.us/>, Bouguer gravity anomaly map: <http://bgi.omp.obs-mip.fr/>), satellite images (7ETM+ from Landsat USGS: <https://earthexplorer.usgs.gov/>) data, geological maps (Berger et al., 2014; Bertrand and Caby, 1978; Black et al., 1994; Caby, 2003; Fezaa et al., 2010; Liégeois et al., 1994, 2003, 2005, 2013), and geochronological data (e.g. U-Pb radiochronology, see supplementary data 5 1). Geochronological data from published studies were compiled and georeferenced (Fig. 1). Thermo-tectonic ages were grouped into eight main thermo-orogenic events (Fig. 1): The Liberian-Ouzzalian event (Arcehan, >2500 Ma), (the Archean, Eburnean (i.e. Paleoproterozoic, 2500-1600 Ma), the Kibarian (i.e. Mesoproterozoic, 1600-1100 Ma), the Neoproterozoic oceanization-rifting (1100-750 Ma), the ~~Neoproterozoic~~ syn-Pan-African orogeny (i.e. Neoproterozoic, 750-541 Ma), the post-Pan-African (i.e. Neoproterozoic, 541-443 Ma), the Caledonian orogeny (i.e. Siluro-Devonian, 443-358 Ma), and the Hercynian orogeny (i.e. Carbo-Permian, 358-252 Ma).

#### **4 Structural framework and tectono-sedimentary structure analyses**

The structural architecture of the North Saharan Platform (~~Fig. 1~~) is characterized by ~~an~~ ~~association of syncline basins and anticlines (i.e. arches, domes, etc.). The basins (or sub-basins) are~~ mostly circular to oval ~~shaped~~. ~~They are bounded by arches which correspond to the mainly N-S Azzel Matti, Arak Foum Belrem, Amguid El Biod, and Tihemboka arches, the NE-SW Bou Bernous, Ahara, and Gargaf arches, and the NW-SE Saoura and Azzene arches (Fig. 1).~~ The basins ~~are~~ structured by major faults frequently associated with broad asymmetrical folds displayed by three main trends (Fig. 1): (1) near-N-S, varying from N0° to N10° or N160°, (2) from N40° to 60°, and (3) N100° to N140° directions (Figs 1, 3A, and 4).

These fault zones are about 100 km (e.g. faults F1 and F2, Fig. 4 5) to tens of kilometers ~~lengths~~ long (e.g. faults F3 to F8, Fig. 4 5). They correspond to the mainly N–S Azzel-Matti, Arak-Foum Belrem, Amguid El Biod, and Tihemboka arches, the NE–SW Bou Bernous, Ahara, and Gargaf arches, and the NW–SE Saoura and Azzene arches (Fig. 1).

#### 4.1 Syntectonic extensional markers

Extensional markers are characterized by the settlement of steeply west- or eastward-dipping basement normal faults associated with colinear syndepositional folds of several kilometers in length (e.g. Fig. ~~6A to E~~ ~~5A–A', 5B–B', 5C–C', 5E–E'~~ and ~~6 7A~~), represented by footwall anticline and hanging wall syncline-shaped forced folds. They are located in the vicinity of different arches (Fig. 3 2) such as the Tihemboka arch (Figs ~~45BB', 5A–A'~~ and ~~56A–B–B'~~), Arak-Foum Belrem arch (Figs ~~4 5A–A', 5 6C–C'~~ to ~~5 6F–F'~~ and ~~6 7A, 6 7C~~), Azzel Matti arch (Fig. ~~6 7B~~), and Bahar El Hamar area intra-basin arch (Fig. ~~6 7D~~). These tectonic structures can be featured by basement blind faults (e.g. ~~fault F5 in Fig. 5 6C–C', fault F1 in Figs 5D–D', 5E–E', and 6A~~ fault F1 in Fig. 7A). The deformation pattern is mainly characterized by brittle faulting in Cambrian–Ordovician series down to the basement and fault-damping in Silurian series (e.g. ~~fault F2 in Fig. 5AA'~~, faults F1 to F6 in Fig. ~~6 7B~~). The other terms of the series (i.e. Silurian to Carboniferous) are usually affected by folding except (see F1 faults in Figs ~~5 6F–F', 6 7B, 6 7D and 6 7C~~) where the brittle deformation can be propagated to the Upper Devonian (due to reactivation and/or inversion as suggested in the next paragraph).

In association with the extensional markers, thickness variations and tilted divergent onlaps of the sedimentary series (i.e. wedge-shaped units, progressive unconformities) in the hanging wall syncline of the fault escarpments are observed (Figs ~~5 6~~ and ~~6 7~~). These are attested using photogeological analysis of satellite images (Fig. ~~5 6~~) and are marked by a gentler dip angle of the stratification planes away from the fault plane (i.e. fault core zone). The markers of

syndepositional deformation structures are visible in the hanging-wall synclines of Precambrian to Upper Devonian series (Figs [5 6](#) and [6 7](#)).

The footwall anticline and hanging-wall syncline-shaped forced folds recognized in this study are very similar to those described in the literature by Grasemann et al., (2005); Khalil and McClay, (2002); Schlische, (1995); Stearns, (1978); Withjack et al., (1990), (2002); Withjack and Callaway, (2000). The wedge-shaped units (DO0 to DO3; Figs [4 5](#), [5 6](#) and [6 7](#)) associated with the hanging-wall synclines are interpreted as synsedimentary normal fault-related folding. The whole tectonic framework forms broad extensional horsts and graben related to synsedimentary forced folds controlling basin shape and sedimentation ([Figs 4, 5 and 6](#)).

Following Khalil and McClay, (2002); Lewis et al., (2015); Shaw et al., (2005); Withjack et al., (1990), we use the ages of the growth strata (i.e. wedge-shaped units) to determine the timing of the deformation. The main four wedge-shaped units identified (DO0 to DO3) are indicative of the activation and/or reactivation of the normal faults (extensional settings) during Neoproterozoic ([DO0](#)), Cambrian–Ordovician ([DO1](#)), Early to Mid Silurian ([DO2](#)) and Mid to Late Devonian ([DO3](#)) times.

In planar view, straight (F1 in Fig. [4 5A–A'](#)) and sinuous faults (F2, F3, F3', F4, F4', and F5 in Fig. [4 5AA'](#)) can be identified. The sinuous faults are arranged “en echelon” into several segments with relay ramps. These faults are 10 to several tens of kilometers long with vertical throws of hundreds of meters that fade rapidly toward the fault tips. The sinuous geometry of normal undulated faults as well as the rapid lateral variation in fault throw are controlled by the propagation and the linkage of growing parent and tip synsedimentary normal faults (Marchal et al., 2003, 1998; [Fig. 4A–A'](#)). We use the stratigraphic age of impacted layers (here Tamadjert Fm.) to date (re)activation of the faults.

According to Holbrook and Schumm, (1999), river patterns are extremely sensitive to tectonic structure activity. Here we find that the synsedimentary activity of the extensional structures is also evidenced by the influence of the fault scarp on the distribution and orientation of sinuous channelized sandstone body systems (dotted red lines in Fig. 4 ~~5B-B'~~). It highlights the (re)activation of the faults during the deposition of these channels, i.e. late Hirnantian dated by (Girard et al., 2012).

#### **4.2 Synsedimentary compressional markers (inversion tectonics)**

After the development of the extensional tectonism described previously, evidence of synsedimentary compressional markers can be identified. These markers are located and preferentially observable near the Arak-Foum Belrem arch (Fig. 5 ~~6F-F'~~, F2 in Fig. 6 ~~7C~~), the Azzel Matti arch (2 in Figs 6 ~~7B~~), and the Bahar El Hamar area intra-basin arch (2 in Fig. 6 ~~7D~~). The tectonic structures take the form of inverse faulting reactivating former basement faults (F1' in Fig. 5 ~~6F-F'~~, F1 in Fig. 6 ~~7C~~, F1' in Fig. 6 ~~7D~~, F1 in Fig. 6 ~~7B~~). The synsedimentary inverse faulting is demonstrated by the characterization of asymmetric anticlines especially observable in satellite images and restricted to the fault footwalls (Figs 4 ~~5A-A'~~ along F1-F2).

Landsat image analysis combined with the line drawing of certain seismic lines reveals several thickness variations reflecting divergent onlaps (i.e. wedge-shaped units) which are restricted to the hanging-wall asymmetric anticlines (2 in Figs 5 ~~6F-F'~~, 6 ~~7B~~, 6 ~~7C~~ and 6 ~~7D~~). The compressional synsedimentary markers clearly post-date extensional divergent onlaps at hanging-wall syncline-shaped forced folds (1 in Figs 6 ~~7B~~, 6 ~~7C~~ and 6 ~~7D~~). This architecture is very similar to classical positive inversion structures of former inherited normal faults (Bellahsen and Daniel, 2005; Bonini et al., 2012; Buchanan and McClay, 1991; Ustaszewski et al., 2005). Tectonic transport from the paleo-graben hanging-wall toward the paleo-horst

footwall (F1, F2-F2', F4-F4' in Fig. 6 7B; F1-F1' in Fig. 6B 7D) is evidenced. Further positive tectonic inversion architecture is identified by tectonic transport from the paleo-horst footwall to the paleo-graben hanging wall (F1-F1' in Fig. 5 6F-F'; F1, F5, and F6 in Fig. 6 7C). This second type of tectonic inversion is very similar to the transported fault models defined by (Butler, 1989; Madritsch et al., 2008). The local positive inversions of inherited normal faults occurred during Silurian–Devonian (F4' Fig. 6 7B) and Mid to Late Devonian times (Figs 6 7B, 6 7C and 6 7D). A late significant compression event between the end of the Carboniferous and the Early Mesozoic was responsible for the exhumation and erosion of the tilted Paleozoic series. This series is related to the Hercynian angular unconformity surface (Fig. 6 7B).

## 5 Stratigraphy and sedimentology

The whole sedimentary series described in the literature is composed ~~of fluvatile Cambrian of fluvatile to Braid-deltaic plain Cambrian, not only fluvatile (e.g. Brahmaputra River analogue), with a transitional facies from continental to shallow marine~~ (Beuf et al., 1968b, 1968a, 1971; Eschard et al., 2005, 2010; Sabaou et al., 2009), ~~glacial–Ordovician Upper Ordovician glaciogenic deposits~~ (Beuf et al., 1968a, 1968b, 1971; Eschard et al., 2005, 2010), ~~argillaceous deep marine Silurian argillaceous deep marine Silurian deposits~~ (Djouder et al., 2018; Eschard et al., 2005, 2010; Legrand, 1986, 2003b; Lüning et al., 2000) and offshore to embayment Carboniferous deposits (Wendt et al., 2009). In this complete sedimentary succession, we have focused on the Devonian deposits as they are very sensitive to and representative of basin dynamics. The architecture of the Devonian deposits allows us to approximate the main forcing factors controlling the sedimentary infilling of the basin and its syndepositional deformation. ~~Nine~~ Eleven facies associations organized into four depositional environments (Table 1) are defined to reconstruct the architecture and the lateral and vertical sedimentary evolution of the basins (Figs 9 10, 10 11, supplementary data 2 and 3 12 and 13).

## 5.1 Facies association, depositional environments, and erosional unconformities

Based on the compilation and synthesis of internal studies (Eschard et al., 1999), published papers on the ~~Algerian platform~~ Saharan platform (Beuf et al., 1971; Eschard et al., 2005, 2010; Henniche, 2002) and on the Ahnet and Mouydir basins (Biju-Duval et al., 1968; Wendt et al., 2006) ~~plus the present study~~, eleven main facies associations (AF1 to AF5) and four depositional environments are proposed for the Devonian succession (Table 1). They are associated with their gamma-ray responses (Figs [7](#) [8](#) and [8](#) [9](#)). They are organized into two continental/fluvial (AF1 to AF2), four transitional/coastal plain (AF3a to AF3d), three shoreface (AF4a to AF4c), and two offshore (AF5a to AF5b) sedimentary environments.

### 5.1.1 Continental fluvial environments

This depositional environment features the AF1 (fluvial) and the AF2 (flood plain) facies association (Table 1). Facies association AF1 is mainly characterized by a thinning-up sequence with a basal erosional surface and trough cross-bedded intraformational conglomerates with mud clast lag deposits, quartz pebbles, and imbricated grains (Table 1). It passes into medium to coarse trough cross-bedded sandstones, planar cross-bedded siltstones, and laminated shales. These deposits are associated with rare bioturbations (except at the surface of the sets), ironstones, phosphorites, corroded quartz grains, and phosphatized pebbles. Laterally, facies association AF2 is characterized by horizontally laminated and very poorly sorted silt to argillaceous fine sandstones. They contain frequent root traces, plant debris, well-developed paleosols, bioturbations, nodules, and ferruginous horizons. Current ripples and climbing ripples are associated in prograding thin sandy layers.

In AF1, the basal erosional reworking and high energy processes are characteristic of channel-filling of fluvial systems (Allen, 1983; Owen, 1995). Eschard et al., (1999) identify three fluvial systems (see A, B, and C in Fig. [8](#) [9](#)) in the Tassili-N-Ajjers outcrops: braided dominant (AF1a),

meandering dominant (AF1b), and straight dominant (AF1c). They differentiate them by their different sinuosity, directions of accretion (lateral or frontal), the presence of mud drapes, bioturbations, and giant epsilon cross-bedding. Gamma-ray signatures of these facies associations (A, B, and C in Fig. 8 9) are cylindrical with an average value of 20 gAPI. The gamma ray shapes are largely representative of fluvial environments (Rider, 1996; Serra and Serra, 2003; Wagoner et al., 1990). The bottom is sharp with high value peaks and the tops are frequently fining-up, which may be associated with high values caused by argillaceous flood plain deposits and roots (Eschard et al., 1999). AF2 is interpreted as humid floodplain deposits (Allen, 1983; Owen, 1995) with crevasse splays or preserved levees of fluvial channels (Eschard et al., 1999). Gamma-ray curves of AF2 (D, Fig. 8 9) show a rapid succession of low to very high peak values, ranging from 50 to ~~200~~ 120 gAPI. AF1 and AF2 are typical of the Pragian “Oued Samene” Formation (Wendt et al., 2006). In the Illizi basin, these facies are mainly recorded in the ~~Cambrian~~ Ajjers Formation ([dated Upper Cambrian? to Ordovician see Fabre, 2005; Vecoli, 2000; Vecoli et al., 1995, 1999, 2008; Vecoli and Playford, 1997](#)) and the Lochkovian to Pragian ~~“Middle-Barre”~~ [“Barre Moyenne”](#) and ~~“Upper-Barre”~~ [“Barre Supérieure”](#) Formations (Beuf et al., 1971; Eschard et al., 2005).

### 5.1.2 Transitional coastal plain environments

This depositional environment comprises facies associations AF3a (delta/estuarine), AF3b (fluvial/tidal distributary channels), AF3c (tidal sand flat), AF3d (lagoon/mudflat) (table 1). AF3a is mainly dominated by sigmoidal cross-bedded heterolithic rocks with mud drapes. It is also characterized by fine to coarse, poorly sorted sandstones and siltstones often structured by combined flow ripples, flaser bedding, wavy bedding, and some rare planar bedding. Mud clasts, root traces, desiccation cracks, water escape features, and shale pebbles are common. The presence of epsilon bedding is attested, which is formed by lateral accretion of a river point bar (Allen, 1983). The bed surface sets are intensively bioturbated (*Skolithos* and *Planolites*)

indicating a shallow marine subtidal setting (Pemberton and Frey, 1982). Faunas such as brachiopods, trilobites, tentaculites, and graptolites are present. AF3b exhibits a fining-up sequence featured by a sharp erosional surface, trough cross-bedded, very coarse-grained, poorly sorted sandstone at the base and sigmoidal cross-bedding at the top (Figs 7 8 and 8 9). AF3c is formed by fine-grained to very coarse-grained sigmoidal cross-bedded heterolithic sandstones with multidirectional tidal bundles. They are also structured by lenticular, flaser bedding and occasional current and oscillation ripples with mud cracks. They reveal intense bioturbation composed of *Skolithos* (Sk), *Thalassinoides* (Th), and *Planolites* (Pl) ichnofacies indicating a shallow marine subtidal setting (Frey et al., 1990; Pemberton and Frey, 1982). AF4d is characterized by horizontally laminated mudstones associated with varicolored shales and fine-grained sandstones. They exhibit mud cracks, occasional wave ripples, and rare multidirectional current ripples. These sedimentary structures are poorly preserved because of intense bioturbation composed of *Skolithos* (Sk), *Thalassinoides* (Th), and *Planolites* (Pl). Fauna includes ammonoids (rare), goniatites, calymenids, pelecypod molds, and brachiopod coquinas.

In AF3a, both tidal and fluvial systems in the same facies association can be interpreted as an estuarine system (Dalrymple et al., 1992; Dalrymple and Choi, 2007). The gamma-ray signature is characterized by a convex bell shape with rapidly alternating low to ~~high~~ mid values (30 to 60 gAPI) due to the mud draping of the sets (see E Fig. 8 9). These forms of gamma ray are typical of fluvial-tidal influenced environments with upward-fining parasequences (Rider, 1996; Serra and Serra, 2003; Wagoner et al., 1990). AF3a is identified at the top of the Pragian “Oued Samene” Formation and in Famennian “Khenig” Formation (Wendt et al., 2006) in the Ahnet and Mouydir basins. In the Illizi basin, AF3a is mostly recorded at the top Cambrian of the Ajjers Formation, in the Lochkovian ~~“Middle-bar”~~ “Barre Moyenne”, and at the top Pragian of the ~~“Upper-bar”~~ “Barre Supérieure” Formation (Beuf et al., 1971; Eschard et al., 2005). The

AF3b association can be characterized by a mixed fluvial and tidal dynamic based on criteria such as erosional basal contacts, fining-upward trends or heterolythic facies (Dalrymple et al., 1992; Dalrymple and Choi, 2007). They are associated with abundant mud clasts, mud drapes, and bioturbation indicating tidal influences (Dalrymple et al., 1992, 2012; Dalrymple and Choi, 2007). The major difference with the estuarine facies association (AF3a) is the slight lateral extent of the channels which are only visible in outcrops (Eschard et al., 1999). The gamma-ray pattern is very similar to the estuarine electrofacies (see F Fig. 8 9). AF3c is interpreted as a tidal sandflat laterally present near a delta (Lessa and Masselink, 1995) and associated with an estuarine environment (Leuven et al., 2016). The gamma-ray signature (see G Fig. 8 9) is distinguishable by its concave funnel shape with alternating low and **high mid** peaks (25 to 60 gAPI) due to the heterogeneity of the deposits and rapid variations in the sand/shale ratio. These facies are observed in the ~~“Tigillites–Talus”~~ “Talus à Tigillites” Formation of the Illizi basin (Eschard et al., 2005). In AF4d, both ichnofacies and facies are indicative of tidal mudflat/lagoonal depositional environments (Dalrymple et al., 1992; Dalrymple and Choi, 2007; Frey et al., 1990). The gamma-ray signature has a distinctively high value (80 to 130 gAPI) and an erratic shape (see H Fig. 8 9). AF4d is observed in the “Atafaita fa” Formation and in the Emsian prograding shoreface sequence of the Illizi basin (Eschard et al., 2005). It is also recorded in the Lochkovian “Oued Samene” Formation and the Famennian “Khenig” Sandstones (Wendt et al., 2006).

### **5.1.3 Shoreface environments**

This depositional environment is composed of AF4a (subtidal), AF4b (upper shoreface), and AF4c (lower shoreface) facies associations (Table 1). AF4a is characterized by the presence of brachiopods, crinoids, and diversified bioturbations, by the absence of emersion, and by the greater amplitude of the sets in a dominant mud lithology (Eschard et al., 1999). AF4b is heterolithic and composed of fine to medium-grained sandstones (brownish) interbedded with

argillaceous siltstones and bioclastic carbonated sandstones. Sedimentary structures include oscillation ripples, swaley cross-bedding, flaser bedding, cross-bedding, convolute bedding, wavy bedding, and low-angle planar cross-stratification. Sediments were affected by moderate to highly diversified bioturbation by *Skolithos* (Sk), *Cruziana*, *Planolites*, (Pl) *Chondrites* (Ch), *Teichichnus* (Te), *Spirophytons* (Sp) and are composed of ooids, crinoids, bryozoans, stromatoporoids, tabulate and rugose corals, pelagic styliolinids, neritic tentaculitids, and brachiopods. AF4c can be distinguished by a low sand/shale ratio, thick interbeds, abundant HCS, deep groove marks, slumping, and intense bioturbation (Table 1).

AF4a is interpreted as a lagoonal shoreface. The gamma-ray pattern (see I Fig. 8 9) is characterized by a concave bell shape influenced by a low sand/shale ratio with values fluctuating between 100 and 200 gAPI. AF4a is identified in the ~~“Tigillites-Talus”~~ “Talus à Tigillites” Formation and the Emsian sequence of the Illizi basin (Eschard et al., 2005) and in the Lochkovian “Oued Samene” Formation (Wendt et al., 2006). AF4b is interpreted as a shoreface environment. The presence of swaley cross-bedding produced by the amalgamation of storm beds (Dumas and Arnott, 2006) and other cross-stratified beds is indicative of upper shoreface environments (Loi et al., 2010). The gamma-ray pattern (see J and K Fig. 8 9) displays concave erratic egg shapes with a very regularly decreasing-upward trend and ranging from offshore shale with high mid values (80 to 60 gAPI) to clean sandstone with lower values at the top (40 to 60 gAPI). AF4b is observed in the “Atafaitafa” Formation corresponding to the ~~“Passage-zone”~~ “Zone de passage” Formation of the Illizi basin (Eschard et al., 2005). AF4c is interpreted as a lower shoreface environment (Dumas and Arnott, 2006; Suter, 2006). The gamma-ray pattern displays the same features as the upper shoreface deposits with ~~lower~~ higher values (i.e. muddier facies) ranging from 100 to 80 gAPI (see J and K Fig. 8 9).

#### 5.1.4 Offshore marine environments

This depositional environment is composed of AF5a and AF5b facies associations (Table 1). AF5a is mainly defined by wavy to planar-bedded heterolithic silty-shales interlayered with fine-grained sandstones. It also contains bundles of skeletal wackestones and calcareous mudstones. The main sedimentary structures are lenticular sandstones, rare hummocky cross-bedding (HCS), mud mounds, low-angle cross-bedding, tempestite bedding, slumping, and deep groove marks. Sediments can present rare horizontal bioturbation such as *Zoophycos* (Z), *Teichichnus* (Te), and *Planolites* (Pl). AF5b is characterized by an association of black silty shales with occasional bituminous wackestones and packstones. It is composed of graptolites, goniatites, orthoconic nautiloids, pelagic pelecypods, limestone nodules, tentaculitids, ostracods, and rare fish remains. Rare bioturbation such as *Zoophycos* (Z) is visible.

In AF5a, the occurrence of HCS, the decrease in sand thickness and grain size together with the fossil-traces bioturbation and the floro-faunal associations indicate a deeper marine environment under the influence of storms (Aigner, 1985; Dott and Bourgeois, 1982; Reading and Collinson, 2009). AF5a is interpreted as upper offshore deposits (i.e. offshore transitional).

The gamma-ray pattern is serrated and erratic with values well grouped around high values from 120 to 140 gAPI (see L Fig. 8 9). Positive peaks may indicate siltstone to sandstone ripple beds. AF5b is interpreted as lower offshore deposits (Aigner, 1985; Stow et al., 2001; Stow and Piper, 1984). Here again the gamma-ray signature is serrated and erratic with values well grouped around 140 gAPI (see L Fig. 8 9). Hot shales with anoxic conditions are characterized by gamma-ray peaks (>140 gAPI). These gamma-ray patterns are typical of offshore environments dominated by shales (Rider, 1996; Serra and Serra, 2003; Wagoner et al., 1990). AF5a and AF5b are observed in the Silurian “Graptolites-shales” “Argiles à Graptolites” Formation and the Emsian “Orsine” Formation of the Illizi basin (Beuf et al., 1971; Eschard et

al., 2005; Legrand, 1986, 2003b). The “Argiles de Mehden Yahia” and “Tematasset” “Argiles de Temertasset” shales have the same facies (Wendt et al., 2006).

## 5.2 Sequential framework and unconformities

The high-resolution facies analysis, depositional environments, stacking patterns, and surface geometries observed in the Paleozoic Devonian succession reveal at least two different orders of depositional sequences (large and medium scale, Fig. 7 8) considered as transgressive/regressive T/R (Catuneanu et al., 2009). The sequential framework proposed in Fig. 7 8B result from the integration of the vertical evolution the main surfaces (Fig. 7 8A) and the gamma-ray pattern (Fig. 8 9). The Devonian series under focus exhibits nine medium-scale sequences (D1 to D9, Fig. 7 8; Figs 9 10, 10 11, supplementary data 2 and 3 12 and 13) bounded by 10 major sequence boundaries (HD0 to HD9), and nine major flooding surfaces (MFS1 to MFS9). The correlation of the different sequences at the scale of the different basins and arches is used to build two E–W (Figs 9 10, 10 11, supplementary data 2 and 12) and one N–S (supplementary data 3 Fig. 13) cross-sections.

The result of the analysis of the general pattern displayed by the successive sequences reveal two major patterns (Figs 9 10, 12 and 10 13) limited by a major flooding surface MFS5. The first pattern extends from the Oued Samene to Adrar Morrat Formations and is dated from the Lochkovian to Givetian. D1 to D5 medium-scale sequences indicate a general proximal clastic depositional environment (dominated by fluvial to transitional and shoreface facies) with intensive lateral facies evolution. This first pattern is thin (from 500 m in the basin depocenter to 200 m around the basin rim) and with successive amalgamated surfaces on the edge of the arches between the “Passage-zone” “Zone de passage” and “Oued Samene” Formations (e.g. Figs 5 C-C’, 6A, 6C, 6D, 10 and 9 13). It is delimited at the bottom by the HD0 surface corresponding to the Silurian/Devonian boundary. D1 to D3 are composed of T-R sequences

with a first deepening transgressive trend indicative of a transition from continental to marine deposits bounded by a major MFS and evolving into a second shallowing trend from deep marine to shallow marine depositional environments. D1 to D3 thin progressively toward the edge and the continental deposits, in the central part of the basin, pass laterally into a major unconformity. The amalgamation of the surfaces and **rapid** lateral variations of facies between the Ahnet basin and Azzel Matti and Arak-Foum Belrem arches demonstrate a tectonic control related to the presence of subsiding basins and paleo-highs (i.e. arches).

D4 and D5 display the same T-R pattern with a reduced continental influence and upward decrease in lateral facies variations and thicknesses where the MFS4 marks the beginning of a marine-dominated regime in the entire area. It is identified as the early Eifelian transgression defined by Wendt et al., (2006). The D5 sequence is mainly composed of shoreface carbonates. Evidence of mud mounds preferentially located along faults are well-documented in the area for that time (Wendt et al., 1993, 1997, 2006; Wendt and Kaufmann, 1998). This change in the general pattern indicates reduced tectonic influence.

MFS5, at the transition between the two main patterns, represents a major flooding surface on the platform and is featured worldwide by deposition of “hot shales” during the early Frasnian (Lüning et al., 2003, 2004; Wendt et al., 2006).

The second pattern extends from the “**Meh**den Yahia”, “Temertasset” to “Khenig” Formations dated Frasnian to Lower Tournaisian. This pattern is composed of part of D5 to D9 medium-scale sequences. It corresponds to homogenous offshore depositional environments with no lateral facies variations. However, local deltaic (fluvio-marine) conditions are observed during the Frasnian at the Arak Foum Belrem arch (“Grès de Mehden Yahia” in Fig. 40 12). A successive alternation of shoreface and offshore deposits is organized into five medium-scale sequences (part of D5, and D6 to D9; Figs 9 10, 11 and 40 12). They in particular show some

regressive phases with the deposition of both “Grès de Mehden Yahia” and “Grès du Khnig” sandstones (bounded by HD6 and HD9). This pattern (i.e. part of D5 to D9) corresponds to the general maximum flooding (Lüning et al., 2003, 2004; Wendt et al., 2006) under eustatic control with no tectonic influences.

## **6 Subsidence and tectonic history: An association of low rate extensional subsidence and positive inversion pulses**

The backstripping approach (Fig. 44 14) was applied to five wells (W1, W5, W7, W17, and W21). The morphology of the backstripped curve and subsidence rates can provide clues as to the nature of the sedimentary basin (Xie and Heller, 2006). In intracratonic basins, reconstructed tectonic subsidence curves are almost linear to gently exponential in shape, similar to those of passive margins and rifts (Xie and Heller, 2006). The compilation of tectonic backstripped curves from several wells in peri-Hoggar basins (Fig. 44 14A, see Fig. 1 for location) and from wells in the study area (Fig. 44 14B) display low rates of subsidence (from 5 to 50 m/Myr) organized in subsidence patterns of: Inversion of the Low Rate Subsidence (ILRS type c, red line, Fig. 44 14C), Deceleration of the Low Rate Subsidence (DLRS type b, black line), and Acceleration of the Low Rate Subsidence (ALRS type a, blue line).

Each period of ILRS, DLRS, and ALRS may be synchronous among the different wells studied (see B1 to J, Fig. 44 14B) and some wells of published data (see D to J Fig. 44 14A).

The Saharan Platform is marked by a rejuvenation of basement structures, around arches (Figs 1, 2, 3, and 4 3), linked to regional geodynamic pulses during Neoproterozoic to Paleozoic times (Fig. 44 14). A compilation of the literature shows that the main geodynamic events are associated with discriminant association of subsidence patterns:

(A) Late Pan-African compression and collapse (patterns a, b, and c, A Fig. 44 14A). The Infra-Cambrian (i.e. top Neoproterozoic) is characterized by horst and graben architecture associated

with wedge-shaped unit DO0 in the basement (~~Fig. 9 and 10~~ Fig. 7). This structuring probably related to Pan-African post-orogenic collapse is illustrated by intracratonic basins infilled with volcano-sedimentary molasses series (Ahmed and Moussine-Pouchkine, 1987; Coward and Ries, 2003; Fabre et al., 1988; Oudra et al., 2005).

(B) Cambrian-Ordovician geodynamic pulse (Fig. ~~11A-B~~ 14). Highlighted by the wedge-shaped units DO1 (Figs ~~5 6A-A'~~ and ~~6 7~~), the horst-graben system is correlated with deceleration (DLRS pattern a, B1) and with local acceleration of the subsidence (ALRS pattern b, B2). The Cambrian-Ordovician extension is documented on arches (Arak-Foum Belrem, Azzel Matti, Amguid El Biod, Tihemboka, Gargaf, Murizidié, Dor El Gussa, etc.) of the Saharan Platform by synsedimentary normal faults, reduced sedimentary successions (Bennacef et al., 1971; Beuf et al., 1968b, 1968a, 1971; Beuf and Montadert, 1962; Borocco and Nyssen, 1959; Claracq et al., 1958; Echikh, 1998; Eschard et al., 2010; Fabre, 1988; Ghienne et al., 2003, 2013; Zazoun and Mahdjoub, 2011) and by stratigraphic hiatuses (Mélou et al., 1999; Oulebsir and Paris, 1995; Paris et al., 2000; Vecoli et al., 1995, 1999).

(C) Late Ordovician geodynamic pulse (i.e. Hirnantian glacial and isostatic rebound; Fig. ~~11A-B~~ 14). Late Ordovician incisions mainly situated at the hanging walls of normal faults (Fig. ~~6 7C~~ and ~~6 7D~~) are interpreted as ~~Hirnantian glacial valleys~~ Hirnantian glacial-Palaeovalleys (Le Heron, 2010; Smart, 2000) and followed by local inversion of low rate subsidence (ILRS of type c, C in Fig. ~~11A~~ 14).

(D) Silurian extensional geodynamic pulse (D, Figs ~~11A~~ 14). The Silurian post-glaciation period is featured by the reactivation and sealing of the inherited horst and graben fault system (i.e. wedge-shaped unit DO2; Figs ~~5 6B-B'~~, ~~5 6C-C'~~, ~~6 7A~~ and ~~6 7B~~). It is linked to an acceleration of the subsidence (ALRS of pattern b in Fig. ~~11A~~ 14). This tectonic extension is

documented in seismic (Najem et al., 2015) and is associated to the Silurian major transgression on the Saharan platform (e.g. Eschard et al., 2005; Lüning et al., 2000).

(E) Late Silurian to -Early Devonian geodynamic pulse (Caledonian compression; E Fig. 4A 14). Late Silurian times are marked by reactivation and local positive inversion of the former structures (Figs 5 6C-C' and 6 7B); by truncations located at fold hinges (Figs 5 6C-C' and 6 7); and by a major shift from marine to fluvial/transitional environments (e.g. Figs 10 9, 10 supplementary data 2 and 3). Backstripped curves register an inversion of the subsidence (ILRS of pattern c, in Fig. 4A 14). The Caledonian event is mentioned as related to large-scale folding or uplifted arches (e.g. the Gargaff, Tihemboka, Ahara, Murizidé-Dor el Gussa and Amguid El Biod arches) and it is associated with breaks in the series and with angular unconformities (Beuf et al., 1971; Biju-Duval et al., 1968; Boote et al., 1998; Boudjema, 1987; Boumendjel et al., 1988; Carruba et al., 2014; Chavand and Claracq, 1960; Coward and Ries, 2003; Dubois and Mazelet, 1964; Echikh, 1998; Eschard et al., 2010; Fekirine and Abdallah, 1998; Follot, 1950; Frizon de Lamotte et al., 2013; Ghienne et al., 2013; Gindre et al., 2012; Legrand, 1967b, 1967a; Magloire, 1967).

(F) Early Devonian tectonic quiescence (F Figs 4A 14). This is characterized by a deceleration of the low rate subsidence (DLRS of pattern a, F in Figs 4A 14). During this period, we have detected Emsian truncation from satellite images (Figs. 6D and 6E) and erosion and pinch out of upper Emsian to Eifelian series from well cross sections (Figs. 10, 12 and 13). In previous works, these hiatuses/gaps (i.e. Upper Lochkovian, Lower Pragian, Upper Pragian, Upper Emsian, Lower Eifelian) are observed in the Ahnet basin (Kermandji, 2007; Kermandji et al., 2003, 2008, 2009; Wendt et al., 2006), in the Illizi (Boudjema, 1987) and in the Reggane (Jäger et al., 2009).

(G and H) Middle to late Devonian geodynamic pulse (extension and local inversions, G and H Fig. 11A 14). The Mid to Late Devonian period is characterized by large wedge hiatuses and truncations associated with the reactivation of horst and graben structures and local positive inversion (OD3 in Figs ~~5 6D-D<sup>2</sup>, 6E, 6F, 6 7 and 10 to 13~~ 9, 10 supplementary data 2 and 3). This period is characterized by inversion and acceleration of low rate subsidence (patterns c and b: ILRS - ALRS, Fig. 11A 14). Some of the Middle to Late Devonian syn-tectonic structures and hiatuses (Early-Eifelian e.g. Givetian/Frasnian) are noticed in the Ahnet basin (Wendt et al., 2006), ~~in the Reggane (Jäger et al., 2009)~~, on the Amguid Ridge (~~Wendt et al., 2006~~) (Wendt et al., 2009b), in the Illizi basin (Boudjema, 1987; Chaumeau et al., 1961; Eschard et al., 2010; Fabre, 2005; Legrand, 1967a), on the Gargaf (Carruba et al., 2014; Collomb, 1962; Fabre, 2005; Massa, 1988) and elsewhere on the platform (Frizon de Lamotte et al., 2013).

(~~H to K~~ I and J) Pre-Hercynian to Hercynian geodynamic pulses (I and J Fig. 11A 14). This period is organized in Early Carboniferous pre-Hercynian (H I, Fig. 11A 14) to Late Carboniferous–Early Permian Hercynian (K, Fig. 11A B) compressions limited by Mid Carboniferous tectonic quiescence/extension (J, Fig. 11A 14). The Carboniferous period is characterized by a normal reactivation and local positive inversion of the previous structural patterns involving reverse faults, overturned folds, transpressional flower structures along strike-slip fault zones (Figs ~~3, 5 6F-F<sup>2</sup>, 6 7B, 6 7C and 6 7D~~). The major Carboniferous tectonic event on the Saharan Platform impacted all arches and it is mainly controlled by near-vertical basement faults with a strike-slip component (Boote et al., 1998; Caby, 2003; Carruba et al., 2014; Haddoum et al., 2001, 2013; Liégeois et al., 2003; Wendt et al., 2009a; Zazoun, 2001, 2008). According these authors basement fabric features exerted a very strong control on the structural evolution during the Hercynian deformation. Two major hiatuses (i.e. Mid Tournaisian to Mid Viséan–Serpukhovian) are recognized (Wendt et al., 2009a).

The geodynamic pulses attest to the reactivation of the terranes and associated lithospheric fault zones. This observation questions the nature of the Precambrian basement and associated structural heritage.

## **7 Basement characterization: Precambrian structural heritage: accreted lithospheric terranes limited by vertical strike-slip mega shear zones**

~~The 800 km<sup>2</sup> outcrop of basement rocks of the Hoggar shield massif provides an exceptional case of an exhumed mobile belt composed of accreted terranes of different ages. The Hoggar shield massif is composed of several accreted, sutured, and amalgamated terranes of various ages and compositions resulting from multiple phases of geodynamic events (Bertrand and Caby, 1978; Black et al., 1994; Caby, 2003; Liégeois et al., 2003).~~

~~To reconstruct the nature of the basement, a terrane map (Fig. 12 15) was put together by integrating geophysical data (aeromagnetic anomaly map: <https://www.geomag.us/>, Bouguer gravity anomaly map: <http://bgi.omp.obs-mip.fr/>), satellite images (7ETM+ from Landsat USGS: <https://earthexplorer.usgs.gov/>) data, geological maps (Berger et al., 2014; Bertrand and Caby, 1978; Black et al., 1994; Caby, 2003; Fezaa et al., 2010; Liégeois et al., 1994, 2003, 2005, 2013), and geochronological data (e.g. U-Pb radiochronology, see supplementary data 5 1). Geochronological data from published studies were compiled and georeferenced (Fig. 1). Thermo-tectonic ages were grouped into eight main thermo-orogenic events (Fig. 1): The Liberian-Ouzzalian event (Archean, >2500 Ma), (the Archean, Eburnean (i.e. Paleoproterozoic, 2500-1600 Ma), the Kibarian (i.e. Mesoproterozoic, 1600-1100 Ma), the Neoproterozoic oceanization rifting (1100-750 Ma), the Neoproterozoic syn-Pan African orogeny (i.e. Neoproterozoic, 750-541 Ma), the post-Pan African (i.e. Neoproterozoic, 541-443 Ma), the Caledonian orogeny (i.e. Siluro-Devonian, 443-358 Ma), and the Hercynian orogeny (i.e. Carbo-Permian, 358-252 Ma). Geochronological data show that the different terranes were~~

reworked during several main thermo-orogenic events. ~~Twenty three well preserved terranes in the Hoggar were identified and grouped into Archean, Paleoproterozoic, and Mesoproterozoic–Neoproterozoic juvenile Pan African terranes (see legend in Fig. 1). In the West African Craton, the Reguibat shield is composed of Archean terrains in the west and of Paleoproterozoic terranes in the east (Peucat et al., 2003, 2005).~~ The two main events deduced from geochronological data are the Neoproterozoic (i.e. Pan-African) and Paleoproterozoic (i.e. Eburnean) episodes (Bertrand and Caby, 1978). Aeromagnetic anomaly surveys are commonly used to analyze geological features such as rock types and fault zones (e.g. Turner et al., 2007). A similar study was led in the meantime showing similar interpretations (Bournas et al., 2003; Brahimi et al., 2018). In this study, these data highlight the geometries and the extension of the different terranes under the sedimentary cover. Four main domains can be identified from the aeromagnetic anomaly map, delimited by contrasted magnetic signatures and interpreted as suture zones (thick black lines, Fig. ~~12~~ 15A). The study area is bounded to the south by the Tuareg Shield (TS), to the north, by the south Atlasic Range, to the west by the West African Craton (WAC) and at the east by the East Saharan Craton (ESC) or Saharan Metacraton (Abdelsalam et al., 2002).

The magnetic disturbance features (Fig. ~~12~~ 15A) show three main magnetic trends. A major NS sinuous fabric and two minor sinuous 130–140°E and N45°E trends. The major NS lineaments coincide with terrane boundaries and mega-shear zones (e.g. 4°50', 4°10', WOSZ, EOSZ, 8°30', RSZ shear zones; Fig. 1). Sigmoidal-shaped terranes 200 to 500 km long and 100 km wide are characterized (red lines in Fig. ~~12~~ 15A). The whole assemblage forms a typical SC-shaped shear fabric (Choukroune et al., 1987) associated with vertical mega-shear zones and suture zones (e.g. WOSZ, EOSZ, 4°10', 4°50' or 8°30' Hoggar shear zones in Fig. 1). The SC fabrics combined with subvertical lithospheric shear zones (Fig. 16B and C) are typical features of the Paleoproterozoic accretionary orogens (Cagnard et al., 2011; Chardon et al., 2009). This

architecture is concordant with the Neoproterozoic collage of the Tuareg Shield (i.e. mobile belt) between the West African Craton and the East Saharan Craton (i.e. cratonic blocks) described by (Coward and Ries, 2003; Craig et al., 2008).

The gravimetric anomaly map (Fig. ~~12~~ 15B) shows a correlation between gravimetric anomalies and tectonic architecture (intracratonic syncline-shaped basin and neighboring arches). Positive anomalies (> 66 mGal) are mainly associated with arches whereas negative anomalies are related to intracratonic basins (< 66 mGal). Nevertheless, negative anomaly disturbance is found in the Hoggar massif probably due to Cenozoic volcanism and the Hoggar swell (Liégeois et al., 2005) or to Eocene Alpine intraplate lithospheric buckling (Rougier et al., 2013).

The Precambrian structural heritage is characterized by accreted lithospheric terranes limited by vertical strike-slip mega shear zones (Fig. 16B and C). A zonation is observed between the Paleozoic basins and arches configurations and the different terranes (thermo-tectonic age). Arches are linked to Archean to Paleoproterozoic continental terranes in contrast to syncline-shaped basins which are associated with Meso-Neoproterozoic terranes (Figs 1, 2 and ~~12A-B~~ 16A-C).

## **8 Low subsidence rate intracratonic Paleozoic basins of the Central Sahara provide a basis for an integrated modeling study**

Paleozoic intracratonic basins with similar characteristics (architecture, subsidence rate, stratigraphic partitioning, alternating episodes of intraplate extension and short duration compressions with periods of tectonic quiescence, etc.) have been documented in North America (e.g. Allen and Armitage, 2011; Beaumont et al., 1988; Burgess, 2008; Burgess et al., 1997; Eaton and Darbyshire, 2010; Pinet et al., 2013; Potter, 2006; Sloss, 1963; Xie and Heller, 2006), South America (Allen and Armitage, 2011; de Brito Neves et al., 1984; Milani and Zalan, 1999; de Oliveira and Mohriak, 2003; Soares et al., 1978; Zalan et al., 1990), Russia

(Allen and Armitage, 2011; Nikishin et al., 1996) and Australia (Harris, 1994; Lindsay and Leven, 1996; Mory et al., 2017). However, the nature of the potential driving processes (lithospheric folding, far-field stresses, local increase in the geotherm, mechanical anisotropy from lithospheric rheological heterogeneity, etc.) associated with the formation of intracratonic Paleozoic basins remains highly speculative (Allen and Armitage, 2011; Armitage and Allen, 2010; Braun et al., 2014; Burgess and Gurnis, 1995; Burov and Cloetingh, 2009; Cacace and Scheck-Wenderoth, 2016; C  lerier et al., 2005; Gac et al., 2013; Heine et al., 2008; Leeder, 1991; Vauchez et al., 1998).

The multiscale and multidisciplinary analysis performed in this study enable us to document a model of Paleozoic intracratonic Central Saharan basins coupling basin architecture and basement structures (Fig. 13 17). While we do not provide any quantitative explanations for the dynamics of these basins, our synthesis highlights that their subsidence is not the result of a single process and we attempt here to make a check-list of the properties that a generic model of formation of such basins must capture:

(A) The association of syncline-shaped wide basins and neighboring arches (i.e. paleo-highs). The structural framework shows a close association of syncline-shaped basins, inter-basin principal to secondary arches, and intra-basin secondary arches (see Fig. 3 2).

(B) By local horst and graben architecture linked to steep-dipping planar normal faults and associated with normal fault-related fold structures (i.e. forced folds; a, Fig. 13 17A). Locally, the extensional structures are disrupted by positive inversion structures (b, Fig. 13 17A) or transported normal faults (c, Fig. 13 17A).

(C) A low rate of subsidence ranging between 5 to 50 m/Myr (Fig. 14 14).

(D) Long periods of extension and tectonic quiescence are interrupted by brief periods of compression or glaciation/deglaciation events (Beuf et al., 1971; Denis et al., 2007; Le Heron

et al., 2006). These periods of compression are possibly related to intraplate compression linked to distal orogenies (i.e. Late Silurian Caledonian event, Late Carboniferous Hercynian, (Frizon de Lamotte et al., 2013) or to intraplate arch uplift related to magmatism (Derder et al., 2016; Fabre, 2005; Frizon de Lamotte et al., 2013; Moreau et al., 1994).

(E) Syndimentary divergent onlaps and local unconformities are identified from integrated seismic data, satellite images, and borehole data (Figs 4, 5, 6, 7, 9 and 10 to 13). The periods of tectonic activity are characterized by normal to reverse reactivation of border faults, emplacement of wedge-shaped units, and erosional unconformities neighboring the arches (Figs 3, 4, 5, 6, 9, 10 and 13).

(F) The stratigraphic architecture displays a lateral facies variation and partitioning between distal marine facies infilling the intracratonic basins (i.e. offshore deposits) and proximal amalgamated facies (i.e. fluvio-marine, shoreface) associated with prominent stratigraphic hiatus and erosional unconformities in the vicinity of the arches.

(G) A close connection is evidenced between the period of tectonic deformation and the presence of erosional unconformities (i.e. 2, 3, 6, 8, 10 geodynamic events in Fig. 13 17B). By contrast, the periods of tectonic quiescence and extension are characterized by low lateral facies variations, thin deposits, and the absence of erosional surfaces.

(H) The Precambrian heritage corresponds to Archean to Paleoproterozoic terranes identified in the Hoggar massif and reactivated during the Meso-Neoproterozoic Pan-African cycle (Fig. 1). The Precambrian lithospheric heterogeneity illustrated by the different characteristics of Precambrian terranes (wavelength, age, nature, fault zones) spatially control the emplacement of the syncline-shaped intracratonic basins underlain by Meso-Neoproterozoic oceanic terranes and the arches underlain by Archean to Paleoproterozoic continental terranes (Figs 1, 3 2 and 13 16). Many authors suggest control of the basement fabrics is inherited from the Pan-African

orogeny in the Saharan basins (Beuf et al., 1968b, 1971; Boote et al., 1998; Carruba et al., 2014; Coward and Ries, 2003; Eschard et al., 2010; Guiraud et al., 2005; Sharata et al., 2015).

## 9 **Conclusion**

Our integrated approach using both geophysical (seismic, gravity, aeromagnetic, etc.) and geological (well, seismic, satellite images, etc.) data has enabled us to decrypt the characteristics of the intracratonic Paleozoic Saharan basins and the control of the heterogeneous lithospheric heritage of the horst and graben architecture, low rate subsidence, association of long-lived broad synclines and anticlines (i.e. arches swells, domes, highs or ridges) with very different wavelengths ( $\lambda$ ) (tens to hundreds of kilometers). A coupled basin architecture and basement structures model is proposed ([Fig. 17](#)).

This study highlights a tight control of the heterogeneous lithosphere [zonation](#) over the structuring of the intracratonic Central Saharan basin. This particular type of basin is characterized by a low rate of subsidence and fault activation controlling the homogeneity of sedimentary facies and the distribution of the main unconformities. The low rate activation of vertical mega-shear zones bounding the intracratonic basin during Paleozoic times contrasts markedly with classic rift kinematics and architecture. Three different periods of tectonic compressional pulses ([i.e. Caledonian, Middle to Late Devonian, Pre-Hercynian](#)), extension and quiescence are identified and controlled the sedimentary distribution ([Fig. 17](#)). An understanding of tectono-sedimentary interaction is key to understanding the distribution of the Paleozoic petroleum reservoirs of this first-order oil province.

## **Acknowledgements**

We are most grateful to ENGIE/NEPTUNE who provided the database used in this paper and who funded the work. Special thanks to the data management service of ENGIE/NEPTUNE (especially Aurelie Galvani) for their help with the database. [Specific appreciations for detailed](#)

reviews/comments from Jobst Wendt, Réda Samy Zazoun and Fabio Lottaroli, along with a short comment from Alexander Peace, which have considerably enriched and improved this paper.

## References

Abdelsalam, M. G., Liégeois, J.-P. and Stern, R. J.: The saharan metacraton, *J. Afr. Earth Sci.*, 34(3), 119–136, 2002.

Abdesselam-Rouighi, F.: Etude palynologique du sondage Sebkheth El Melah (unpublished), Entreprise nationale Sonatrach division hydrocarbures direction Laboratoire central des hydrocarbures, Boumerdès., 1977.

Abdesselam-Rouighi, F.: Résultats de l'étude palynologiques des sondage Garet El Guefoul Bassin de l'Ahnet-Mouydir (unpublished), Entreprise nationale Sonatrach division hydrocarbures direction Laboratoire central des hydrocarbures, Boumerdès., 1991.

Ahmed, A. A.-K. and Moussine-Pouchkine, A.: Lithostratigraphie, sédimentologie et évolution de deux bassins molassiques intramontagneux de la chaîne Pan-Africaine: la Série pourprée de l'Ahnet, Nord-Ouest du Hoggar, Algérie, *J. Afr. Earth Sci.* 1983, 6(4), 525–535, 1987.

Aigner, T.: Storm depositional systems: dynamic stratigraphy in modern and ancient shallow-marine sequences, *Lect. Notes Earth Sci. Berl. Springer Verl.*, 3, 1–158, 1985.

Allen, J. R. L.: Studies in fluvial sedimentation: bars, bar-complexes and sandstone sheets (low-sinuosity braided streams) in the Brownstones (L. Devonian), Welsh Borders, *Sediment. Geol.*, 33(4), 237–293, 1983.

Allen, P. A. and Allen, J. R.: Subsidence and thermal history, in *Basin analysis: Principles and applications*, pp. 349–401, Wiley-Blackwell, Oxford., 2005.

Allen, P. A. and Armitage, J. J.: Cratonic Basins, in *Tectonics of Sedimentary Basins*, edited by C. Busby and A. Azor, pp. 602–620, John Wiley & Sons, Ltd., 2011.

Angevine, C. L., Heller, P. L. and Paola, C.: *Quantitative sedimentary basin modeling*, American Association of Petroleum Geologists., 1990.

Armitage, J. J. and Allen, P. A.: Cratonic basins and the long-term subsidence history of continental interiors, *J. Geol. Soc.*, 167(1), 61–70, doi:10.1144/0016-76492009-108, 2010.

Askri, H., Belmecheri, A., Benrabah, B., Boudjema, A., Boumendjel, K., Daoudi, M., Drid, M., Ghalem, T., Docca, A. M., Ghandriche, H. and others: *Geology of Algeria*, in *Well Evaluation Conference Algeria*, pp. 1–93, Schlumberger-Sonatrach., 1995.

Azzoune, N.: *Analyse palynologique de trois (03) échantillons de carottes du sondages W7, Sonatrach* (unpublished), Entreprise nationale Sonatrach division hydrocarbures direction Laboratoire central des hydrocarbures, Boumerdès., 1999.

Badalini, G., Redfern, J. and Carr, I. D.: A synthesis of current understanding of the structural evolution of North Africa, *J. Pet. Geol.*, 25(3), 249–258, 2002.

Beaumont, C., Quinlan, G. and Hamilton, J.: Orogeny and stratigraphy: Numerical models of the Paleozoic in the eastern interior of North America, *Tectonics*, 7(3), 389–416, 1988.

Bellahsen, N. and Daniel, J. M.: Fault reactivation control on normal fault growth: an experimental study, *J. Struct. Geol.*, 27(4), 769–780, doi:10.1016/j.jsg.2004.12.003, 2005.

Bennacef, A., Beuf, S., Biju-Duval, B., Charpal, O. de, Gariel, O. and Rognon, P.: *Example of Cratonic Sedimentation: Lower Paleozoic of Algerian Sahara*, *AAPG Bull.*, 55(12), 2225–2245, 1971.

Bennacef, A., Attar, A., Froukhi, R., Beuf, S., Philippe, G., Schmerber, G. and Vermeire, J. C.: Cartes Géologiques d'Iherir-Dider (NG-32-IX), Iherir (NG-32-X), Illizi (NG-32-XV), Aharhar (NG-32-VIII), Oued Samène (NG-32-XIV), Erg Tihodaine (NG-32-VII), Tin Alkoum (NG-32-V), Djanet (NG-32-IV), Ta-N-Mellet (NG-32-XIII), Ta-N-Elak (NG-32-XIX), Fort Tarat (NG-32-XVI), Tilmas El Mra (NG-31-XXIV), Ers Oum El Lil (NG-31-XXII), Amguid (NG-31-XVIII), 1/200000 Sonatrach-Ministère de l'Industrie et des Mines, Algérie, 1974.

Bensalah, A., Beuf, S., Gabriel, O., Philippe, G., Lacot, R., Paris, A., Basseto, D., Conrad, J. and Moussine-Pouchkine, A.: Cartes Géologiques de Khanguet El Hadid (NG-31-XVII), Aïn Tidjoubar (NG-31-XVI), Oued Djaret (NG-31-XV), Aoulef El Arab (NG-31-XIV), Reggane (NG-31-XIII), Ifetessene (NG-31-IX), Arak (NG-31-X et NG-31-IV), Meredoua (NG-31-XIII), Tanezrouft (NG-31-VII et NG-31-I), In Heguis (NG-31-IX), Tin Senasset (NG-31-III), Ouallene (NG-31-II) 1/200000 Sonatrach-Ministère de l'Industrie et des Mines, Algérie, 1971.

Berger, J., Ouzegane, K., Bendaoud, A., Liégeois, J.-P., Kiénast, J.-R., Bruguier, O. and Caby, R.: Continental subduction recorded by Neoproterozoic eclogite and garnet amphibolites from Western Hoggar (Tassendjanet terrane, Tuareg Shield, Algeria), *Precambrian Res.*, 247, 139–158, doi:10.1016/j.precamres.2014.04.002, 2014.

Bertrand, J. M. L. and Caby, R.: Geodynamic evolution of the Pan-African orogenic belt: A new interpretation of the Hoggar shield (Algerian Sahara), *Geol. Rundsch.*, 67(2), 357–388, doi:10.1007/BF01802795, 1978.

Beuf, S. and Montadert, L.: Géologie-sur une discordance angulaire entre les unités II et III du Cambro-Ordovicien au sud-est de la plaine de Dider (Tassili des Ajjers), *Compte Rendus Hebd. Séances L'Académie Sci.*, 254(6), 1108, 1962.

Beuf, S., Biju-Duval, B., Mauvier, A. and Legrand, P.: Nouvelles observations sur le ‘Cambro-Ordovicien’ du Bled El Mass (Sahara central), Publ. Serv. Géologique Algér. Bull., 38, 39–51, 1968a.

Beuf, S., Biju-Duval, B., De Charpal, O., Gariel, O., Bennacef, A., Black, R., Arene, J., Boissonnas, J., Chachau, F., Guérangé, B. and others: Une conséquence directe de la structure du bouclier Africain: L’ébauche des bassins de l’Ahnet et du Mouydir au Paléozoïque inférieur, Publ. Serv. Géologique L’Algérie Nouv. Sér. Bull., 38, 105–34, 1968b.

Beuf, S., Biju-Duval, B., De Charpal, O. and Gariel, O.: Homogénéité des directions des paléocourants du Dévonien inférieur au Sahara central, Comptes Rendus L’Académie Sci. Sér. D, 268, 2026–9, 1969.

Beuf, S., Biju-Duval, B., de Charpal, O., Rognon, P., Gabriel, O. and Bennacef, A.: Les grès du Paléozoïque inférieur au Sahara: Sédimentation et discontinuités évolution structurale d’un craton, Technip., Paris., 1971.

Biju-Duval, B., de Charpal, O., Beuf, S. and Bennacef, A.: Lithostratigraphie du Dévonien inférieur dans l’Ahnet et le Mouydir (Sahara Central), Bull Serv Géologique Algérie, (38), 83–104, 1968.

Black, R., Latouche, L., Liégeois, J. P., Caby, R. and Bertrand, J. M.: Pan-African displaced terranes in the Tuareg shield (central Sahara), Geology, 22(7), 641–644, 1994.

Bonini, M., Sani, F. and Antonielli, B.: Basin inversion and contractional reactivation of inherited normal faults: A review based on previous and new experimental models, Tectonophysics, 522–523, 55–88, doi:10.1016/j.tecto.2011.11.014, 2012.

Boote, D. R. D., Clark-Lowes, D. D. and Traut, M. W.: Palaeozoic petroleum systems of North Africa, *Geol. Soc. Lond. Spec. Publ.*, 132(1), 7–68, doi:10.1144/GSL.SP.1998.132.01.02, 1998.

Borocco, J. and Nyssen, R.: Nouvelles observations sur les “gres inférieurs” cambro-ordoviciens du Tassili interne (Nord-Hoggar), *Bull. Société Géologique Fr.*, S7-I(2), 197–206, doi:10.2113/gssgfbull.S7-I.2.197, 1959.

Boudjema, A.: Evolution structurale du bassin pétrolier "triasique" du Sahara nord oriental (Algérie), Doctoral dissertation, Paris 11, France., 1987.

Boumendjel, K.: Les chitinozoaires du silurien supérieur et du dévonien du Sahara algérien (cadre géologique, systématique, biostratigraphie), Doctoral dissertation, Rennes 1, France., 1987.

Boumendjel, K., Loboziak, S., Paris, F., Steemans, P. and Strel, M.: Biostratigraphie des Miospores et des Chitinozoaires du Silurien supérieur et du Dévonien dans le bassin d'Illizi (S.E. du Sahara algérien), *Geobios*, 21(3), 329–357, doi:10.1016/S0016-6995(88)80057-3, 1988.

Bournas, N., Galdeano, A., Hamoudi, M. and Baker, H.: Interpretation of the aeromagnetic map of Eastern Hoggar (Algeria) using the Euler deconvolution, analytic signal and local wavenumber methods, *J. Afr. Earth Sci.*, 37(3–4), 191–205, doi:10.1016/j.jafrearsci.2002.12.001, 2003.

Brahimi, S., Liégeois, J.-P., Ghienne, J.-F., Munsch, M. and Bourmatte, A.: The Tuareg shield terranes revisited and extended towards the northern Gondwana margin: Magnetic and gravimetric constraints, *Earth-Sci. Rev.*, 185, 572–599, doi:10.1016/j.earscirev.2018.07.002, 2018.

Braun, J., Simon-Labric, T., Murray, K. E. and Reiners, P. W.: Topographic relief driven by variations in surface rock density, *Nat. Geosci.*, 7(7), 534–540, doi:10.1038/ngeo2171, 2014.

de Brito Neves, B. B., Fuck, R. A., Cordani, U. G. and Thomaz F<sup>o</sup>, A.: Influence of basement structures on the evolution of the major sedimentary basins of Brazil: A case of tectonic heritage, *J. Geodyn.*, 1(3), 495–510, doi:10.1016/0264-3707(84)90021-8, 1984.

Buchanan, P. G. and McClay, K. R.: Sandbox experiments of inverted listric and planar fault systems, *Tectonophysics*, 188(1), 97–115, doi:10.1016/0040-1951(91)90317-L, 1991.

Burgess, P. M.: Phanerozoic evolution of the sedimentary cover of the North American craton, in *Sedimentary Basins of the World*, vol. 5, pp. 31–63, Elsevier., 2008.

Burgess, P. M. and Gurnis, M.: Mechanisms for the formation of cratonic stratigraphic sequences, *Earth Planet. Sci. Lett.*, 136(3), 647–663, doi:10.1016/0012-821X(95)00204-P, 1995.

Burgess, P. M., Gurnis, M. and Moresi, L.: Formation of sequences in the cratonic interior of North America by interaction between mantle, eustatic, and stratigraphic processes, *Geol. Soc. Am. Bull.*, 109(12), 1515–1535, 1997.

Burke, K., MacGregor, D. S. and Cameron, N. R.: Africa's petroleum systems: four tectonic 'Aces' in the past 600 million years, *Geol. Soc. Lond. Spec. Publ.*, 207(1), 21–60, 2003.

Burov, E. and Cloetingh, S.: Controls of mantle plumes and lithospheric folding on modes of intraplate continental tectonics: differences and similarities, *Geophys. J. Int.*, 178(3), 1691–1722, doi:10.1111/j.1365-246X.2009.04238.x, 2009.

Butler, R. W. H.: The influence of pre-existing basin structure on thrust system evolution in the Western Alps, *Geol. Soc. Lond. Spec. Publ.*, 44(1), 105–122, doi:10.1144/GSL.SP.1989.044.01.07, 1989.

Caby, R.: Terrane assembly and geodynamic evolution of central–western Hoggar: a synthesis, *J. Afr. Earth Sci.*, 37(3–4), 133–159, doi:10.1016/j.jafrearsci.2003.05.003, 2003.

Cacace, M. and Scheck-Wenderoth, M.: Why intracontinental basins subside longer: 3-D feedback effects of lithospheric cooling and sedimentation on the flexural strength of the lithosphere: Subsidence at Intracontinental Basins, *J. Geophys. Res. Solid Earth*, 121(5), 3742–3761, doi:10.1002/2015JB012682, 2016.

Cagnard, F., Barbey, P. and Gapais, D.: Transition between “Archaean-type” and “modern-type” tectonics: Insights from the Finnish Lapland Granulite Belt, *Precambrian Res.*, 187(1–2), 127–142, doi:10.1016/j.precamres.2011.02.007, 2011.

Carr, I. D.: Second-Order Sequence Stratigraphy of the Palaeozoic of North Africa, *J. Pet. Geol.*, 25(3), 259–280, doi:10.1111/j.1747-5457.2002.tb00009.x, 2002.

Carruba, S., Perotti, C., Rinaldi, M., Bresciani, I. and Bertozzi, G.: Intraplate deformation of the Al Qarqaf Arch and the southern sector of the Ghadames Basin (SW Libya), *J. Afr. Earth Sci.*, 97, 19–39, doi:10.1016/j.jafrearsci.2014.05.001, 2014.

Catuneanu, O., Abreu, V., Bhattacharya, J. P., Blum, M. D., Dalrymple, R. W., Eriksson, P. G., Fielding, C. R., Fisher, W. L., Galloway, W. E., Gibling, M. R., Giles, K. A., Holbrook, J. M., Jordan, R., Kendall, C. G. S. C., Macurda, B., Martinsen, O. J., Miall, A. D., Neal, J. E., Nummedal, D., Pomar, L., Posamentier, H. W., Pratt, B. R., Sarg, J. F., Shanley, K. W., Steel, R. J., Strasser, A., Tucker, M. E. and Winker, C.: Towards the standardization of sequence stratigraphy, *Earth-Sci. Rev.*, 92(1–2), 1–33, doi:10.1016/j.earscirev.2008.10.003, 2009.

Célérier, J., Sandiford, M., Hansen, D. L. and Quigley, M.: Modes of active intraplate deformation, Flinders Ranges, Australia, *Tectonics*, 24(6), 1–17, doi:10.1029/2004TC001679, 2005.

Chardon, D., Gapais, D. and Cagnard, F.: Flow of ultra-hot orogens: A view from the Precambrian, clues for the Phanerozoic, *Tectonophysics*, 477(3–4), 105–118, doi:10.1016/j.tecto.2009.03.008, 2009.

Chaumeau, J., Legrand, P. and Renaud, A.: Contribution a l'étude du Couvinien dans le bassin de Fort-de-Polignac (Sahara), *Bull. Société Géologique Fr.*, S7-III(5), 449–456, doi:10.2113/gssgfbull.S7-III.5.449, 1961.

Chavand, J. C. and Claracq, P.: La disparition du Tassili externe à l'E de Fort-Polignac (Sahara central), *CR Soc Géol Fr*, 1959, 172–174, 1960.

Choukroune, P., Gapais, D. and Merle, O.: Shear criteria and structural symmetry, *J. Struct. Geol.*, 9(5–6), 525–530, doi:10.1016/0191-8141(87)90137-4, 1987.

Claracq, P., Fabre, C., Freulon, J. M. and Nougarede, F.: Une discordance angulaire dans les “Grès inférieurs” de l'Adrar Tan Elak (Sahara central), *C. r. Somm. Séances Soc. Géologique Fr.*, 309–310, 1958.

Collomb, G. R.: Étude géologique du Jebel Fezzan et de sa bordure paléozoïque, *Compagnie française des pétroles.*, 1962.

Conrad, J.: Les grandes lignes stratigraphiques et sédimentologiques du Carbonifère de l'Ahnet-Mouydir (Sahara central algérien), *Rev. Inst. Fr. Pétrole*, 28, 3–18, 1973.

Conrad, J.: Les séries carbonifères du Sahara central algérien: stratigraphie, sédimentation, évolution structurale, *Doctoral dissertation, Université Aix-Marseille III, France.*, 1984.

Coward, M. P. and Ries, A. C.: Tectonic development of North African basins, *Geol. Soc. Lond. Spec. Publ.*, 207(1), 61–83, doi:10.1144/GSL.SP.2003.207.4, 2003.

Cózar, P., Somerville, I. D., Vachard, D., Coronado, I., García-Frank, A., Medina-Varea, P., Said, I., Del Moral, B. and Rodríguez, S.: Upper Mississippian to lower Pennsylvanian biostratigraphic correlation of the Sahara Platform successions on the northern margin of Gondwana (Morocco, Algeria, Libya), *Gondwana Res.*, 36, 459–472, doi:10.1016/j.gr.2015.07.019, 2016.

Craig, J., Rizzi, C., Said, F., Thusu, B., Luning, S., Asbali, A. I., Keeley, M. L., Bell, J. F., Durham, M. J. and Eales, M. H.: Structural styles and prospectivity in the Precambrian and Palaeozoic hydrocarbon systems of North Africa, *Geol. East Libya*, 4, 51–122, 2008.

Dalrymple, R. W. and Choi, K.: Morphologic and facies trends through the fluvial–marine transition in tide-dominated depositional systems: A schematic framework for environmental and sequence-stratigraphic interpretation, *Earth-Sci. Rev.*, 81(3–4), 135–174, doi:10.1016/j.earscirev.2006.10.002, 2007.

Dalrymple, R. W., Zaitlin, B. A. and Boyd, R.: A conceptual model of estuarine sedimentation, *J. Sediment. Petrol.*, 62(1130–1146), 116, 1992.

Dalrymple, R. W., Mackay, D. A., Ichaso, A. A. and Choi, K. S.: Processes, Morphodynamics, and Facies of Tide-Dominated Estuaries, in *Principles of Tidal Sedimentology*, pp. 79–107, Springer, Dordrecht., 2012.

Denis, M., Buoncristiani, J.-F., Konaté, M., Ghienne, J.-F. and Guiraud, M.: Hirnantian glacial and deglacial record in SW Djado Basin (NE Niger), *Geodin. Acta*, 20(3), 177–195, doi:10.3166/ga.20.177-195, 2007.

Derder, M. E. M., Maouche, S., Liégeois, J. P., Henry, B., Amenna, M., Ouabadi, A., Bellon, H., Bruguier, O., Bayou, B., Bestandji, R., Nouar, O., Bouabdallah, H., Ayache, M. and Beddiaf, M.: Discovery of a Devonian mafic magmatism on the western border of the Murzuq basin (Saharan metacraton): Paleomagnetic dating and geodynamical implications, *J. Afr. Earth Sci.*, 115, 159–176, doi:10.1016/j.jafrearsci.2015.11.019, 2016.

Djouder, H., Lüning, S., Da Silva, A.-C., Abdallah, H. and Boulvain, F.: Silurian deltaic progradation, Tassili n'Ajjer plateau, south-eastern Algeria: Sedimentology, ichnology and sequence stratigraphy, *J. Afr. Earth Sci.*, 142, 170–192, 2018.

Dokka, A. M.: Sedimentological core description WELL: W7, Block - 340, (District - 3) (unpublished), Core description, Sonatrach division exploration direction des operations département assistance aux opérations service géologique, Algérie., 1999.

Dott, R. H. and Bourgeois, J.: Hummocky stratification: Significance of its variable bedding sequences, *Geol. Soc. Am. Bull.*, 93(8), 663, doi:10.1130/0016-7606(1982)93<663:HSSOIV>2.0.CO;2, 1982.

Dubois, P.: Stratigraphie du Cambro-Ordovicien du Tassili n'Ajjer (Sahara central), *Bull. Société Géologique Fr.*, S7-III(2), 206–209, doi:10.2113/gssgfbull.S7-III.2.206, 1961.

Dubois, P. and Mazelet, P.: Stratigraphie du Silurien du Tassili N'Ajjer, *Bull. Société Géologique Fr.*, S7-VI(4), 586–591, doi:10.2113/gssgfbull.S7-VI.4.586, 1964.

Dubois, P., Beuf, S. and Biju-Duval, B.: Lithostratigraphie du Dévonien inférieur gréseux du Tassili n'Ajjer, in *Symposium on the Lower Devonian and its limits: Bur. Recherche Geol. et Minieres Mem*, pp. 227–235., 1967.

Dumas, S. and Arnott, R. W. C.: Origin of hummocky and swaley cross-stratification—the controlling influence of unidirectional current strength and aggradation rate, *Geology*, 34(12), 1073–1076, 2006.

Eaton, D. W. and Darbyshire, F.: Lithospheric architecture and tectonic evolution of the Hudson Bay region, *Tectonophysics*, 480(1–4), 1–22, doi:10.1016/j.tecto.2009.09.006, 2010.

Echikh, K.: Geology and hydrocarbon occurrences in the Ghadames basin, Algeria, Tunisia, Libya, *Geol. Soc. Lond. Spec. Publ.*, 132(1), 109–129, 1998.

Eschard, R., Desaubliaux, G., Deschamps, R., Montadert, L., Ravenne, C., Bekkouche, D., Abdallah, H., Belhaouas, S., Benkouider, M., Braïk, F., Henniche, M., Maache, N. and Mouaïci, R.: Illizi-Berkine Devonian Reservoir Consortium (unpublished), Institut Française du Pétrole - Sontrach, unpublished, Algérie., 1999.

Eschard, R., Abdallah, H., Braïk, F. and Desaubliaux, G.: The Lower Paleozoic succession in the Tassili outcrops, Algeria: sedimentology and sequence stratigraphy, *First Break*, 23(10), 2005.

Eschard, R., Braïk, F., Bekkouche, D., Rahuma, M. B., Desaubliaux, G., Deschamps, R. and Proust, J. N.: Palaeohighs: their influence on the North African Palaeozoic petroleum systems, *Pet. Geol. Mature Basins New Front. 7th Pet. Geol. Conf.*, 707–724, 2010.

Fabre, J.: Les séries paléozoïques d’Afrique: une approche, *J. Afr. Earth Sci. Middle East*, 7(1), 1–40, doi:10.1016/0899-5362(88)90051-6, 1988.

Fabre, J.: Géologie du Sahara occidental et central, Musée royal de l’Afrique centrale., 2005.

Fabre, J., Kaci, A. A., Bouima, T. and Moussine-Pouchkine, A.: Le cycle molassique dans le Rameau trans-saharien de la chaîne panafricaine, *J. Afr. Earth Sci.*, 7, 41–55, doi:10.1016/0899-5362(88)90052-8, 1988.

Fekirine, B. and Abdallah, H.: Palaeozoic lithofacies correlatives and sequence stratigraphy of the Saharan Platform, Algeria, *Geol. Soc. Lond. Spec. Publ.*, 132(1), 97–108, doi:10.1144/GSL.SP.1998.132.01.05, 1998.

Fezaa, N., Liégeois, J.-P., Abdallah, N., Cherfouh, E. H., De Waele, B., Bruguier, O. and Ouabadi, A.: Late Ediacaran geological evolution (575–555Ma) of the Djanet Terrane, Eastern Hoggar, Algeria, evidence for a Murzukian intracontinental episode, *Precambrian Res.*, 180(3–4), 299–327, doi:10.1016/j.precamres.2010.05.011, 2010.

Follet, J.: Sur l'existence de mouvements calédoniens au Mouydir (Sahara Central), *Compte Rendus Hebd. Séances L'Académie Sci.*, 230(25), 2217–2218, 1950.

Frey, R. W., Pemberton, S. G. and Saunders, T. D.: Ichnofacies and bathymetry: a passive relationship, *J. Paleontol.*, 64(1), 155–158, 1990.

Frizon de Lamotte, D., Tavakoli-Shirazi, S., Leturmy, P., Averbuch, O., Mouchot, N., Raulin, C., Leparmentier, F., Blanpied, C. and Ringenbach, J.-C.: Evidence for Late Devonian vertical movements and extensional deformation in northern Africa and Arabia: Integration in the geodynamics of the Devonian world: Devonian evolution Northern Gondwana, *Tectonics*, 32(2), 107–122, doi:10.1002/tect.20007, 2013.

Fröhlich, S., Petitpierre, L., Redfern, J., Grech, P., Bodin, S. and Lang, S.: Sedimentological and sequence stratigraphic analysis of Carboniferous deposits in western Libya: Recording the sedimentary response of the northern Gondwana margin to climate and sea-level changes, *J. Afr. Earth Sci.*, 57(4), 279–296, doi:10.1016/j.jafrearsci.2009.09.007, 2010.

Gac, S., Huismans, R. S., Simon, N. S. C., Podladchikov, Y. Y. and Faleide, J. I.: Formation of intracratonic basins by lithospheric shortening and phase changes: a case study from the ultra-deep East Barents Sea basin, *Terra Nova*, 25(6), 459–464, doi:10.1111/ter.12057, 2013.

Galeazzi, S., Point, O., Haddadi, N., Mather, J. and Druésne, D.: Regional geology and petroleum systems of the Illizi–Berkine area of the Algerian Saharan Platform: An overview, *Mar. Pet. Geol.*, 27(1), 143–178, doi:10.1016/j.marpetgeo.2008.10.002, 2010.

Galloway, W. E.: Genetic Stratigraphic Sequences in Basin Analysis I: Architecture and Genesis of Flooding-Surface Bounded Depositional Units, *AAPG Bull.*, 73(2), 125–142, 1989.

Galushkin, Y. I. and Eloghbi, S.: Thermal history of the Murzuq Basin, Libya, and generation of hydrocarbons in its source rocks, *Geochem. Int.*, 52(6), 486–499, doi:10.1134/S0016702914060032, 2014.

Gariel, O., de Charpal, O. and Bennacef, A.: Sur la sédimentation des grès du Cambro-Ordovicien (Unité II) dans l’Ahnet et le Mouydir (Sahara central): *Algerie, Serv. Geol, Bull N Ser*, (38), 7–37, 1968.

Ghienne, J.-F., Deynoux, M., Manatschal, G. and Rubino, J.-L.: Palaeovalleys and fault-controlled depocentres in the Late-Ordovician glacial record of the Murzuq Basin (central Libya), *Comptes Rendus Geosci.*, 335(15), 1091–1100, doi:10.1016/j.crte.2003.09.010, 2003.

Ghienne, J.-F., Moreau, J., Degermann, L. and Rubino, J.-L.: Lower Palaeozoic unconformities in an intracratonic platform setting: glacial erosion versus tectonics in the eastern Murzuq Basin (southern Libya), *Int. J. Earth Sci.*, 102(2), 455–482, doi:10.1007/s00531-012-0815-y, 2013.

Gindre, L., Le Heron, D. and Bjørnseth, H. M.: High resolution facies analysis and sequence stratigraphy of the Siluro-Devonian succession of Al Kufrah basin (SE Libya), *J. Afr. Earth Sci.*, 76, 8–26, doi:10.1016/j.jafrearsci.2012.08.002, 2012.

Girard, F., Ghienne, J.-F. and Rubino, J.-L.: Channelized sandstone bodies ('cordons') in the Tassili N'Ajjer (Algeria & Libya): snapshots of a Late Ordovician proglacial outwash plain, *Geol. Soc. Lond. Spec. Publ.*, 368(1), 355–379, doi:10.1144/SP368.3, 2012.

Grasemann, B., Martel, S. and Passchier, C.: Reverse and normal drag along a fault, *J. Struct. Geol.*, 27(6), 999–1010, doi:10.1016/j.jsg.2005.04.006, 2005.

Greigertt, J. and Pougnet, R.: Carte Géologique du Niger, 1/2000000, BRGM, République du Niger, 1965.

Guiraud, R., Bosworth, W., Thierry, J. and Delplanque, A.: Phanerozoic geological evolution of Northern and Central Africa: An overview, *J. Afr. Earth Sci.*, 43(1–3), 83–143, doi:10.1016/j.jafrearsci.2005.07.017, 2005.

Haddoum, H., Guiraud, R. and Moussine-Pouchkine, A.: Hercynian compressional deformations of the Ahnet–Mouydir Basin, Algerian Saharan Platform: far-field stress effects of the Late Palaeozoic orogeny, *Terra Nova*, 13(3), 220–226, 2001.

Haddoum, H., Mokri, M., Ouzegane, K., Ait-Djaffer, S. and Djemai, S.: Extrusion de l'In Ouzal vers le Nord (Hoggar occidental, Algérie): une conséquence d'un poinçonnement panafricain, *J. Hydrocarb. Mines Environ. Res. Vol.*, 4(1), 6–16, 2013.

Haq, B. U. and Schutter, S. R.: A Chronology of Paleozoic Sea-Level Changes, *Science*, 322(5898), 64–68, doi:10.1126/science.1161648, 2008.

Harris, L. B.: Structural and tectonic synthesis for the Perth basin, Western Australia, *J. Pet. Geol.*, 17(2), 129–156, 1994.

Hartley, R. W. and Allen, P. A.: Interior cratonic basins of Africa: relation to continental break-up and role of mantle convection, *Basin Res.*, 6(2–3), 95–113, 1994.

Hassan, A.: Etude palynologique Paléozoïque du sondage Razzal-Allah-Nord (unpublished), Entreprise nationale Sonatrach division hydrocarbures direction Laboratoire central des hydrocarbures, Boumerdès., 1984.

Heine, C., Dietmar Müller, R., Steinberger, B. and Torsvik, T. H.: Subsidence in intracontinental basins due to dynamic topography, *Phys. Earth Planet. Inter.*, 171(1–4), 252–264, doi:10.1016/j.pepi.2008.05.008, 2008.

Henniche, M.: Architecture et modèle de dépôts d'une série sédimentaire paléozoïque en contexte cratonique, Rennes 1, France., 2002.

Holbrook, J. and Schumm, S. A.: Geomorphic and sedimentary response of rivers to tectonic deformation: a brief review and critique of a tool for recognizing subtle epeirogenic deformation in modern and ancient settings, *Tectonophysics*, 305(1), 287–306, 1999.

Hollard, H., Choubert, G., Bronner, G., Marchand, J. and Sougy, J.: Carte géologique du Maroc, scale 1: 1,000,000, *Serv Carte Géol Maroc*, 260(2), 1985.

Holt, P. J., Allen, M. B., van Hunen, J. and Bjørnseth, H. M.: Lithospheric cooling and thickening as a basin forming mechanism, *Tectonophysics*, 495(3–4), 184–194, doi:10.1016/j.tecto.2010.09.014, 2010.

Jacquemont, P., Jutard, G., Plauchut, B., Grégoire, J. and Mouflard, R.: Etude du bassin du Djado, *Bur. Rech. Pétroles Rapp.*, 1215, 1959.

Jäger, H., Lewandowski, E. and Lampart, V.: Palynology of the upper Silurian to middle Devonian in the Reggane Basin, southern Algeria, Ext. Abstr. DGMK-Tagungsbericht 2009-1 DGMKÖGEW Spring Meet. Celle, 47–51, 2009.

Jardiné, S. and Yapaudjian, L.: Lithostratigraphie et palynologie du Dévonien-Gothlandien gréseux du Bassin de Polignac (Sahara), Rev. L'Institut Fr. Pétrole, 23(4), 439–469, 1968.

Joulia, F.: Carte géologique de reconnaissance de la bordure sédimentaire occidentale de l'Aïr au 1/500 000, Éditions BRGM Orléans Fr., 1963.

Kermandji, A. M.: Silurian–Devonian miospores from the western and central Algeria, Rev. Micropaléontologie, 50(1), 109–128, doi:10.1016/j.revmic.2007.01.003, 2007.

Kermandji, A. M. H., Kowalski, M. W. and Pharisat, A.: Palynologie et séquences de l'Emsien de la région d'In Salah, Sahara central Algérien, Bull. Société D'Histoire Nat. Pays Montbél., 301–306, 2003.

Kermandji, A. M. H., Kowalski, W. M. and Touhami, F. K.: Miospore stratigraphy of Lower and early Middle Devonian deposits from Tidikelt, Central Sahara, Algeria, Geobios, 41(2), 227–251, doi:10.1016/j.geobios.2007.05.002, 2008.

Kermandji, A. M. H., Touhami, F. K., Kowalski, W. M., Abbés, S. B., Boularak, M., Chabour, N., Laïfa, E. L. and Hannachi, H. B.: Stratigraphie du Dévonien Inférieur du Plateau du Tidikelt d'In Salah (Sahara Central Algérie), Comun. Geológicas, (t. 96), 67–82, 2009.

Khalil, S. M. and McClay, K. R.: Extensional fault-related folding, northwestern Red Sea, Egypt, J. Struct. Geol., 24(4), 743–762, 2002.

Khiar, S.: Résultats palynologiques du sondage Garet El Guefoul (unpublished), Entreprise nationale Sonatrach division hydrocarbures direction Laboratoire central des hydrocarbures, Alger., 1974.

Kracha, N.: Relation entre sédimentologie, fracturation naturelle et diagénèse d'un réservoir à faible perméabilité application aux réservoirs de l'Ordovicien bassin de l'Ahnet, Sahara central, Algérie, Doctoral dissertation, Université des sciences et technologies de Lille, France., 2011.

Le Heron, D. P.: Interpretation of Late Ordovician glaciogenic reservoirs from 3-D seismic data: an example from the Murzuq Basin, Libya, *Geol. Mag.*, 147(01), 28, doi:10.1017/S0016756809990586, 2010.

Le Heron, D. P., Craig, J., Sutcliffe, O. E. and Whittington, R.: Late Ordovician glaciogenic reservoir heterogeneity: An example from the Murzuq Basin, Libya, *Mar. Pet. Geol.*, 23(6), 655–677, doi:10.1016/j.marpetgeo.2006.05.006, 2006.

Le Heron, D. P., Craig, J. and Etienne, J. L.: Ancient glaciations and hydrocarbon accumulations in North Africa and the Middle East, *Earth-Sci. Rev.*, 93(3–4), 47–76, doi:10.1016/j.earscirev.2009.02.001, 2009.

Leeder, M. R.: Denudation, vertical crustal movements and sedimentary basin infill, *Geol. Rundsch.*, 80(2), 441–458, doi:10.1007/BF01829376, 1991.

Legrand, P.: Le Devonien du Sahara Algerien, *Can. Soc. Pet. Geol.*, 1, 245–284, 1967a.

Legrand, P.: Nouvelles connaissances acquises sur la limite des systèmes Silurien et Dévonien au Sahara algérien, *Bull. Bur. Rech. Géologiques Minières*, 33, 119–37, 1967b.

Legrand, P.: The lower Silurian graptolites of Oued In Djerane: a study of populations at the Ordovician-Silurian boundary, *Geol. Soc. Lond. Spec. Publ.*, 20(1), 145–153, doi:10.1144/GSL.SP.1986.020.01.15, 1986.

Legrand, P.: Late Ordovician-early Silurian paleogeography of the Algerian Sahara, *Bull. Société Géologique Fr.*, 174(1), 19–32, 2003a.

Legrand, P.: Silurian stratigraphy and paleogeography of the northern African margin of Gondwana, in *Silurian Lands and Seas: Paleogeography Outside of Laurentia*, edited by E. Landing and M. E. Johson, pp. 59–104, New York., 2003b.

Legrand-Blain, M.: Dynamique des Brachiopodes carbonifères sur la plate-forme carbonatée du Sahara algérien: paléoenvironnements, paléobiogéographie, évolution, Doctoral dissertation, Université de Bordeaux 1, France., 1985.

Lessa, G. and Masselink, G.: Morphodynamic evolution of a macrotidal barrier estuary, *Mar. Geol.*, 129(1–2), 25–46, 1995.

Leuven, J. R. F. W., Kleinhans, M. G., Weisscher, S. A. H. and van der Vegt, M.: Tidal sand bar dimensions and shapes in estuaries, *Earth-Sci. Rev.*, 161, 204–223, doi:10.1016/j.earscirev.2016.08.004, 2016.

Lewis, M. M., Jackson, C. A.-L., Gawthorpe, R. L. and Whipp, P. S.: Early synrift reservoir development on the flanks of extensional forced folds: A seismic-scale outcrop analog from the Hadahid fault system, Suez rift, Egypt, *AAPG Bull.*, 99(06), 985–1012, doi:10.1306/12011414036, 2015.

Liégeois, J. P., Latouche, L., Boughrara, M., Navez, J. and Guiraud, M.: The LATEA metacraton (Central Hoggar, Tuareg shield, Algeria): behaviour of an old passive margin during

the Pan-African orogeny, *J. Afr. Earth Sci.*, 37(3–4), 161–190, doi:10.1016/j.jafrearsci.2003.05.004, 2003.

Liégeois, J.-P., Black, R., Navez, J. and Latouche, L.: Early and late Pan-African orogenies in the Air assembly of terranes (Tuareg Shield, Niger), *Precambrian Res.*, 67(1), 59–88, 1994.

Liégeois, J.-P., Benhallou, A., Azzouni-Sekkal, A., Yahiaoui, R. and Bonin, B.: The Hoggar swell and volcanism: Reactivation of the Precambrian Tuareg shield during Alpine convergence and West African Cenozoic volcanism, *Geol. Soc. Am. Spec. Pap.*, 388, 379–400, doi:10.1130/0-8137-2388-4.379, 2005.

Liégeois, J.-P., Abdelsalam, M. G., Ennih, N. and Ouabadi, A.: Metacraton: Nature, genesis and behavior, *Gondwana Res.*, 23(1), 220–237, doi:10.1016/j.gr.2012.02.016, 2013.

Lindsay, J. F. and Leven, J. H.: Evolution of a Neoproterozoic to Palaeozoic intracratonic setting, Officer Basin, South Australia, *Basin Res.*, 8(4), 403–424, doi:10.1046/j.1365-2117.1996.00223.x, 1996.

Logan, P. and Duddy, I.: An investigation of the thermal history of the Ahnet and Reggane Basins, Central Algeria, and the consequences for hydrocarbon generation and accumulation, *Geol. Soc. Lond. Spec. Publ.*, 132(1), 131–155, 1998.

Loi, A., Ghienne, J.-F., Dabard, M. P., Paris, F., Botquelen, A., Christ, N., Elaouad-Debbaj, Z., Gorini, A., Vidal, M., Videt, B. and Destombes, J.: The Late Ordovician glacio-eustatic record from a high-latitude storm-dominated shelf succession: The Bou Ingarf section (Anti-Atlas, Southern Morocco), *Palaeogeogr. Palaeoclimatol. Palaeoecol.*, 296(3–4), 332–358, doi:10.1016/j.palaeo.2010.01.018, 2010.

Lubeseder, S.: Silurian and Devonian sequence stratigraphy of North Africa; Regional correlation and sedimentology (Marocco, Algeria, Libya), Doctoral dissertation, University of Manchester, UK., 2005.

Lubeseder, S., Redfern, J., Petitpierre, L. and Fröhlich, S.: Stratigraphic trapping potential in the Carboniferous of North Africa: developing new play concepts based on integrated outcrop sedimentology and regional sequence stratigraphy (Morocco, Algeria, Libya), in Geological Society, London, Petroleum Geology Conference series, vol. 7, pp. 725–734, Geological Society of London., 2010.

Lüning, S.: North African Phanerozoic, in Phanerozoic in the Northern african basins, Encyclopedia of Geology, pp. 152–172, Elsevier., 2005.

Lüning, S., Craig, J., Loydell, D. K., Štorch, P. and Fitches, B.: Lower Silurian 'hot shales' in North Africa and Arabia: regional distribution and depositional model, Earth-Sci. Rev., 49(1–4), 121–200, doi:10.1016/S0012-8252(99)00060-4, 2000.

Lüning, S., Adamson, K. and Craig, J.: Frasnian organic-rich shales in North Africa: regional distribution and depositional model, Geol. Soc. Lond. Spec. Publ., 207(1), 165–184, doi:10.1144/GSL.SP.2003.207.9, 2003.

Lüning, S., Wendt, J., Belka, Z. and Kaufmann, B.: Temporal–spatial reconstruction of the early Frasnian (Late Devonian) anoxia in NW Africa: new field data from the Ahnet Basin (Algeria), Sediment. Geol., 163(3–4), 237–264, doi:10.1016/S0037-0738(03)00210-0, 2004.

Madritsch, H., Schmid, S. M. and Fabbri, O.: Interactions between thin-and thick-skinned tectonics at the northwestern front of the Jura fold-and-thrust belt (eastern France), Tectonics, 27(5), 1–31, doi:10.1029/2008TC002282, 2008.

Magloire, L.: Étude stratigraphique, par la Palynologie, des dépôts argilo-gréseux du Silurien et du Dévonien inférieur dans la Région du Grand Erg Occidental (Sahara Algérien), *Can. Soc. Pet. Geol.*, 2, 473–491, 1967.

Makhous, M. and Galushkin, Y. I.: Burial history and thermal evolution of the northern and eastern Saharan basins, *AAPG Bull.*, 87(10), 1623–1651, doi:10.1306/04300301122, 2003a.

Makhous, M. and Galushkin, Y. I.: Burial history and thermal evolution of the southern and western Saharan basins: Synthesis and comparison with the eastern and northern Saharan basins, *AAPG Bull.*, 87(11), 1799–1822, 2003b.

Marchal, D., Guiraud, M., Rives, T. and van den Driessche, J.: Space and time propagation processes of normal faults, *Geol. Soc. Lond. Spec. Publ.*, 147(1), 51–70, doi:10.1144/GSL.SP.1998.147.01.04, 1998.

Marchal, D., Guiraud, M. and Rives, T.: Geometric and morphologic evolution of normal fault planes and traces from 2D to 4D data, *J. Struct. Geol.*, 25(1), 135–158, doi:10.1016/S0191-8141(02)00011-1, 2003.

Massa, D.: Paléozoïque de Libye occidentale : stratigraphie et paléogéographie, Doctoral dissertation, Université de Nice, France., 1988.

Mélou, M., Oulebsir, L. and Paris, F.: Brachiopodes et chitinozoaires ordoviciens dans le NE du Sahara algérien: Implications stratigraphiques et paléogéographiques, *Geobios*, 32(6), 822–839, doi:10.1016/S0016-6995(99)80865-1, 1999.

Milani, E. J. and Zalan, P. V.: An outline of the geology and petroleum systems of the Paleozoic interior basins of South America, *Episodes*, 22, 199–205, 1999.

Milton, N. J., Bertram, G. T. and Vann, I. R.: Early Palaeogene tectonics and sedimentation in the Central North Sea, *Geol. Soc. Lond. Spec. Publ.*, 55(1), 339–351, 1990.

Moreau, C., Demaiffe, D., Bellion, Y. and Boullier, A.-M.: A tectonic model for the location of Palaeozoic ring complexes in Air (Niger, West Africa), *Tectonophysics*, 234(1), 129–146, 1994.

Mory, A. J., Zhan, Y., Haines, P. W., Hocking, R. M., Thomas, C. M. and Copp, I. A.: A paleozoic perspective of Western Australia, *Geological Survey of Western Australia.*, 2017.

Najem, A., El-Arnauti, A. and Bosnina, S.: Delineation of Paleozoic Tecto-stratigraphic Complexities in the Northern Part of Murzuq Basin-Southwest Libya, in *SPE North Africa Technical Conference and Exhibition*, Society of Petroleum Engineers., 2015.

Nikishin, A. M., Ziegler, P. A., Stephenson, R. A., Cloetingh, S., Furne, A. V., Fokin, P. A., Ershov, A. V., Bolotov, S. N., Korotaev, M. V. and Alekseev, A. S.: Late Precambrian to Triassic history of the East European Craton: dynamics of sedimentary basin evolution, *Tectonophysics*, 268(1–4), 23–63, 1996.

Ogg, J. G., Ogg, G. and Gradstein, F. M.: Introduction, in *A Concise Geologic Time Scale: 2016*, p. 3, Elsevier., 2016.

de Oliveira, D. C. and Mohriak, W. U.: Jaibaras trough: an important element in the early tectonic evolution of the Parnaíba interior sag basin, Northern Brazil, *Mar. Pet. Geol.*, 20(3), 351–383, doi:[https://doi.org/10.1016/S0264-8172\(03\)00044-8](https://doi.org/10.1016/S0264-8172(03)00044-8), 2003.

Oudra, M., Beraaouz, H., Ikenne, M., Gasquet, D. and Soulimani, A.: La Tectonique Panafricaine du Secteur d'Igherm: Implication des dômes extensifs tardi à post-orogéniques (Anti-Atlas occidental, Maroc), *Estud. Geológicas*, 61(3–6), 177–189, 2005.

Oulebsir, L. and Paris, F.: Chitinozoaires ordoviciens du Sahara algérien: biostratigraphie et affinités paléogéographiques, *Rev. Palaeobot. Palynol.*, 86(1), 49–68, doi:10.1016/0034-6667(94)00098-5, 1995.

Owen, G.: Senni Beds of the Devonian Old Red Sandstone, Dyfed, Wales: anatomy of a semi-arid floodplain, *Sediment. Geol.*, 95(3–4), 221–235, 1995.

Paris, F.: The Ordovician chitinozoan biozones of the Northern Gondwana domain, *Rev. Palaeobot. Palynol.*, 66(3–4), 181–209, doi:10.1016/0034-6667(90)90038-K, 1990.

Paris, F., Bourahrouh, A. and Hérisse, A. L.: The effects of the final stages of the Late Ordovician glaciation on marine palynomorphs (chitinozoans, acritarchs, leiospheres) in well NI-2 (NE Algerian Sahara), *Rev. Palaeobot. Palynol.*, 113(1–3), 87–104, doi:10.1016/S0034-6667(00)00054-3, 2000.

Peace, A., McCaffrey, K., Imber, J., van Hunen, J., Hobbs, R. and Wilson, R.: The role of pre-existing structures during rifting, continental breakup and transform system development, offshore West Greenland, *Basin Res.*, 30(3), 373–394, 2018.

Pemberton, S. G. and Frey, R. W.: Trace fossil nomenclature and the Planolites-Palaeophycus dilemma, *J. Paleontol.*, 56(4), 843–881, 1982.

Peucat, J. J., Drareni, A., Latouche, L., Deloule, E. and Vidal, P.: U–Pb zircon (TIMS and SIMS) and Sm–Nd whole-rock geochronology of the Gour Oumelalen granulitic basement, Hoggar massif, Tuareg shield, Algeria, *J. Afr. Earth Sci.*, 37(3–4), 229–239, doi:10.1016/j.jafrearsci.2003.03.001, 2003.

Peucat, J.-J., Capdevila, R., Drareni, A., Mahdjoub, Y. and Kahoui, M.: The Eglab massif in the West African Craton (Algeria), an original segment of the Eburnean orogenic belt:

petrology, geochemistry and geochronology, *Precambrian Res.*, 136(3–4), 309–352, doi:10.1016/j.precamres.2004.12.002, 2005.

Phillips, T. B., Jackson, C. A.-L., Bell, R. E. and Duffy, O. B.: Oblique reactivation of lithosphere-scale lineaments controls rift physiography – the upper-crustal expression of the Sorgenfrei–Tornquist Zone, offshore southern Norway, *Solid Earth*, 9(2), 403–429, doi:10.5194/se-9-403-2018, 2018.

Pinet, N., Lavoie, D., Dietrich, J., Hu, K. and Keating, P.: Architecture and subsidence history of the intracratonic Hudson Bay Basin, northern Canada, *Earth-Sci. Rev.*, 125, 1–23, doi:10.1016/j.earscirev.2013.05.010, 2013.

Potter, D.: Relationships of Cambro-Ordovician Stratigraphy to Paleotopography on the Precambrian Basement, Williston Basin, *Sask. Geol. Soc.*, 63–73, 2006.

Reading, H. G. and Collinson, J. D.: Clastic coasts, in *Sedimentary environments: processes, facies, and stratigraphy*, pp. 154–231, John Wiley & Sons, Oxford ; Cambridge, Mass., 2009.

Rider, M. H.: Facies, Sequences and Depositional Environments from Logs, in *The geological interpretation of well logs*, pp. 226–238, Whittles Publishing, Caithness, Scotland., 1996.

Rougier, S., Missenard, Y., Gautheron, C., Barbarand, J., Zeyen, H., Pinna, R., Liégeois, J.-P., Bonin, B., Ouabadi, A., Derder, M. E.-M. and Lamotte, D. F. de: Eocene exhumation of the Tuareg Shield (Sahara Desert, Africa), *Geology*, 41(5), 615–618, doi:10.1130/G33731.1, 2013.

Sabaou, N., Ait-Salem, H. and Zazoun, R. S.: Chemostratigraphy, tectonic setting and provenance of the Cambro-Ordovician clastic deposits of the subsurface Algerian Sahara, *J. Afr. Earth Sci.*, 55(3–4), 158–174, doi:10.1016/j.jafrearsci.2009.04.006, 2009.

Schlische, R. W.: Geometry and origin of fault-related folds in extensional settings, *AAPG Bull.*, 79(11), 1661–1678, 1995.

Slater, J. G. and Christie, P. A. F.: Continental stretching: An explanation of the Post-Mid-Cretaceous subsidence of the central North Sea Basin, *J. Geophys. Res. Solid Earth*, 85(B7), 3711–3739, doi:10.1029/JB085iB07p03711, 1980.

Scotese, C. R., Boucot, A. J. and McKerrow, W. S.: Gondwanan palaeogeography and paleoclimatology, *J. Afr. Earth Sci.*, 28(1), 99–114, doi:10.1016/S0899-5362(98)00084-0, 1999.

Serra, O. and Serra, L.: Well logging, facies, sequence and environment, in *Well logging and geology*, pp. 197–238, Technip Editions, France., 2003.

Sharata, S., Röth, J. and Reicherter, K.: Basin evolution in the North African Platform, *Geotecton. Res.*, 97(1), 80–81, doi:10.1127/1864-5658/2015-31, 2015.

Shaw, J. H., Connors, C. D. and Suppe, J.: Recognizing growth strata, in *Seismic interpretation of contractional fault-related folds: an AAPG seismic atlas*, vol. 53, pp. 11–14, American Association of Petroleum Geologists, Tulsa, Okla., U.S.A., 2005.

Sloss, L. L.: Sequences in the cratonic interior of North America, *Geol. Soc. Am. Bull.*, 74(2), 93–114, 1963.

Smart, J.: Seismic expressions of depositional processes in the upper Ordovician succession of the Murzuq Basin, SW Libya, in *Geological Exploration in Murzuq Basin*, edited by M. A. Sola and D. Worsley, pp. 397–415, Elsevier Science B.V., Amsterdam., 2000.

Soares, P. C., Landim, P. M. B. and Fulfaro, V. J.: Tectonic cycles and sedimentary sequences in the Brazilian intracratonic basins, *GSA Bull.*, 89(2), 181–191, doi:10.1130/0016-7606(1978)89<181:TCASSI>2.0.CO;2, 1978.

Stearns, D. W.: Faulting and forced folding in the Rocky Mountains foreland, Laramide Fold. Assoc. Basement Block Faulting West. U. S. Geol. Soc. Am. Mem., 151, 1–37, 1978.

Stow, D. a. V. and Piper, D. J. W.: Deep-water fine-grained sediments: facies models, *Geol. Soc. Lond. Spec. Publ.*, 15(1), 611–646, doi:10.1144/GSL.SP.1984.015.01.38, 1984.

Stow, D. A. V., Huc, A.-Y. and Bertrand, P.: Depositional processes of black shales in deep water, *Mar. Pet. Geol.*, 18(4), 491–498, doi:10.1016/S0264-8172(01)00012-5, 2001.

Suter, J. R.: Facies models revisited: clastic shelves, *Spec. Publ.-SEPM*, 84, 339, 2006.

Tournier, F.: Mécanismes et contrôle des phénomènes diagénétiques en milieu acide dans les grès de l'Ordovicien glaciaire du bassin de Sbaa, Algérie, Doctoral dissertation, Université de Paris 11, France., 2010.

Trompette, R.: Gondwana evolution; its assembly at around 600 Ma, *Comptes Rendus Académie Sci.-Ser. IIA-Earth Planet. Sci.*, 330(5), 305–315, 2000.

Turner, G. M., Rasson, J. L. and Reeves, C. V.: Observation and Measurement Techniques, in *Treatise on Geophysics*, vol. 5, edited by G. Schubert, pp. 33–75, Blackwell Pub, Malden, MA., 2007.

Ustaszewski, K., Schumacher, M., Schmid, S. and Nieuwland, D.: Fault reactivation in brittle–viscous wrench systems—dynamically scaled analogue models and application to the Rhine–Bresse transfer zone, *Quat. Sci. Rev.*, 24(3–4), 363–380, doi:10.1016/j.quascirev.2004.03.015, 2005.

Van Hinte, J. E.: Geohistory analysis—application of micropaleontology in exploration geology, *AAPG Bull.*, 62(2), 201–222, 1978.

Vauchez, A., Tommasi, A. and Barruol, G.: Rheological heterogeneity, mechanical anisotropy and deformation of the continental lithosphere, *Tectonophysics*, 296(1–2), 61–86, doi:10.1016/S0040-1951(98)00137-1, 1998.

Vecoli, M.: Palaeoenvironmental interpretation of microphytoplankton diversity trends in the Cambrian–Ordovician of the northern Sahara Platform, *Palaeogeogr. Palaeoclimatol. Palaeoecol.*, 160(3–4), 329–346, doi:10.1016/S0031-0182(00)00080-8, 2000.

Vecoli, M. and Playford, G.: Stratigraphically significant acritarchs in uppermost Cambrian to basal Ordovician strata of Northwestern Algeria, *Grana*, 36(1), 17–28, doi:10.1080/00173139709362585, 1997.

Vecoli, M., Albani, R., Ghomari, A., Massa, D. and Tongiorgi, M.: Précisions sur la limite Cambrien-Ordovicien au Sahara Algérien (Secteur de Hassi-Rmel), *Comptes Rendus Académie Sci. Sér. 2 Sci. Terre Planètes*, 320(6), 515–522, 1995.

Vecoli, M., Tongiorgi, M., Abdesselam-Roughi, F. F., Benzarti, R. and Massa, D.: Palynostratigraphy of upper Cambrian-upper Ordovician intracratonic clastic sequences, North Africa, *Boll.-Soc. Paleontol. Ital.*, 38(2/3), 331–342, 1999.

Vecoli, M., Videt, B. and Paris, F.: First biostratigraphic (palynological) dating of Middle and Late Cambrian strata in the subsurface of northwestern Algeria, North Africa: Implications for regional stratigraphy, *Rev. Palaeobot. Palynol.*, 149(1–2), 57–62, doi:10.1016/j.revpalbo.2007.10.004, 2008.

Videt, B., Paris, F., Rubino, J.-L., Boumendjel, K., Dabard, M.-P., Loi, A., Ghienne, J.-F., Marante, A. and Gorini, A.: Biostratigraphical calibration of third order Ordovician sequences on the northern Gondwana platform, *Palaeogeogr. Palaeoclimatol. Palaeoecol.*, 296(3–4), 359–375, doi:10.1016/j.palaeo.2010.03.050, 2010.

Wagoner, J. C. V., Mitchum, R. M., Campion, K. M. and Rahmanian, V. D.: *Siliciclastic Sequence Stratigraphy in Well Logs, Cores, and Outcrops: Concepts for High-Resolution Correlation of Time and Facies*, AAPG Methods Explor. Ser. No 7, 174, III–55, 1990.

Watts, A. B.: *Isostasy and Flexure of the Lithosphere*, Cambridge University Press, Oxford University., 2001.

Wendt, J.: Disintegration of the continental margin of northwestern Gondwana: Late Devonian of the eastern Anti-Atlas (Morocco), *Geology*, 13(11), 815–818, 1985.

Wendt, J.: Facies Pattern and Paleogeography of the Middle and Late Devonian in the Eastern Anti-Atlas (Morocco), *Can. Soc. Pet. Geol.*, 1(14), 467–480, 1988.

Wendt, J.: Shell directions as a tool in palaeocurrent analysis, *Sediment. Geol.*, 95(3), 161–186, doi:10.1016/0037-0738(94)00104-3, 1995.

Wendt, J. and Kaufmann, B.: Mud buildups on a Middle Devonian carbonate ramp (Algerian Sahara), *Geol. Soc. Lond. Spec. Publ.*, 149(1), 397–415, doi:10.1144/GSL.SP.1999.149.01.18, 1998.

Wendt, J., Belka, Z. and Moussine-Pouchkine, A.: New architectures of deep-water carbonate buildups: Evolution of mud mounds into mud ridges (Middle Devonian, Algerian Sahara), *Geology*, 21(8), 723–726, 1993.

Wendt, J., Belka, Z., Kaufmann, B., Kostrewa, R. and Hayer, J.: The world's most spectacular carbonate mud mounds (Middle Devonian, Algerian Sahara), *J. Sediment. Res.*, 67(3), 424–436, doi:10.1306/D426858B-2B26-11D7-8648000102C1865D, 1997.

Wendt, J., Kaufmann, B., Belka, Z., Klug, C. and Lubeseder, S.: Sedimentary evolution of a Palaeozoic basin and ridge system: the Middle and Upper Devonian of the Ahnet and Mouydir (Algerian Sahara), *Geol. Mag.*, 143(3), 269–299, doi:10.1017/S0016756806001737, 2006.

Wendt, J., Kaufmann, B., Belka, Z. and Korn, D.: Carboniferous stratigraphy and depositional environments in the Ahnet Mouydir area (Algerian Sahara), *Facies*, 55(3), 443–472, doi:10.1007/s10347-008-0176-y, 2009a.

Wendt, J., Kaufmann, B. and Belka, Z.: Devonian stratigraphy and depositional environments in the southern Illizi Basin (Algerian Sahara), *J. Afr. Earth Sci.*, 54(3–4), 85–96, doi:10.1016/j.jafrearsci.2009.03.006, 2009b.

Withjack, M. O. and Callaway, S.: Active normal faulting beneath a salt layer: an experimental study of deformation patterns in the cover sequence, *AAPG Bull.*, 84(5), 627–651, 2000.

Withjack, M. O., Olson, J. and Peterson, E.: Experimental models of extensional forced folds, *AAPG Bull.*, 74(7), 1038–1054, 1990.

Withjack, M. O., Schlische, R. W. and Olsen, P. E.: Rift-basin structure and its influence on sedimentary systems, *Soc. Sediment. Geol. Spec. Publ.*, (73), 57–81, 2002.

Xie, X. and Heller, P.: Plate tectonics and basin subsidence history, *Geol. Soc. Am. Bull.*, 121(1–2), 55–64, doi:10.1130/B26398.1, 2009.

Yahi, N.: Petroleum generation and migration in the Berkine (Ghadames) Basin, Eastern Algeria: an organic geochemical and basin modelling study, Doctoral dissertation, Forschungszentrum, Zentralbibliothek, Jülich., 1999.

Zalan, P. V., Wolff, S., Astolfi, M. A. M., Vieira, I. S., Concelcao, J. C. J., Appi, V. T., Neto, E. V. S., Cerqueira, J. R. and Marques, A.: The Parana Basin, Brazil: Chapter 33: Part II. Selected Analog Interior Cratonic Basins: Analog Basins, , 134, 681–708, 1990.

Zazoun, R. S.: Hercynian deformation in the western Ahnet Basin and Bled El-Mass area, Algerian Sahara: a continuous strain, *J. Afr. Earth Sci.*, 32(4), 869–887, 2001.

Zazoun, R. S.: The Fadnoun area, Tassili-n-Azdjer, Algeria: Fracture network geometry analysis, *J. Afr. Earth Sci.*, 50(5), 273–285, doi:10.1016/j.jafrearsci.2007.10.001, 2008.

Zazoun, R. S. and Mahdjoub, Y.: Strain analysis of Late Ordovician tectonic events in the In-Tahouite and Tamadjert Formations (Tassili-n-Ajjers area, Algeria), *J. Afr. Earth Sci.*, 60(3), 63–78, doi:10.1016/j.jafrearsci.2011.02.003, 2011.

## List of figures

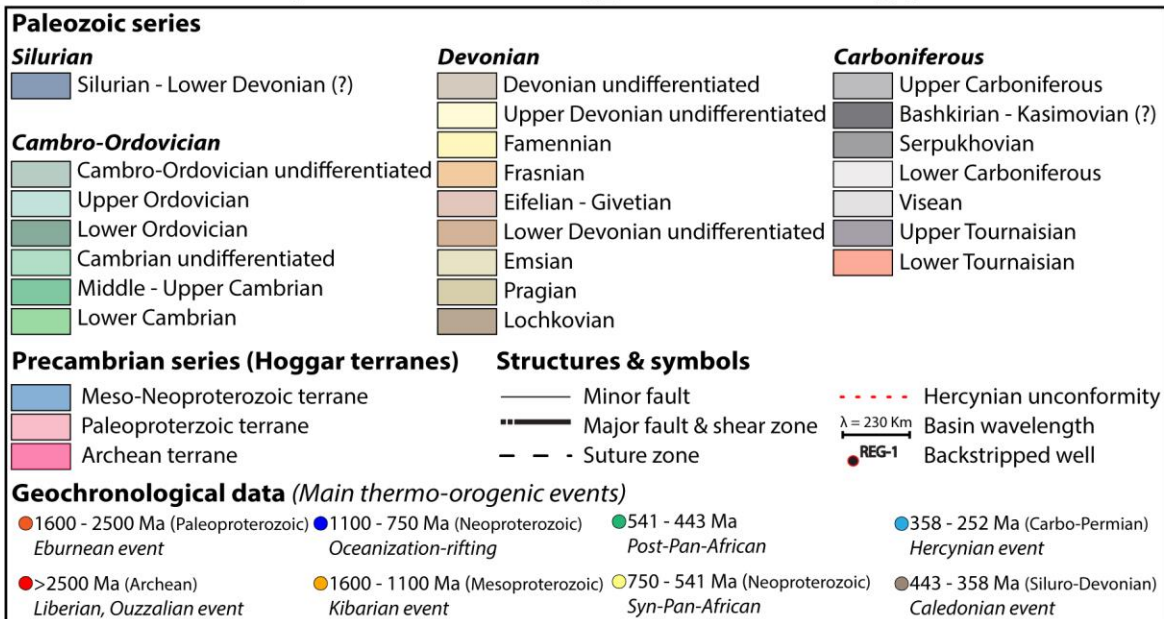
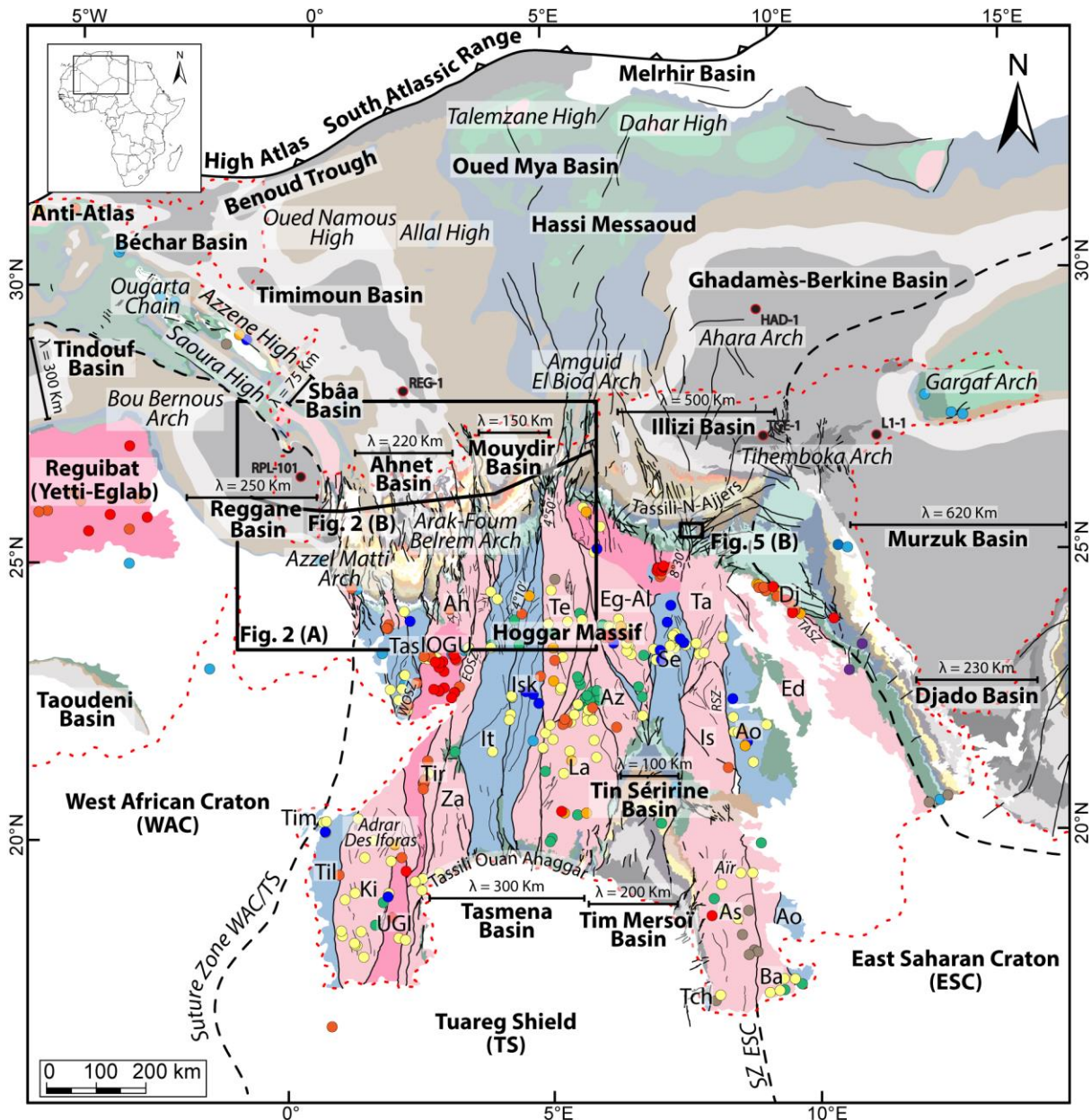


Figure 1: Geological map of the Paleozoic North Saharan Platform (North Gondwana) georeferenced, compiled and modified from (1) Paleozoic subcrop distribution below the Hercynian unconformity geology of the Saharan Platform (Boote et al., 1998; Galeazzi et al., 2010); (2) Geological map (1/500,000) of the Djado basin (Jacquemont et al., 1959); (3) Geological map (1/200,000) of Algeria (Bennacef et al., 1974; Bensalah et al., 1971), (4) Geological map (1/50,000) of Aïr (Joulià, 1963), (5) Geological map (1/2,000,000) of Niger (Greigertt and Pougnet, 1965), (6) Geological map (1/5,000,000) of the Lower Paleozoic of the Central Sahara (Beuf et al., 1971), (7) Geological map (1/1,000,000) of Morocco (Hollard et al., 1985), (8) Geological map of the Djebel Fezzan (Massa, 1988); Basement characterization of the different terranes from geochronological data compilation (see supplementary data) and geological maps (Berger et al., 2014; Bertrand and Caby, 1978; Black et al., 1994; Caby, 2003; Fezaa et al., 2010; Liégeois et al., 1994, 2003, 2005, 2013); Terrane names: Tassendjanet (Tas), Tassendjanet nappe (Tas n.), Ahnet (Ah), In Ouzzal Granulitic Unit (IOGU), Iforas Granulitic Unit (UGI), Kidal (Ki), Timétrine (Tim), Tilemsi (Til), Tirek (Tir), In Zaouatene (Za), In Teidini (It), Iskel (Isk), Tefedest (Te), Laouni (La), Azrou-n-Fad (Az), Egéré-Aleskod (Eg-Al), Serouenout (Se), Tazat (Ta), Issalane (Is), Assodé (As), Barghot (Ba), Tchilit (Tch), Aouzegueur (Ao), Edembo (Ed), Djanet (Dj); Shear zone and lineament names: Suture Zone East Saharan Craton (SZ ESC), West Ouzzal Shear Zone (WOSZ), East Ouzzal Shear Zone (EOSZ), Raghane Shear Zone (RSZ), Tin Amali Shear Zone (TASZ), 4°10' Shear Zone, 4°50' Shear Zone, 8°30' Shear Zone.

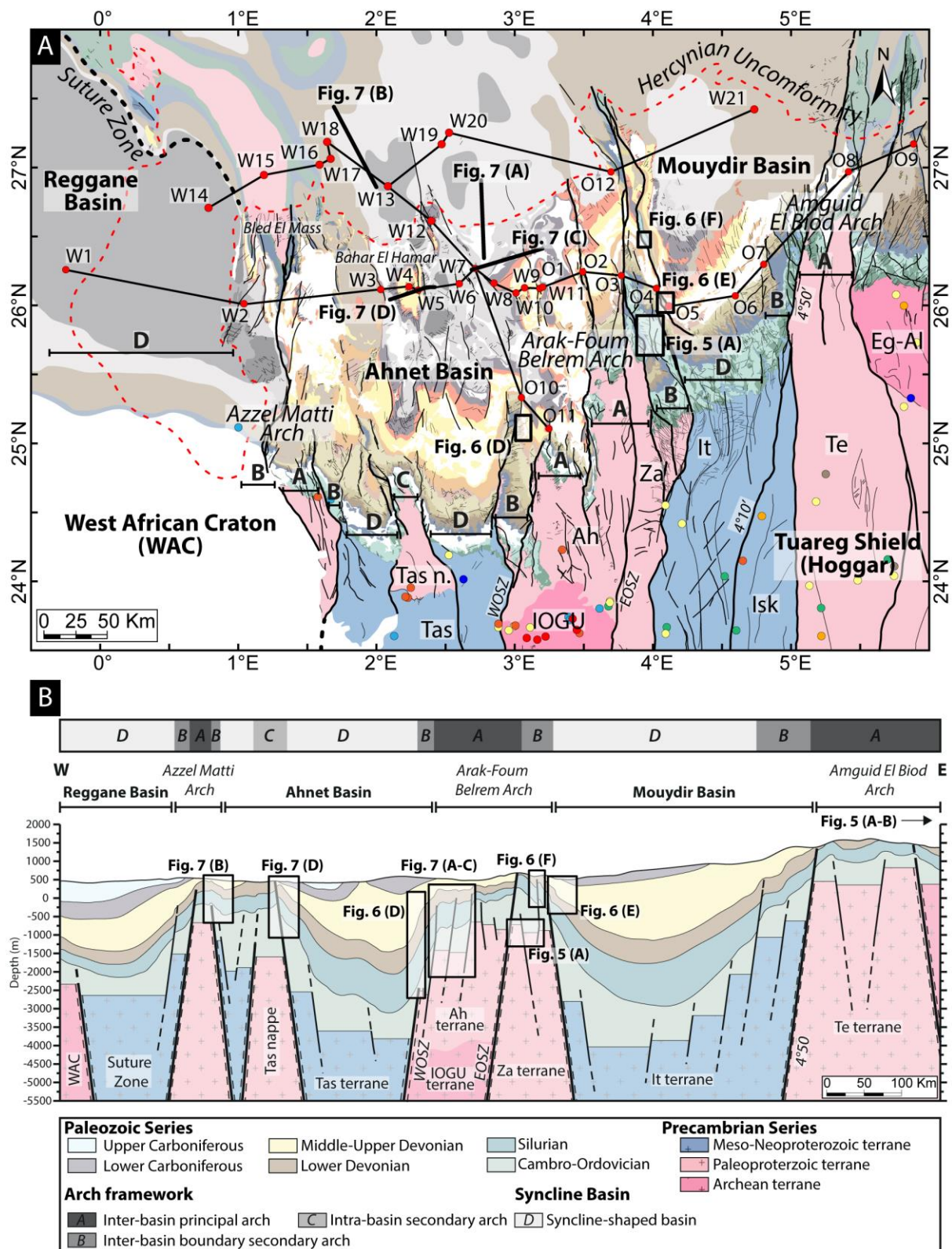


Figure 2: (A) Geological map of the Paleozoic of the Reggane, Ahnet, and Mouydir basins. Legend and references see Fig. 1. **A: Inter-basin principal arch, B: Inter-basin boundary secondary arch, C: Intra-basin secondary arch, D: Syncline-shaped basin.** (B) E-W cross-

section of the Reggane, Ahnet, and Mouydir basins associated with the different terranes and highlighting the classification of the different structural units (~~A: Inter-basin principal arch, B: Inter-basin boundary secondary arch, C: Intra-basin arch, D: Syncline-shaped basin~~). Localization of the interpreted sections (seismic profiles and satellite images). W=Well and O=Outcrop. See figure 1 for location of the geological map A and cross section B.

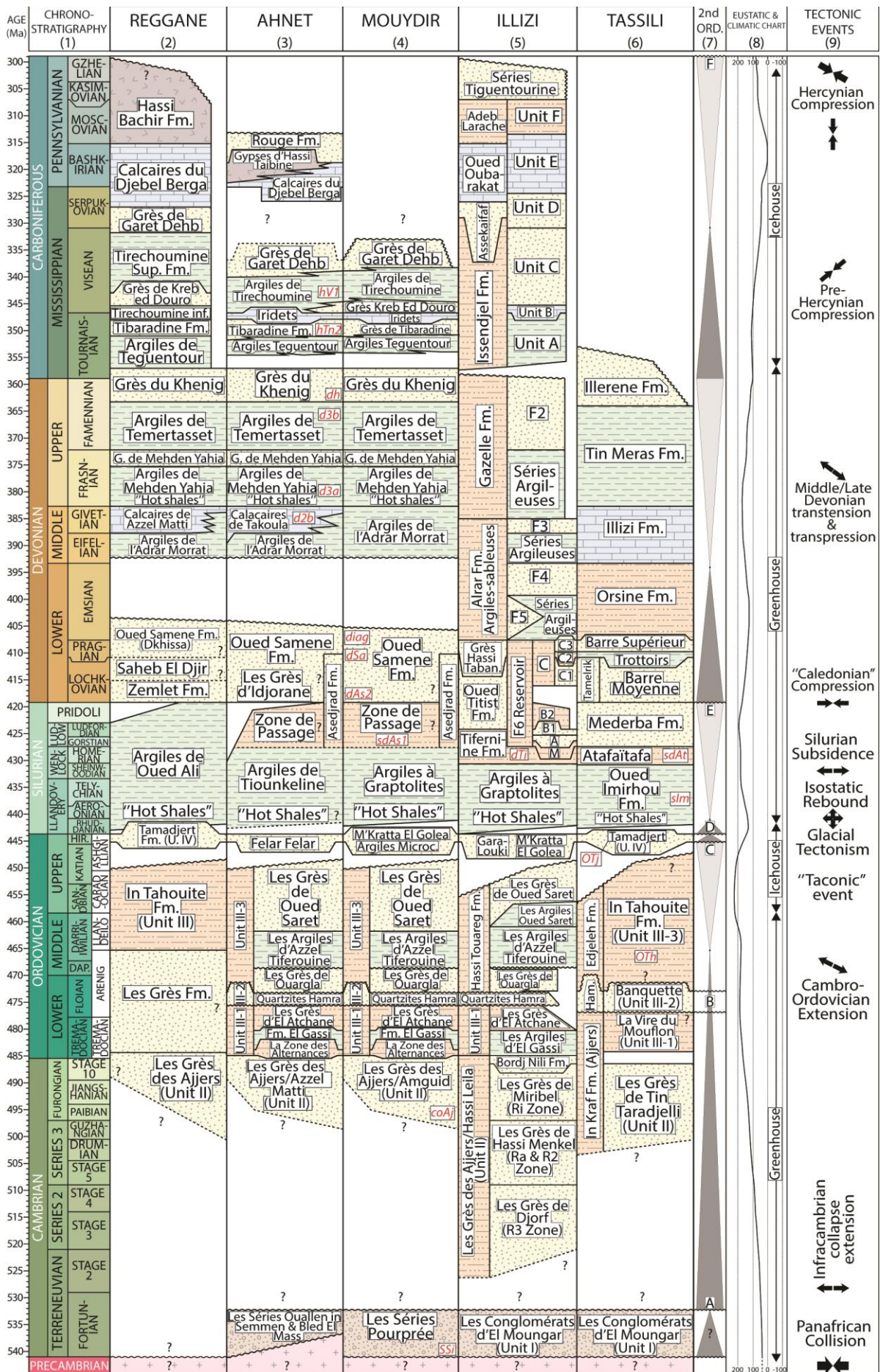


Figure 3.2: Paleozoic litho-stratigraphic, sequence stratigraphy and tectonic framework of the North Peri-Hoggar basins (North African Saharan Platform) compiled from (1) Chronostratigraphic chart (Ogg et al., 2016), (2) The Cambrian–Silurian (Askri et al., 1995) and the Devonian–Carboniferous stratigraphy of the Reggane basin (Cózar et al., 2016; Lubeseder, 2005; Lubeseder et al., 2010; Magloire, 1967; Wendt et al., 2006), (3) The Cambrian–Silurian (Paris, 1990; Wendt et al., 2006) and the Devonian–Carboniferous stratigraphy of the Ahnet basin (Beuf et al., 1971; Conrad, 1973, 1984; Legrand-Blain, 1985; Wendt et al., 2006, 2009a), (4) The Cambrian–Silurian (Askri et al., 1995; Paris, 1990; Videt et al., 2010) and the Devonian–Carboniferous stratigraphy of the Mouydir basin (Askri et al., 1995; Beuf et al., 1971; Conrad, 1973, 1984; Wendt et al., 2006, 2009a), (5) The Cambrian–Silurian (Eschard et al., 2005; Fekirine and Abdallah, 1998; Jardiné and Yapaudjian, 1968; Videt et al., 2010) and the Devonian–Carboniferous stratigraphy of the Illizi basin (Eschard et al., 2005; Fekirine and Abdallah, 1998; Jardiné and Yapaudjian, 1968), (6) The Cambrian–Silurian (Dubois, 1961; Dubois and Mazelet, 1964; Eschard et al., 2005; Henniche, 2002; Videt et al., 2010) and the Devonian–Carboniferous stratigraphy of the Tassili-N-Ajjers (Dubois et al., 1967; Eschard et al., 2005; Henniche, 2002; Wendt et al., 2009a), (7) Sequence stratigraphy of the Saharan Platform (Carr, 2002; Eschard et al., 2005; Fekirine and Abdallah, 1998), (8) Eustatic and climatic chart (Haq and Schutter, 2008; Scotese et al., 1999), (9) Tectonic events (Boudjema, 1987; Coward and Ries, 2003; Craig et al., 2008; Guiraud et al., 2005; Lüning, 2005); (A) Infra-Tassilian (Pan-African) unconformity, (B) Intra-Arenig unconformity, (C) Taconic and glacial unconformity, (D) Isostatic rebound unconformity, (E) Caledonian unconformity, (F) Hercynian unconformity.

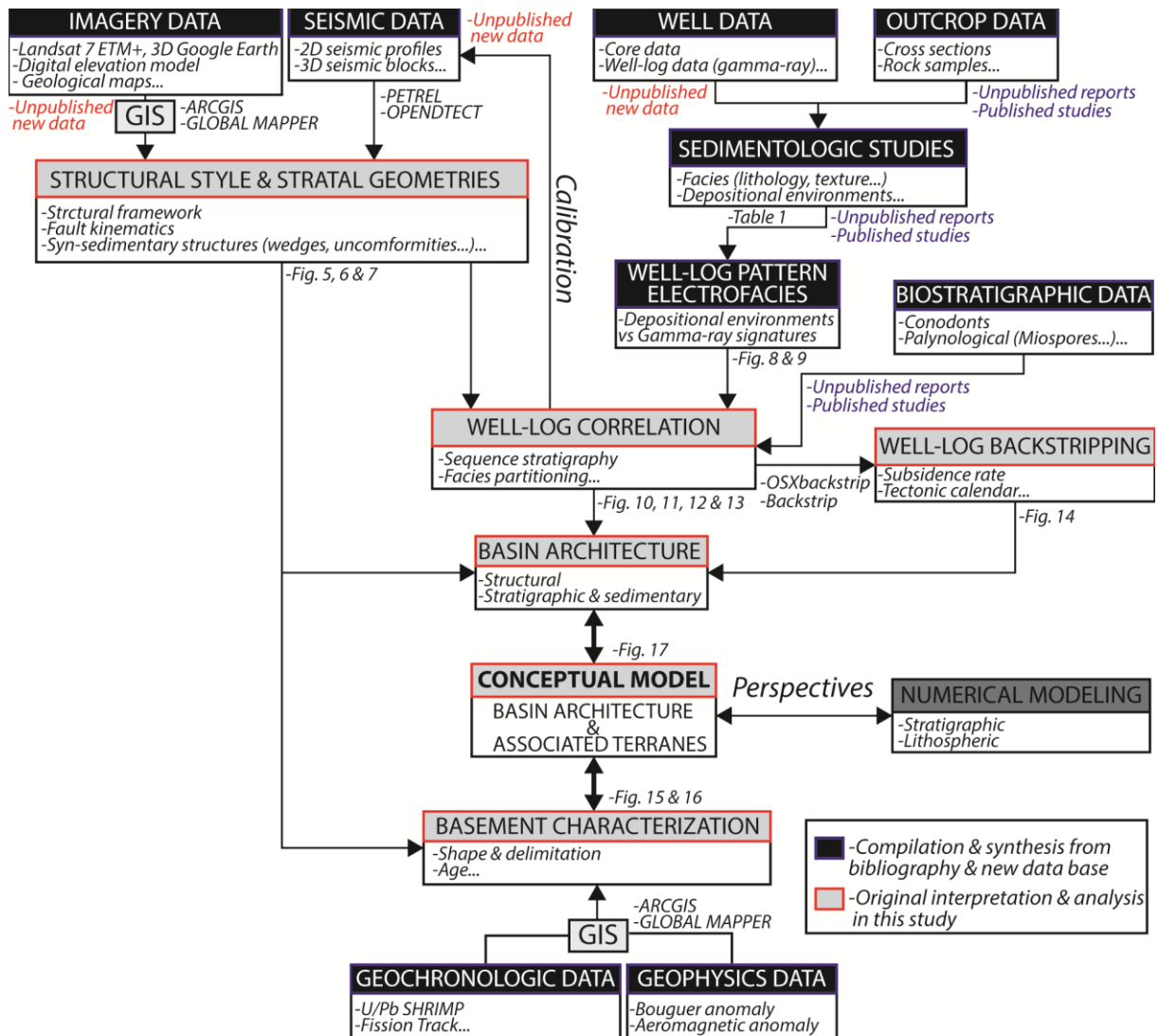


Figure 4: Schematic synthesis of the integrated method of basin analysis in this study.

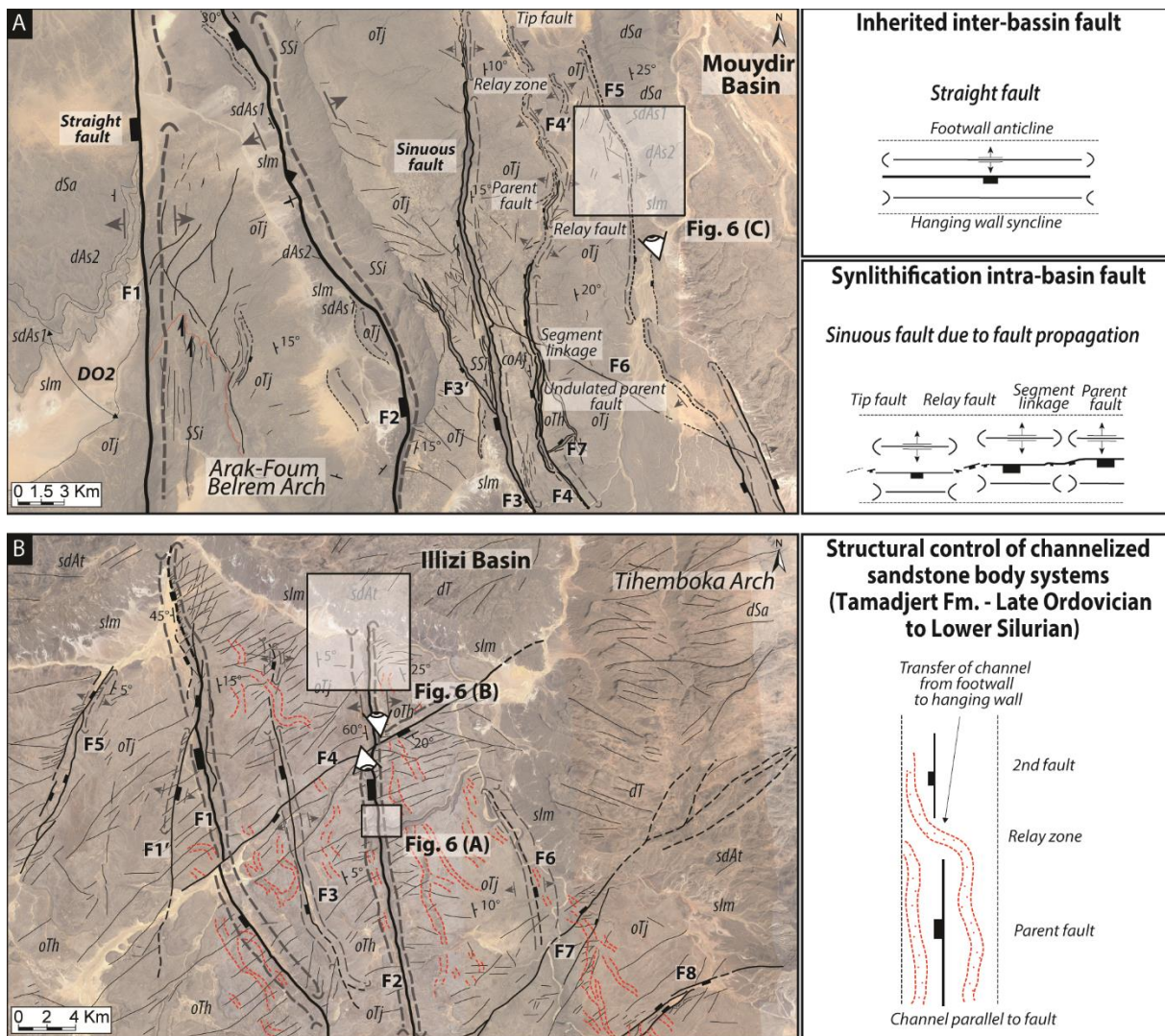


Figure 5 4: (A) Google Earth satellite images Structural interpretation of the Djebel Settaf (Arak Foum Belrem arch; inter basin boundary secondary arch between the Ahnet and Mouydir basins) of the Cambrian Ordovician series showing straight and sinuous normal faults; (A') Typology of different types of faults (inherited straight faults vs sinuous short synlithification propagation faults) in the Cambrian Ordovician series of the Djebel Settaf (Arak-Foum Belrem arch; inter-basin boundary secondary arch between the Ahnet and Mouydir basins). (B) Google Earth satellite images Structural interpretation normal fault propagation in Cambrian Ordovician series of South Adrar Assaouatene, Tassili N Ajjers (Tihemboka inter basin boundary secondary arch between the Illizi and Murzuq basins); (B') Schematic model of Structural control of channelized sandstone bodies in Late Ordovician series of South Adrar

Assaouatene, Tassili-N-Ajjers (Tihemboka inter-basin boundary secondary arch between the Illizi and Murzuq basins). Dotted red line: Tamadjert Fm. channelized sandstone bodies. *OTh*: In Tahouite Fm. (Early to Late Ordovician, Floian to Katian), *OTj*: Tamadjert Fm. (Late Ordovician, Hirnantian), *sIm*: Imirhou Fm. (Early Silurian), *sdAs1*: Asedjrad Fm. 1 (Late Silurian to Early Devonian), *dAs2*: Asedjrad Fm. 2 (Early Devonian, Lochkovian), *dSa*: Oued Samene Fm. (Lower Devonian, Pragian). See Fig. [3 2](#) for map and cross-section location.

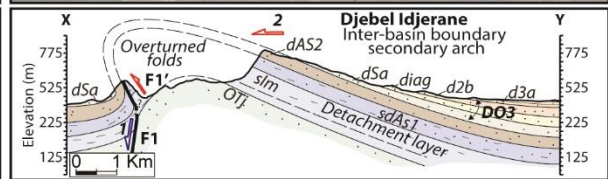
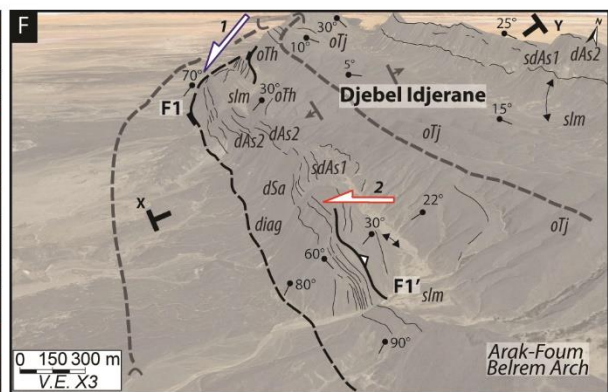
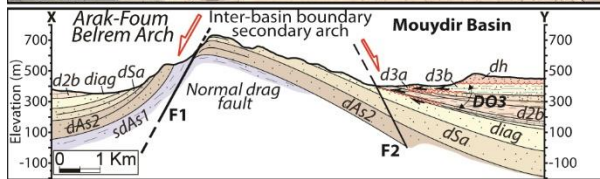
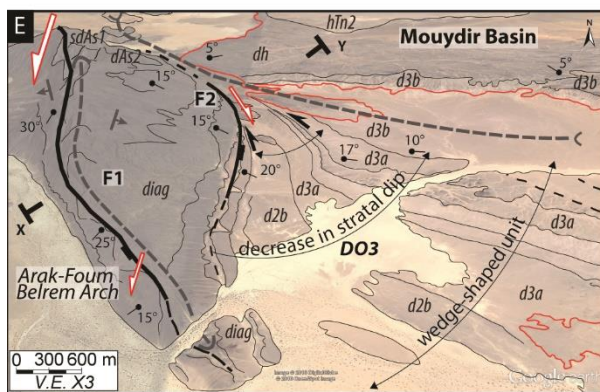
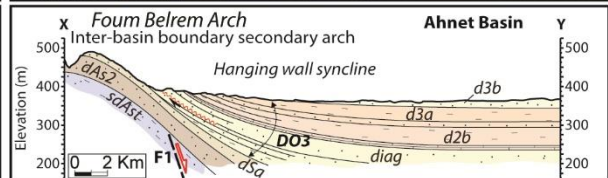
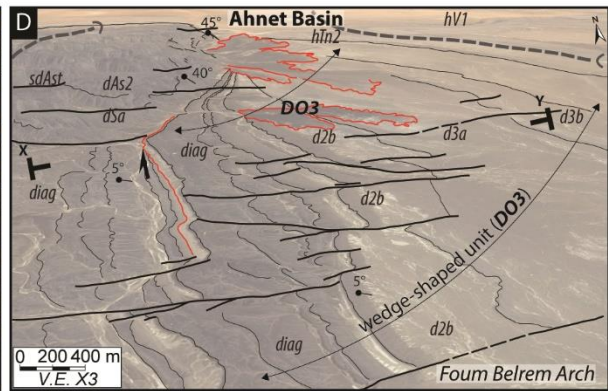
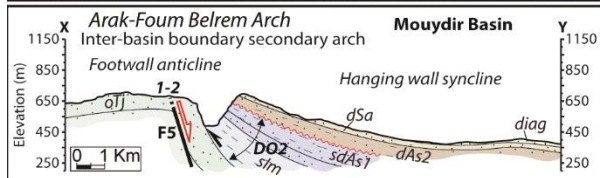
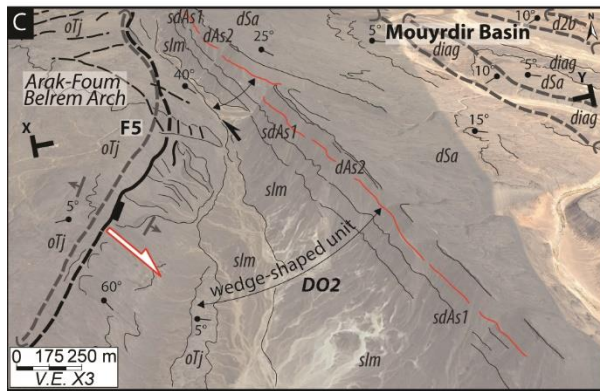
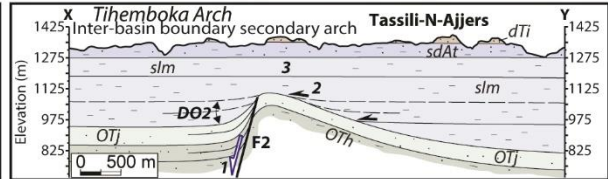
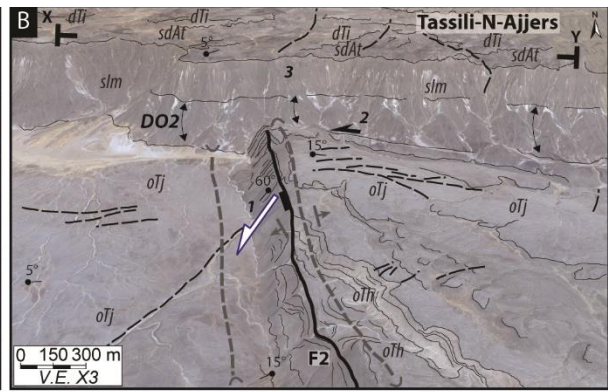
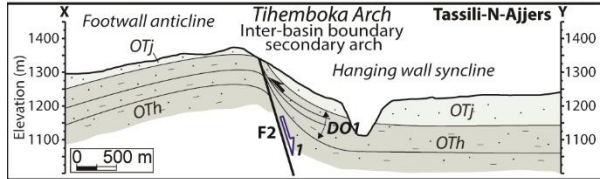
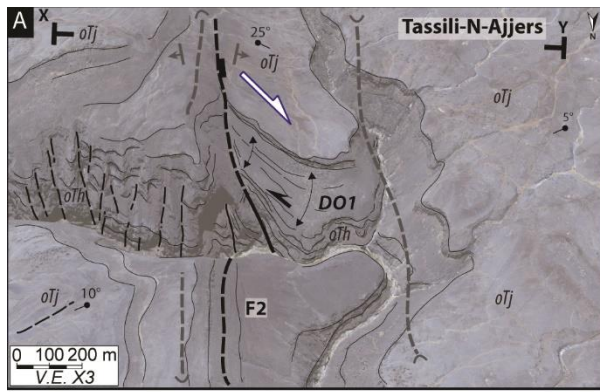


Figure 6 5: (A) ~~Google Earth satellite images structural interpretation of South Adrar Assaouatene, Tassili N Ajjers (Tihemboka inter basin boundary secondary arch between the Illizi and Murzuq basins) showing a Normal fault (F2) associated with a footwall anticline and a hanging wall syncline with divergent onlaps (i.e. wedge-shaped unit DO1) in the Early to Late Ordovician In Tahouite series (Tassili-N-Ajjers, Tihemboka inter-basin boundary secondary arch between the Illizi and Murzuq basins); (A') Cross section between XY. 1: Cambrian–Ordovician extension during the deposition of In Tahouite series (Early to Late Ordovician). See fig. 4B for location.~~ (B) ~~Google Earth satellite images structural interpretation of North Adrar Assaouatene, Tassili N Ajjers (Tihemboka inter basin boundary secondary arch between the Illizi and Murzuq basins) showing an Ancient normal fault F2 escarpment reactivated and sealed during Silurian deposition (poly-historic paleo-reliefs) linked to thickness variation, divergent onlaps (DO2) in the hanging wall synclines, and onlaps on the fold hinge anticline (Tassili-N-Ajjers, Tihemboka inter-basin boundary secondary arch between the Illizi and Murzuq basins); (B') Cross section between X'Y'. 1: Early to Late Ordovician extension, 2: Late Ordovician to Early Silurian extension, 3: Middle to Late Silurian sealing (horizontal drape). See fig. 4B for location.~~ (C) ~~Google Earth satellite images structural interpretation of Dejbél Settaf (Arak Foug Belrem arch; inter basin boundary secondary arch between the Mouydir and Ahnet basins) showing a Normal fault (F5) associated with forced fold with divergent strata (syncline-shaped hanging wall syncline and associated wedge-shaped unit DO2) and truncation in Silurian–Devonian series of Dejbél Settaf (Arak-Foug Belrem arch; inter-basin boundary secondary arch between the Mouydir and Ahnet basins); (C') Cross section between XY. 1: Cambrian–Ordovician extension, 2: Silurian–Devonian extensional reactivation (Caledonian extension). Red line: Unconformity. See fig. 4A for location.~~ (D) ~~Google Earth satellite images structural interpretation in the Ahnet basin (Arak Foug Belrem arch; inter basin boundary secondary arch between the Mouydir and Ahnet basins) showing~~

Blind basement normal fault (F1) associated with forced fold with in the hanging wall syncline divergent onlaps of Lower to Upper Devonian series (wedge-shaped unit DO3) and intra-Emsian truncation (Arak-Foum Belrem arch; inter-basin boundary secondary arch between the Mouydir and Ahnet basins); ~~(D<sup>2</sup>) Cross section between X'Y'~~. (E) ~~Google Earth satellite images structural interpretation in the Mouydir basin (near Arak-Foum Belrem arch, eastward inter-basin boundary secondary arch) showing~~ N170° normal blind faults F1 and F2 forming a horst-graben system associated with forced fold with Lower to Upper Devonian series divergent onlaps (wedge-shaped unit DO3) and intra-Emsian truncation in the hanging-wall syncline (in the Mouydir basin near Arak-Foum Belrem arch, eastward inter-basin boundary secondary arch); ~~(E<sup>2</sup>) Cross section between XY~~. (F) ~~Google Earth satellite images structural interpretation of Djebel Idjerane in the Mouydir basin (Arak-Foum Belrem arch, eastwards inter-basin boundary secondary arch) showing an~~ Inherited normal fault F1 transported from footwall to hanging wall associated with inverse fault F1' and accommodated by a detachment layer in Silurian shales series (thickness variation of Imirhou Fm. between footwall and hanging wall) and spilled dip strata markers of overturned folding (Djebel Idjerane, Arak-Foum Belrem arch, eastwards inter-basin boundary secondary arch); ~~(F<sup>2</sup>) Cross section between X'Y'~~. 1: Cambrian–Ordovician extension, 2: Middle to Late Devonian compression. *OTh*: In Tahouite Fm. (Early to Late Ordovician, Floian to Katian), *OTj*: Tamadjert Fm (Late Ordovician, Hirnantian), *sIm*: Imirhou Fm. (Early to Mid Silurian), *sdAt*: Atafaitafa Fm. (Middle Silurian), *dTi*: Tifernine Fm. (Middle Silurian), *sdAs1*: Asedjrad Fm. 1 (Late Silurian to Early Devonian), *dAs2*: Asedjrad Fm. 2 (Early Devonian, Lochkovian), *dSa*: Oued Samene Fm. (Early Devonian, Pragian), *diag*: Oued Samene shaly-sandstones Fm. (Early Devonian, Emsian?), *d2b*: Givetian, *d3a*: Mehden Yahia Fm. (Late Devonian, Frasnian), *d3b*: Mehden Yahia Fm. (Late Devonian, Famennian), *dh*: Khenig sandstones (late Famennian to early Tournaisian), *hTn2*: late

Tournaisian, *hVI*: early Viséan. Red line: Unconformity. See Figs. 1, 2 and 3 5 for map and cross-section location.

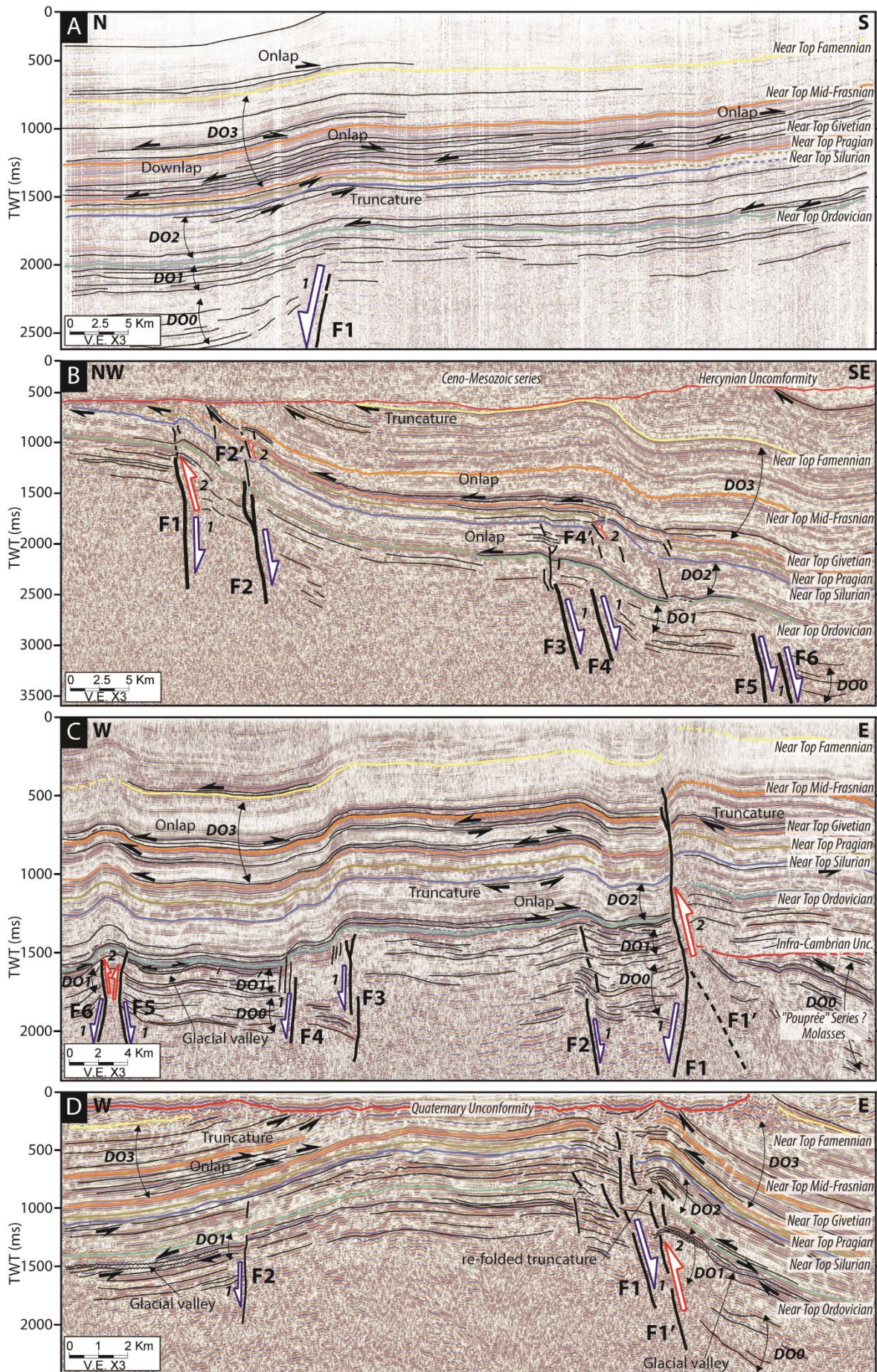


Figure 7 6: (A) N–S interpreted seismic profile in the Ahnet basin near Erg Teguentour (near Arak-Foum Belrem arch, westward inter-basin boundary secondary arch) showing steeply-dipping northward basement normal blind faults associated with forced folding. ~~Strata layout geometries shows Lower Silurian onlaps on the top Ordovician, Upper Silurian and Lower Devonian truncations, onlaps and downlaps of Frasnian series on top Givetian unit and onlap near top Famennian.~~ (B) NW–SE interpreted seismic profile of near Azzel Matti arch (inter-basin principal arch) showing steeply-dipping south-eastwards basement normal blind faults associated with forced folds. The westernmost structures are featured by reverse fault related propagation fold. ~~Strata layout geometries show Silurian onlaps on top Ordovician, Frasnian onlaps, thinning of Frasnian and Silurian series near the arch; truncation of Paleozoic series by Mesozoic unit on Hercynian unconformity.~~ (C) W–E interpreted profile of the Ahnet basin (Arak-Foum Belrem arch, westward inter-basin boundary secondary arch) showing horst and graben structures influencing Paleozoic tectonics associated with forced folds. ~~Strata layout geometries show Precambrian basement tilted structure overlain by Cambrian Ordovician angular unconformity, incised valley in the Ordovician series, Silurian onlaps on top Ordovician, Silurian onlaps on top Ordovician, Silurian Devonian truncation, Frasnian onlaps on top Givetian and near top Famennian onlaps.~~ (D) W–E interpreted seismic profile of Bahar el Hammar in the Ahnet basin (Ahnet intra-basin secondary arch) showing steeply-dipping normal faults F1 and F2 forming a horst positively inverted associated with folding. ~~Strata layout geometries show glacial valley in the Ordovician series, Silurian onlaps on top Ordovician, Silurian onlaps on top Ordovician; Silurian Devonian truncation re folded, Frasnian onlaps on top Givetian.~~ Multiple activation and inversion of normal faults are correlated to divergent onlaps (wedge-shaped units): DO0 Infra-Cambrian extension, DO1 Cambrian–Ordovician extension, DO2 Silurian extension with local Silurian–Devonian positive inversion, and DO3 Frasnian–Famennian extension-local compression (~~transported~~

~~fault with a tectonic transport from footwall to hanging wall~~). See figure [3 2](#) for map and cross-section location.

### A Core descriptions well W7:

### B Wireline well W7:

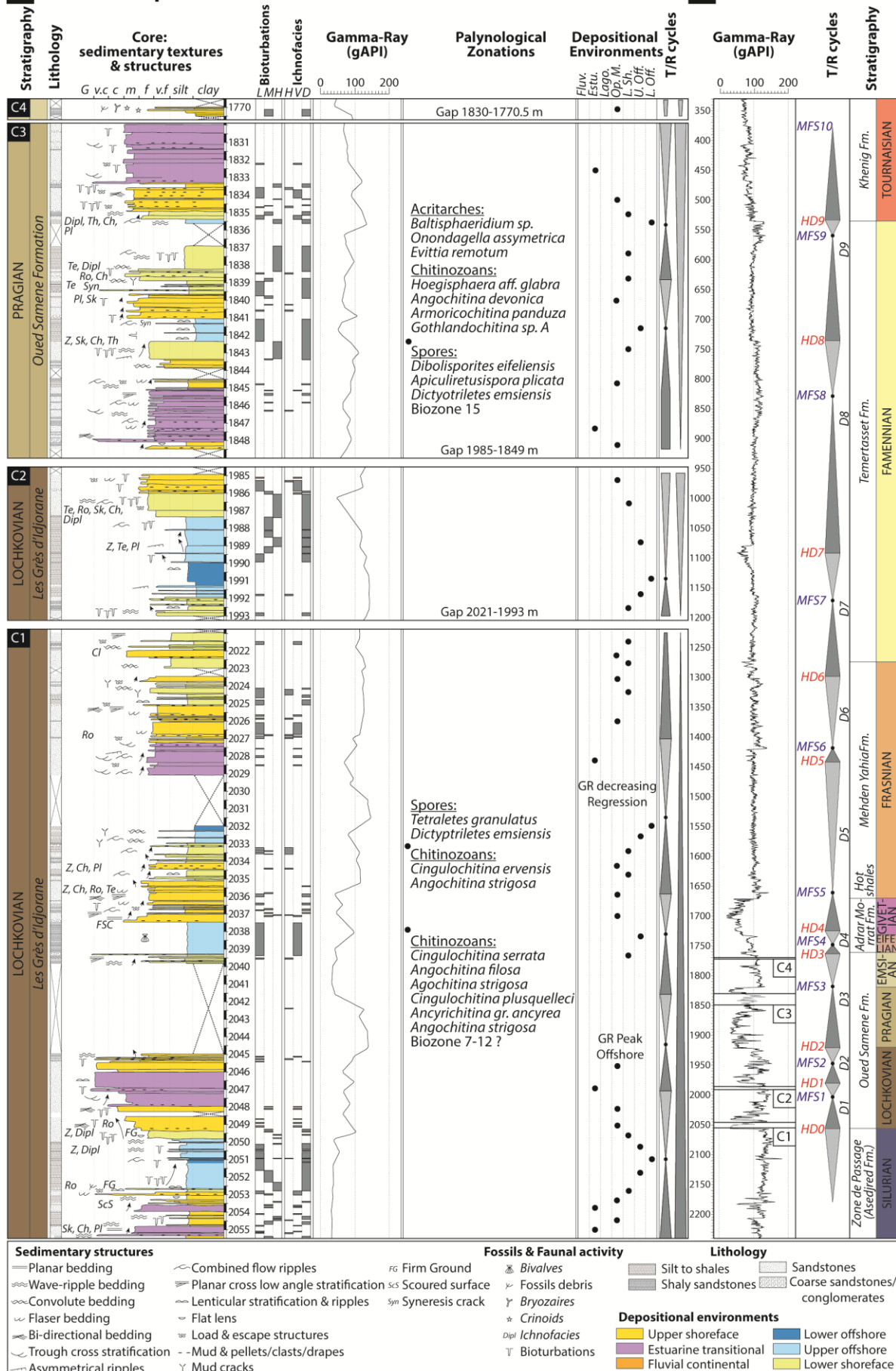


Figure 8.7: (A) Core description, palynological calibration and gamma-ray signatures of well W7 modified from internal core description report (Dokka, 1999) and internal palynological report (Azzoune, 1999). (B) Devonian sequential stratigraphy of well-log W7. For location of well W7 see figure 3A.2A. ~~Lithological and sedimentological studies were synthesized from internal Sonatrach (Dokka, 1999), IFP reports (Eschard et al., 1999), and published articles (Beuf et al., 1971; Biju Duval et al., 1968; Wendt et al., 2006). Biozonations from (Magloire, 1967) and (Boumendjel et al., 1988) are based on palynological data from internal unpublished data (Abdesselam Rouighi, 1991; Azzoune, 1999; Khier, 1974). Well W18 is supported by palynological data and biozonations from (Kermandji et al., 2008).~~

Criteria & characteristics					Formations	Depositional environments	
Facies associations	Textures/Lithology	Sedimentary structures	Biotic/non biotic grains	Ichnofacies			
AF1	Conglomerates, mid to coarse sandstones, siltstones, shales	Trough cross-bedding, mud clasts, lag deposits, fluidal and overturn structures, imbricated grains, lenticular laminations, oblique stratification	Rare oolitic intercalations, imbricated pebbles, sandstones, ironstones, phosphorites, corroded quartz grains, calcareous matrix, brachiopod coquinas, phosphatized pebbles, hematite, azurite, quartz	Rare bioturbation	<a href="#">Oued Samene Fm. Barre Supérieur, Barre Moyenne</a>		
AF2	Silt to argillaceous fine sandstone	Current ripples, climbing ripples, crevasse splay, root traces, paleosols, plant debris	Nodules, ferruginous horizon		<a href="#">Oued Samene Fm. Barre Supérieur, Barre Moyenne</a>	Flood plain	
AF3a	Fine to coarse sandstones, argillaceous siltstones, shales (heterolithic)	Trough cross-bedding, some planar bedding, flaser bedding, mud clasts, mud drapes, root trace, desiccation cracks, water escape, wavy bedding, shale pebble, sigmoidal cross-bedding	Brachiopods, trilobites, tentaculites graptolites	Bioturbations, <i>Skolithos</i> (Sk), <i>Planolites</i> , (Pl)	<a href="#">Oued Samene Fm. Grès du Khenig, Barre Supérieur, Barre Moyenne</a>	Delta/Estuarine channels	Coastal Plain (Transitional Marine/Continental)
AF3b	Very coarse-grained poorly sorted sandstone	Trough cross-bedding, sigmoidal cross-bedding, abundant mud clasts and mud drapes		Increasing upward bioturbation <i>Skolithos</i> (Sk)	<a href="#">Oued Samene Fm. Grès du Khenig, Barre Supérieur, Barre Moyenne</a>	Fluvial/Tidal distributary channels	
AF3c	Fine-grained to very coarse-grained heterolithic sandstone	Sigmoidal cross-bedding with multidirectional tidal bundles, wavy, lenticular, flaser bedding, occasional current and oscillation ripples, occasional mud cracks		Intense bioturbation, <i>Skolithos</i> (Sk), <i>Planolites</i> , (Pl), <i>Thalassinoides</i> (Th)	<a href="#">Talus à Tigillites</a>	Tidal sand flat	
AF3d	Mudstones, varicolored shales, thin sandstone layers	Occasional wave ripples, mud cracks, horizontal lamination, rare multidirectional ripples	Absence of ammonoids, goniatites, calymenids, pelecypod molds, brachiopods coquinas	Intense bioturbation, <i>Skolithos</i> (Sk), <i>Planolites</i> , (Pl), <i>Thalassinoides</i> (Th)	<a href="#">Oued Samene Fm. Grès du Khenig, Atafaitafa Fm.</a>	Lagoon/Mudflat	
AF4a	Silty mudstone associated with coarse to very coarse argillaceous sandstone, poorly sorted, heterolithic silty mudstone	Sigmoidal cross-bedding, abundant mud clasts, wavy, lenticular cross-bedding and flaser bedding, abundant current and oscillation ripples, mud drapes	Shell debris (crinoids, brachiopods)	Strongly bioturbated <i>Skolithos</i> (Sk), <i>Planolites</i> , (Pl)	<a href="#">Oued Samene Fm. Talus à Tigillites</a>	Subtidal	Shoreface
AF4b	Fine to mid grained sandstones interbedded with argillaceous siltstone and mudstone, bioclastic carbonates sandstones, brownish sandstones and clays, silts	Oscillation ripples, swaley cross-bedding, bidirectional bedding, flaser bedding, rare hummocky cross-bedding, mud cracks (syneresis), convolute bedding, wavy bedding, combined flow ripples, planar cross low angle stratification, cross-bedding, ripple marks, centimetric bedding, shale pebbles	Ooids, crinoids, bryozoans, coral clasts, fossil debris, <a href="#">stromatoporoids, tabulates, colonial rugose corals</a> , myriad pelagic styliolids, neritic tentaculitids, brachiopods, iron ooliths, abundant micas	<i>Skolithos</i> (Sk), <i>Cruziana</i> , <i>Planolites</i> , (Pl) <i>Chondrites</i> (Ch), <i>Teichichnus</i> (Te), <i>Spirophytons</i> (Sp)	<a href="#">Atafaitafa Fm. Zone de passage, Grès de Mehden Yahia, Calcaires d'Azzel Matti</a>	Open marine-upper shoreface	
AF4c	Silty shales to fine sandstones (heterolithic)	Hummocky cross-bedding, planar bedding, combined flow ripples, convolute bedding, dish structures, mud drapes, remnant ripples, flat lenses, slumping	Intense bioturbation, <i>Cruziana</i>	<i>Thalassinoides</i> (Th), <i>Planolites</i> (Pl), <i>Skolithos</i> (Sk), <i>Diplocraterion</i> (Dipl), <i>Teichichnus</i> (Te), <i>Chondrites</i> (Ch), <i>Rogerella</i> (Ro), <i>Climactichnites</i> (Cl)	<a href="#">Atafaitafa Fm. Zone de passage, Grès de Mehden Yahia, Calcaires d'Azzel Matti</a>	Lower shoreface	
AF5a	Grey silty-shales, bundles of skeletal wackestones, silty greenish shale interlayers fine grained sandstones, calcareous mudstones, black shales, polychrome clays (black, brown, grey, green, red, pink), grey and reddish shales	Lenticular sandstones, rare hummocky cross-bedding, mud mounds, mud buildups, low-angle cross-bedding, tempestite bedding, slumping, deep groove marks	Intensive burrowing, bivalve debris, horizontal burrows, skeletal remains (goniatites, orthoconic, nautiloids, styliolids, trilobites, crinoids, solitary rugose, corals, limestones nodules, ironstone nodules and layers)	<i>Zoophycos</i> (Z), <i>Teichichnus</i> (Te), <i>Planolites</i> (Pl)	<a href="#">Argiles à Graptolites, Orsine Fm. Argiles de Mehden Yahia, Argiles de Temertasset</a>	Upper offshore	
AF5b	Black silty-shales (mudstones), bituminous mudstones-wackestones, packstones	Rare structures	parallel-aligned styliolids, goniatites, orthoconic nautiloids, pelagic pelecypod <i>Buchiola</i> , anoxic conditions, limestone nodules, goniatites, <i>Buchiola</i> , <i>tentaculitids</i> , ostracods and rare fish remains, <i>Tornoceras</i> , <i>Aulatornoceras</i> , <i>Lobotornoceras</i> , <i>Manticoceras</i> , <i>Costamanticoceras</i> and <i>Virginoceras</i> , graptolites	<i>Zoophycos</i> (Z)	<a href="#">Argiles à Graptolites, Orsine Fm. Argiles de Mehden Yahia, Argiles de Temertasset</a>	Lower offshore	

Table 1: Synthesis of facies associations (AF1 to AF5), depositional environments, and electrofacies in the Devonian series compiled from internal (Eschard et al., 1999) and published studies (Beuf et al., 1971; Biju-Duval et al., 1968; Wendt et al., 2006).

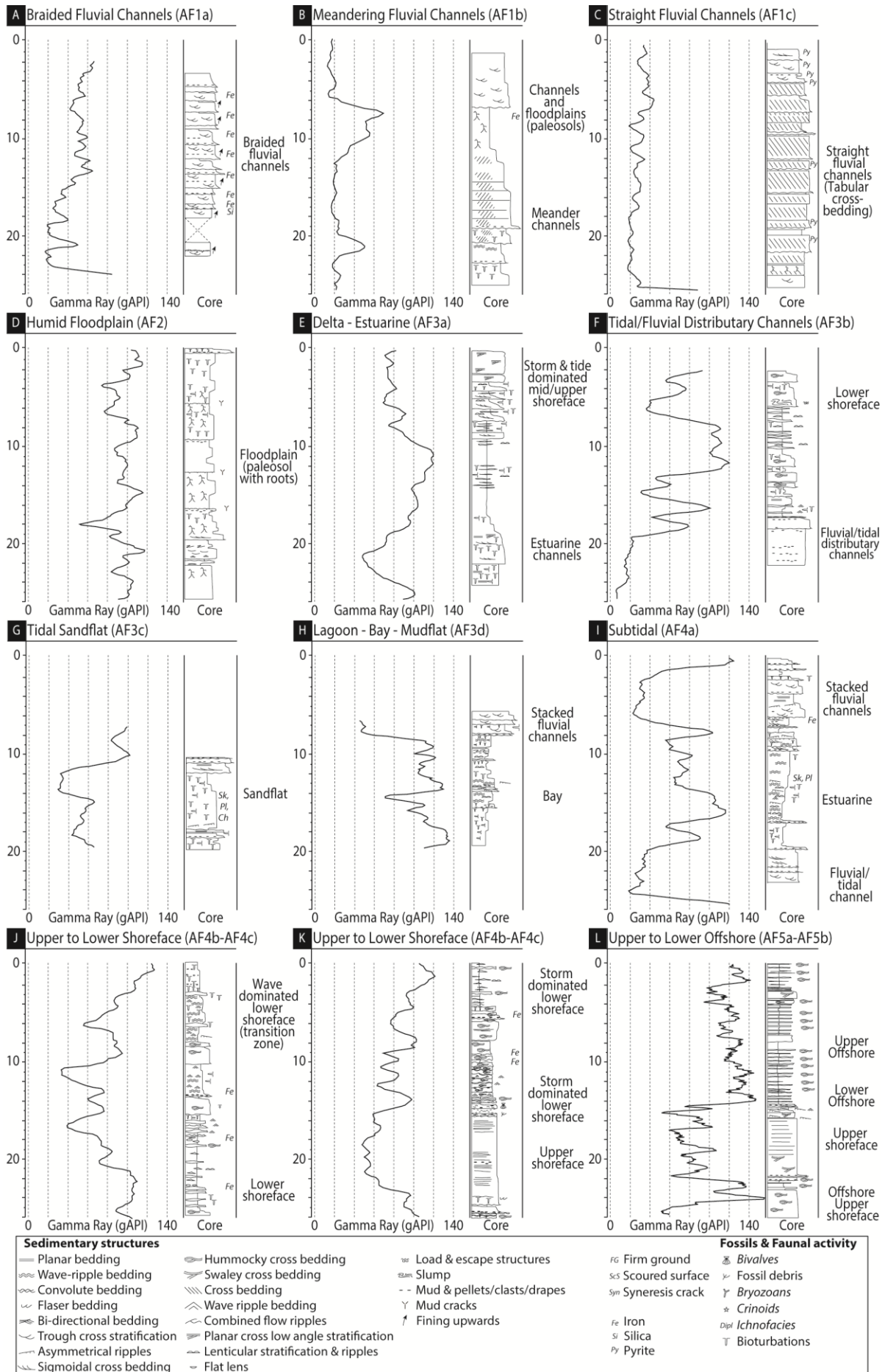


Figure 98: The main depositional environments (A to L) and their associated electrofacies (i.e. gamma-ray patterns) modified and compiled from (Eschard et al., 1999).



Figure 10 9: SE–W cross-section between the Reggane basin, Azzel Matti arch, Ahnet basin, Arak-Foum Belrem arch, Mouydir basin, and Amguid El Biod arch (well locations in fig. 3). Well W1 biozone calibration from Hassan, (1984) internal report is based on Magloire, (1967) classification: biozone G3-H (Wenlock–Ludlow, Upper Silurian), biozone I-K (Lochkovian–Emsian, Lower Devonian), biozone L1-3 (Eifelian–Givetian, Middle Devonian), biozone L4 (Frasnian, Upper Devonian), biozone L5-7 (Famennian, Upper Devonian), biozone M2 (Tournaisian–Lower Carboniferous). Well W7 biozone calibration from Azzoune, (1999) internal report is based on Boumendjel, (1987) classification: biozone 7-12 (Lochkovian, Lower Devonian), biozone 15 (Emsian, Lower Devonian). Interpretation of the basement is based on Figs. 1, 3 and supplementary data 4 2 and 15. Outcrop Well location is in Fig. 3 2.

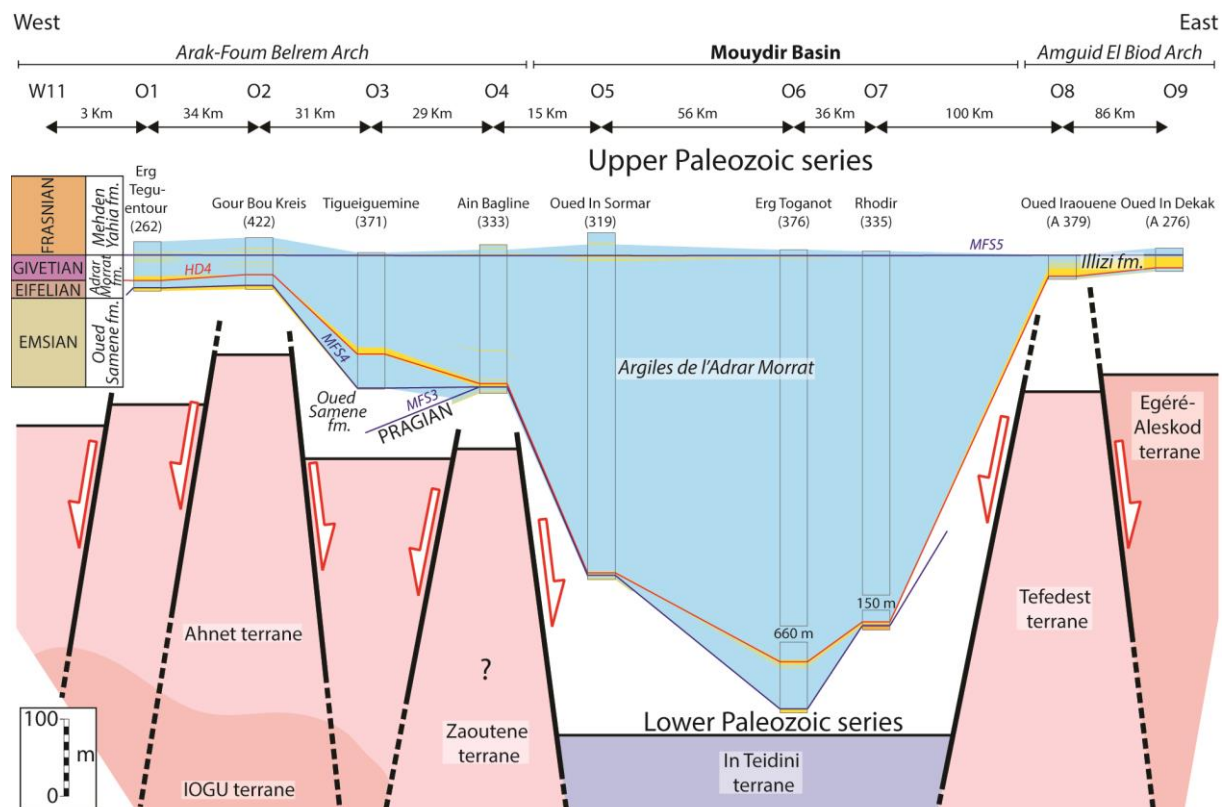


Figure 11: SE–W cross-section between the Arak-Foum Belrem arch, the Mouydir basin and the Amguid El Biod arch. Outcrop cross-section correlations and biostratigraphic calibrations

are based on the compilation of published papers (Wendt et al., 2006, 2009b). Interpretation of the basement is based on Figs. 1, 2 and 15. Outcrop location is in Fig. 2.

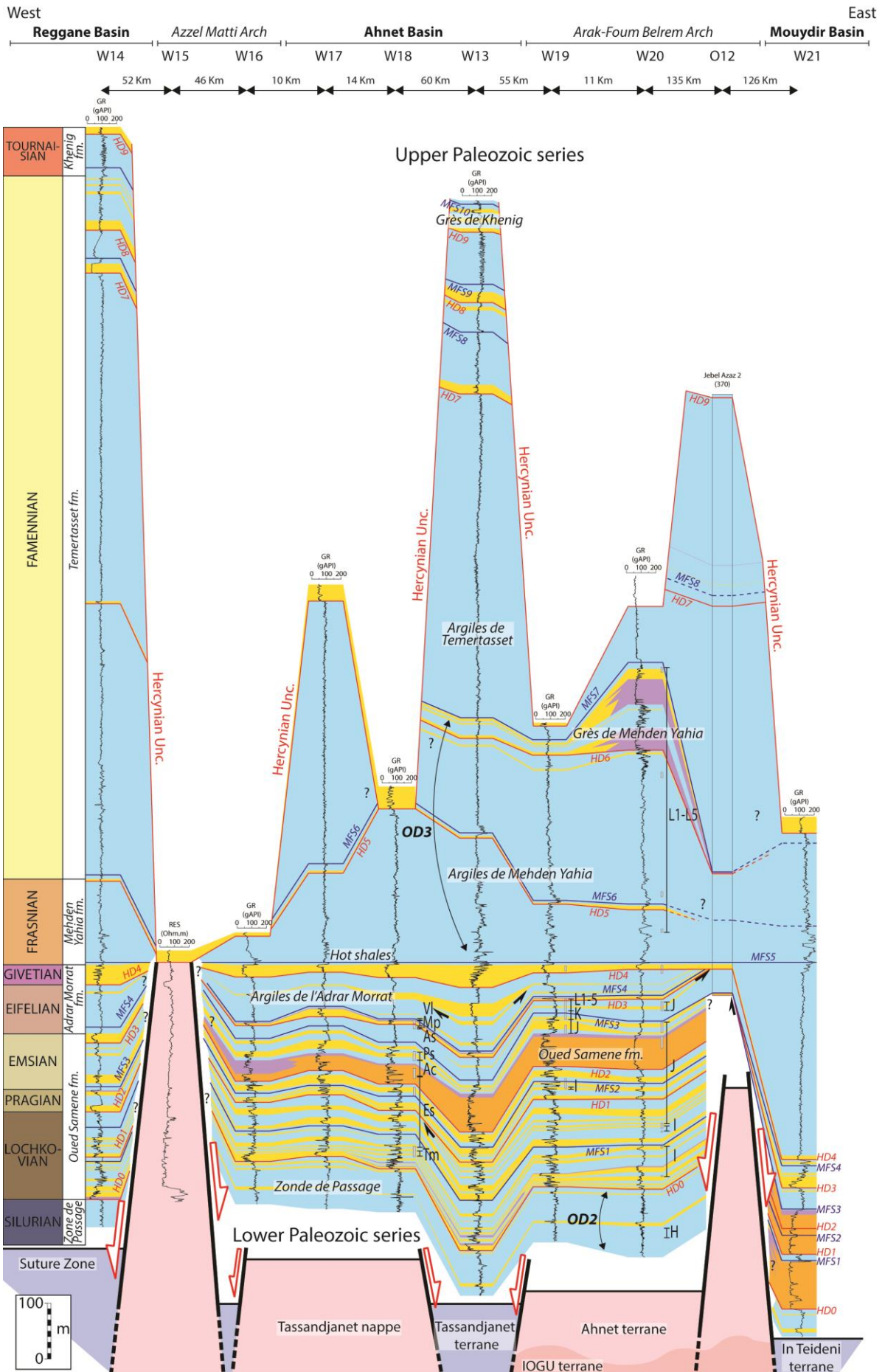


Figure ~~12~~ 10: NE–W cross-section between the Reggane basin, Azzel Matti arch, Ahnet basin, Arak-Foum Belrem arch, Mouydir basin, and Amguid El Biod arch (well locations in fig. 3). Well W18 biozone calibration is based on Kermandji et al., (2009): biozone (Tm) *tidikeltense microbaculatus* (Lochkovian, Lower Devonian), biozone (Es) *emsiensis spinaeformis* (Lochkovian-Pragian, Lower Devonian), biozone (Ac) *arenorugosa caperatus* (Pragian, Lower Devonian), biozone (Ps) *poligonalis subgranifer* (Pragian–Emsian, Lower Devonian), biozone (As) *annulatus svalbardiae* (Emsian, Lower Devonian), biozone (Mp) *microancyreus protea* (Emsian–Eifelian, Lower to Middle Devonian), biozone (VI) *velatus langii* (Eifelian, Middle Devonian). Well W19 and W20 biozones calibration from internal reports (Abdesselam-Roughi, 1991; Khiar, 1974) is based on Magloire, (1967) classification: biozone H (Pridoli, Upper Silurian), biozone I (Lochkovian, Lower Devonian), biozone J (Pragian, Lower Devonian), biozone K (Emsian, Lower Devonian), biozone L1-5 (Middle Devonian to Upper Devonian). Interpretation of the basement is based on Figs. 1, ~~3~~ and supplementary data 4 2 and 15. Outcrop and well location is in Fig. ~~3~~ 2.

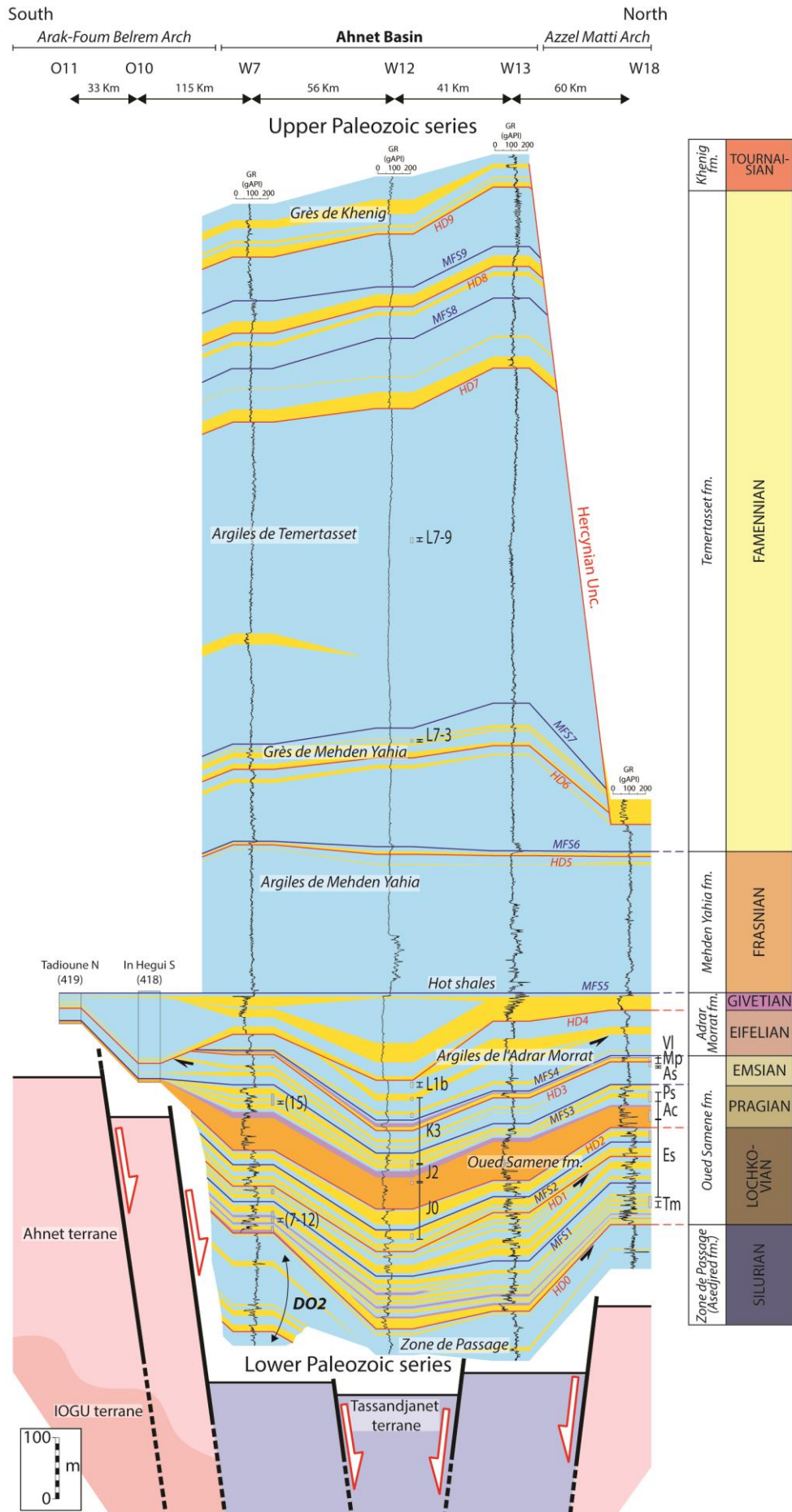


Figure 13: N–S cross-section in the Ahnet basin between Azzel Matti arch and Arak-Foum Belrem arch; Well W7 biozone calibration from Azzoune, (1999) internal report based on Boumendjel, (1987) classification: biozones 7–12 (Lochkovian, Lower Devonian), biozone 15 (Emsian, Lower Devonian). Well W18 biozone calibration is based on Kermadjji et al., (2009): biozone (Tm) *tidikeltense microbaculatus* (Lochkovian, Lower Devonian), biozone (Es) *emsiensis spinaeformis* (Lochkovian-Pragian, Lower Devonian), biozone (Ac) *arenorugosa caperatus* (Pragian, Lower Devonian), biozone (Ps) *poligonalis subgranifer* (Pragian-Emsian, Lower Devonian), biozone (As) *annulatus svalbardiae* (Emsian, Lower Devonian), biozone (Mp) *microancyreus protea* (Emsian-Eifelian, Lower to Middle Devonian), biozone (Vl) *velatus langii* (Eifelian, Middle Devonian). Well W12 biozone calibration from Abdesselam-Rouighi, (1977) internal report is based on (Boumendjel, (1987) classification: biozone J (Pragian, Lower Devonian), biozone K (Emsian, Lower Devonian), biozone L1 (Eifelian, Middle Devonian), biozone L7-3, L7-9 (Frasnian-Famennian, Upper Devonian). Interpretation of the basement is based on Figs. 1, 2 and 15. Outcrop and well location is in Fig. 2.

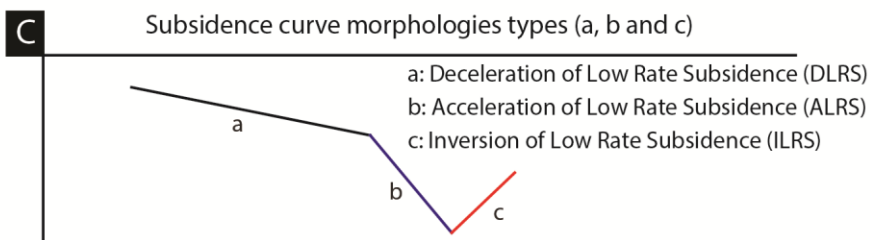
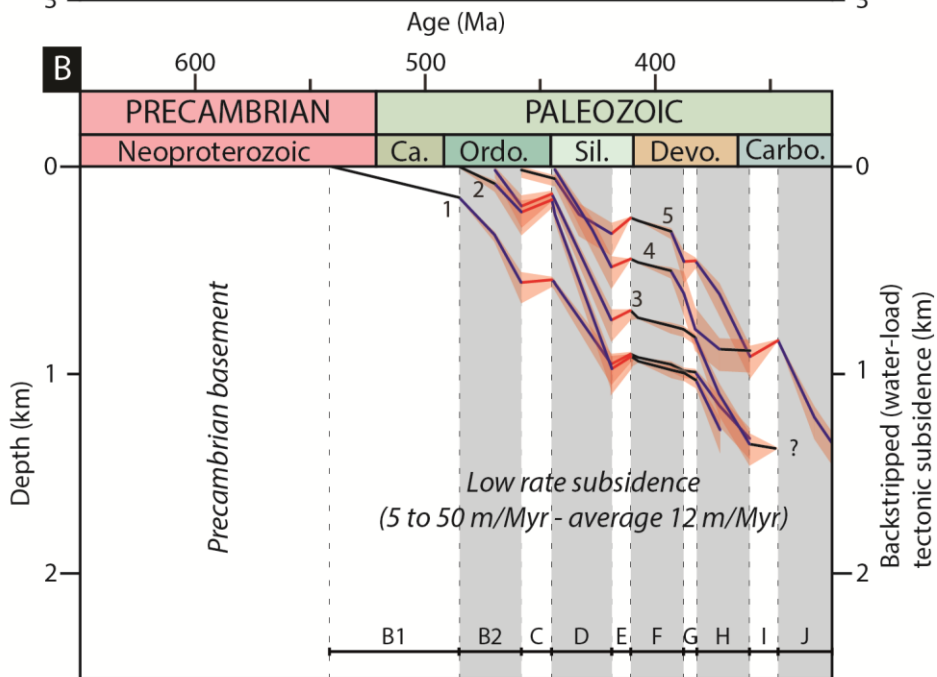
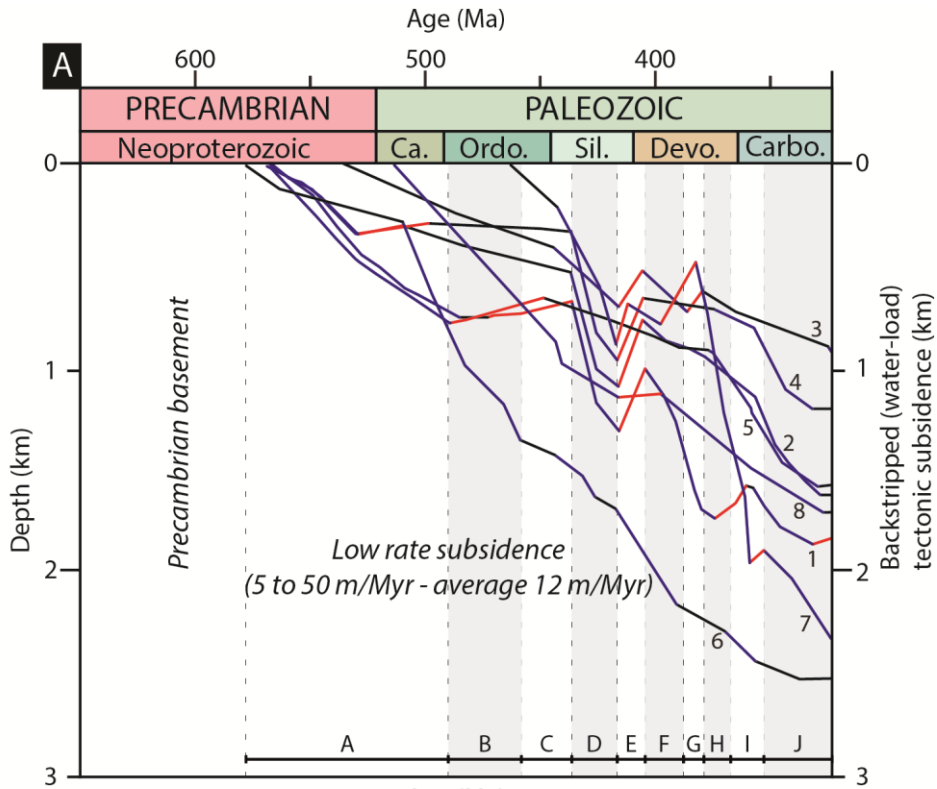


Figure ~~14~~ 11: (A) Tectonic backstripped curves of the Paleozoic North Saharan Platform (peri-Hoggar basins) compiled from literature. 1: HAD-1 well in Ghadamès basin (Makhous and Galushkin, 2003b); 2: Well RPL-101 in Reggane basin (Makhous and Galushkin, 2003b); 3: L1-1 well in Murzuq basin (Galushkin and Eloghbi, 2014); 4: TGE-1 in Illizi basin (Makhous and Galushkin, 2003a); 5: REG-1 in Timimoun basin (Makhous and Galushkin, 2003b); 6: Ghadamès-Berkine basin (Allen and Armitage, 2011; Yahi, 1999); 7: well in Sbâa basin (Tournier, 2010); 8: well B1NC43 in Al Kufrah basin (Holt et al., 2010). (B) Tectonic backstripped curves of wells in the study area (1: well W17 in Ahnet basin; 2: well W5 in Ahnet basin; 3: well W7 in Ahnet basin; 4: well W21 in Mouydir basin; 5: well W1 in Reggane basin; (C) ~~Typologies of subsidence curves morphologies. The data show low rate subsidence with periods of deceleration (Deceleration of Low Rate Subsidence: DLRS), acceleration (Acceleration of Low Rate Subsidence: ALRS), or inversion (Inversion of Low Rate Subsidence: ILRS) synchronous and correlated with regional tectonic pulses (i.e. major geodynamic events).~~ A: Late Pan-African compression and collapse (type a, b, and c subsidence), B: Undifferentiated Cambrian–Ordovician (type a, b, and c subsidence), B1: Cambrian–Ordovician tectonic quiescence (type a subsidence), B2: Cambrian–Ordovician extension (type b subsidence), C: Late Ordovician glacial and isostatic rebound (type c subsidence), D: Silurian extension (type b subsidence), E: Late Silurian Caledonian compression (type c subsidence), F: Early Devonian tectonic quiescence (type a subsidence), G-H: Middle to late Devonian extension with local compression (i.e. inversion structures, type b and c subsidence), I: Early Carboniferous extension with local tectonic pre-Hercynian compression (type c and b subsidence), J: Middle Carboniferous tectonic extension (type b subsidence). ~~K: Late Carboniferous–Early Permian–Hercynian compression (type c subsidence).~~

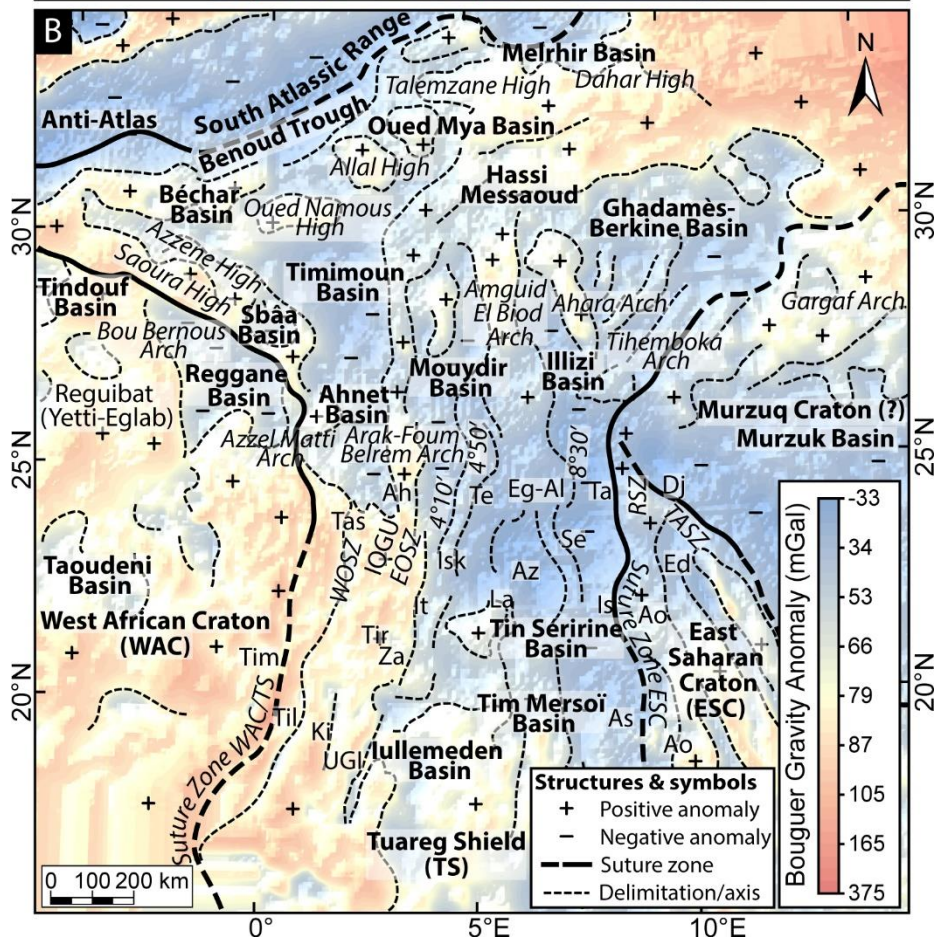
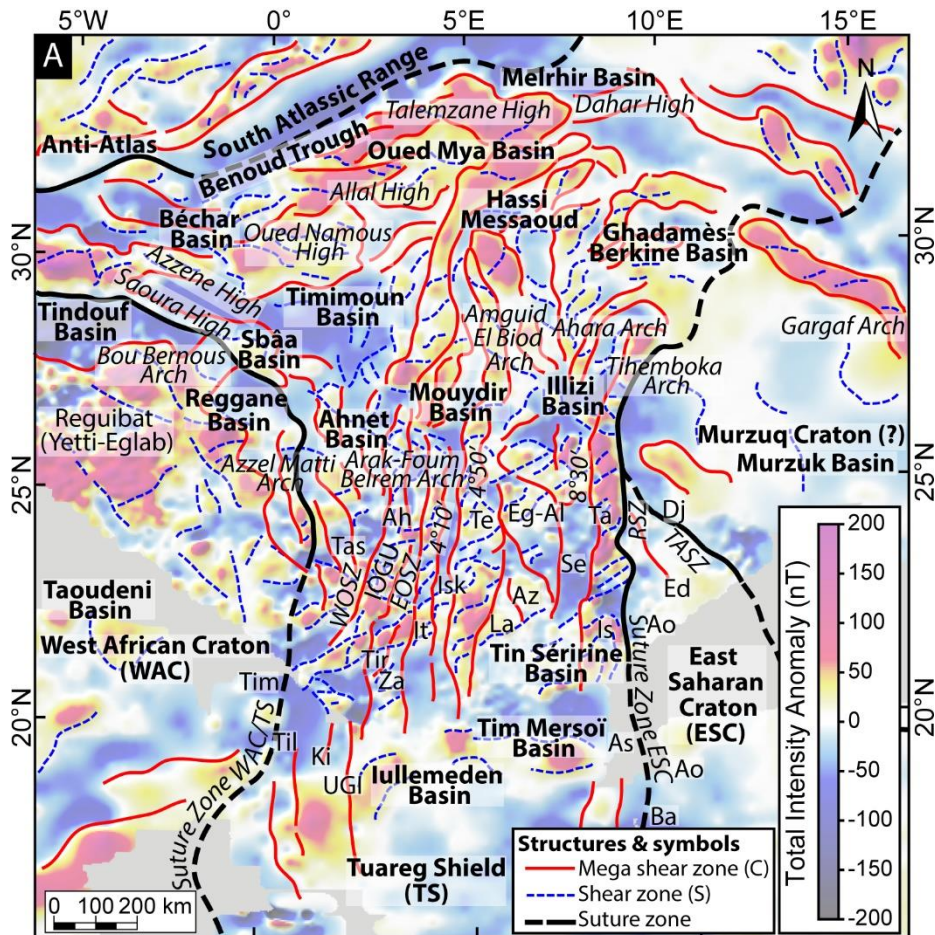


Figure ~~15~~ 12: (A) Interpreted aeromagnetic anomaly map (<https://www.geomag.us/>) of the Paleozoic North Saharan Platform (peri-Hoggar basins) showing the different terranes delimited by NS, NW–SE and NE–SW lineaments and mega-sigmoid structures (SC shear fabrics); (B) Bouguer anomaly map (from International Gravimetric Bureau: <http://bgi.omp.obs-mip.fr/>) of North Saharan Platform (peri-Hoggar basins) presenting evidence of positive anomalies under arches and negative anomalies under basins.

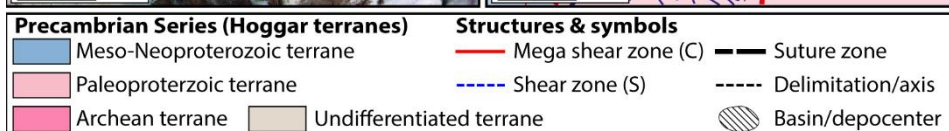
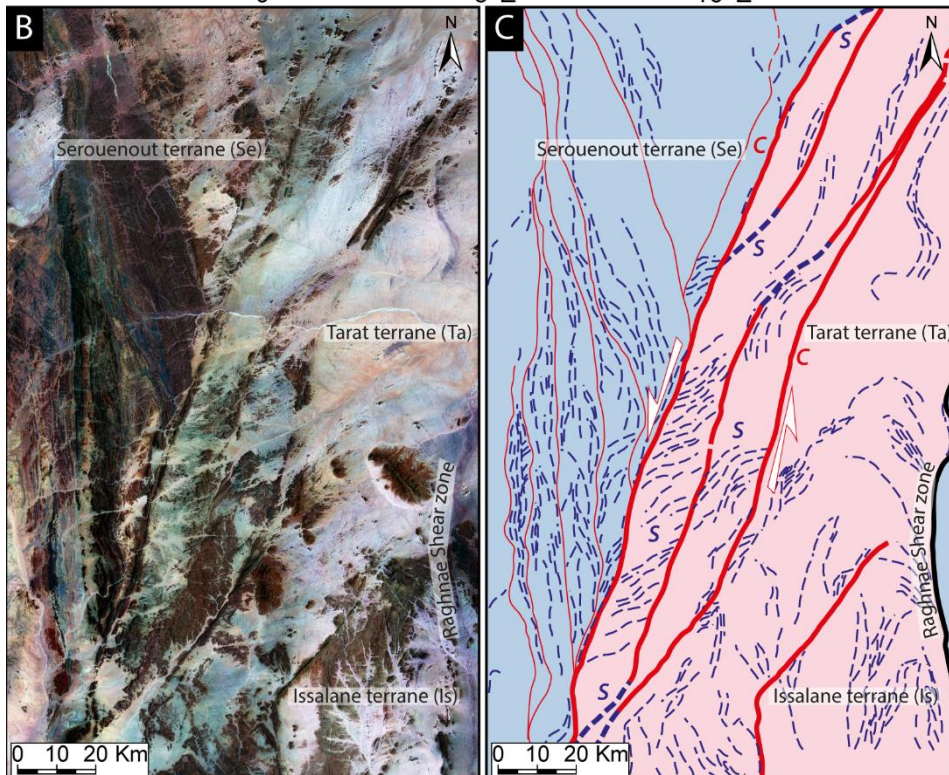
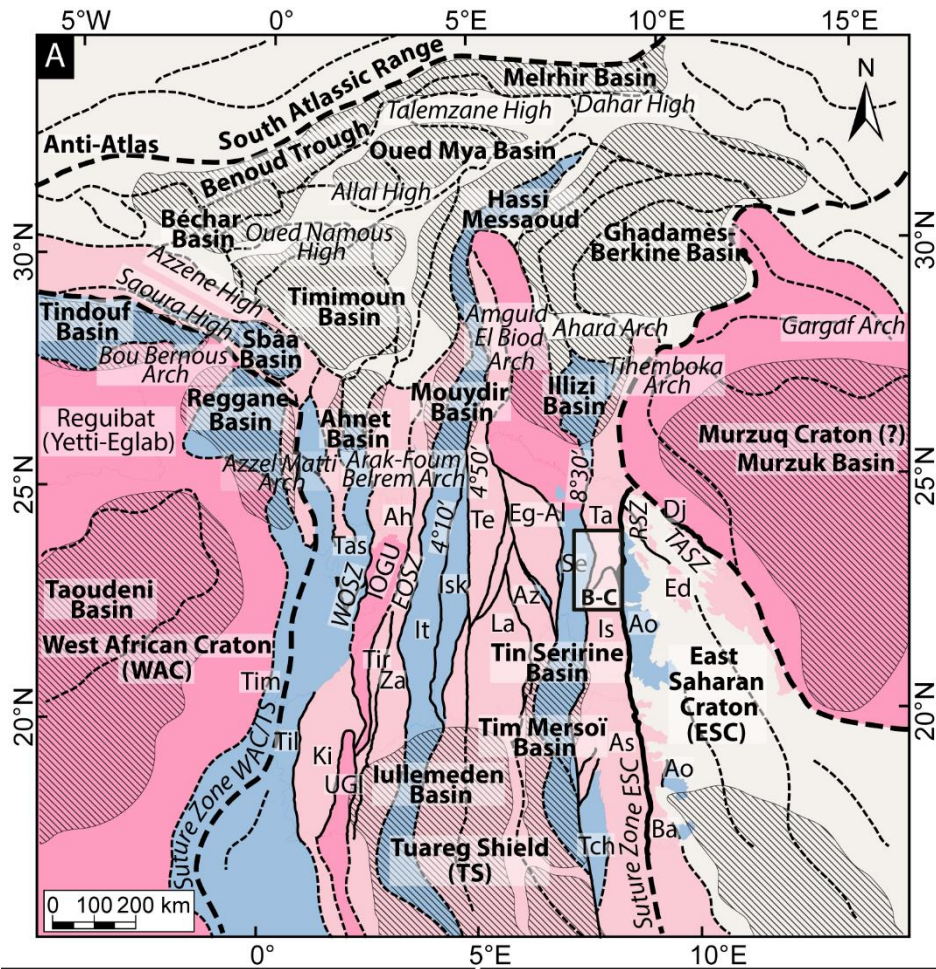


Figure ~~16 12~~: (~~C~~ A) Interpreted map of basement terranes according to their age (compilation of data sets in Fig. 1 and supplementary data 4 1); (~~D~~ B) Satellite images (7ETM+ from USGS: <https://earthexplorer.usgs.gov/>) of Paleoproterozoic Issalane-Tarat terrane, Central Hoggar (see ~~fig. 12~~ C for location); (~~E~~ C) Interpreted satellite images of Paleoproterozoic Issalane-Tarat terrane showing sinistral sigmoid mega-structures associated with transcurrent lithospheric shear fabrics SC.

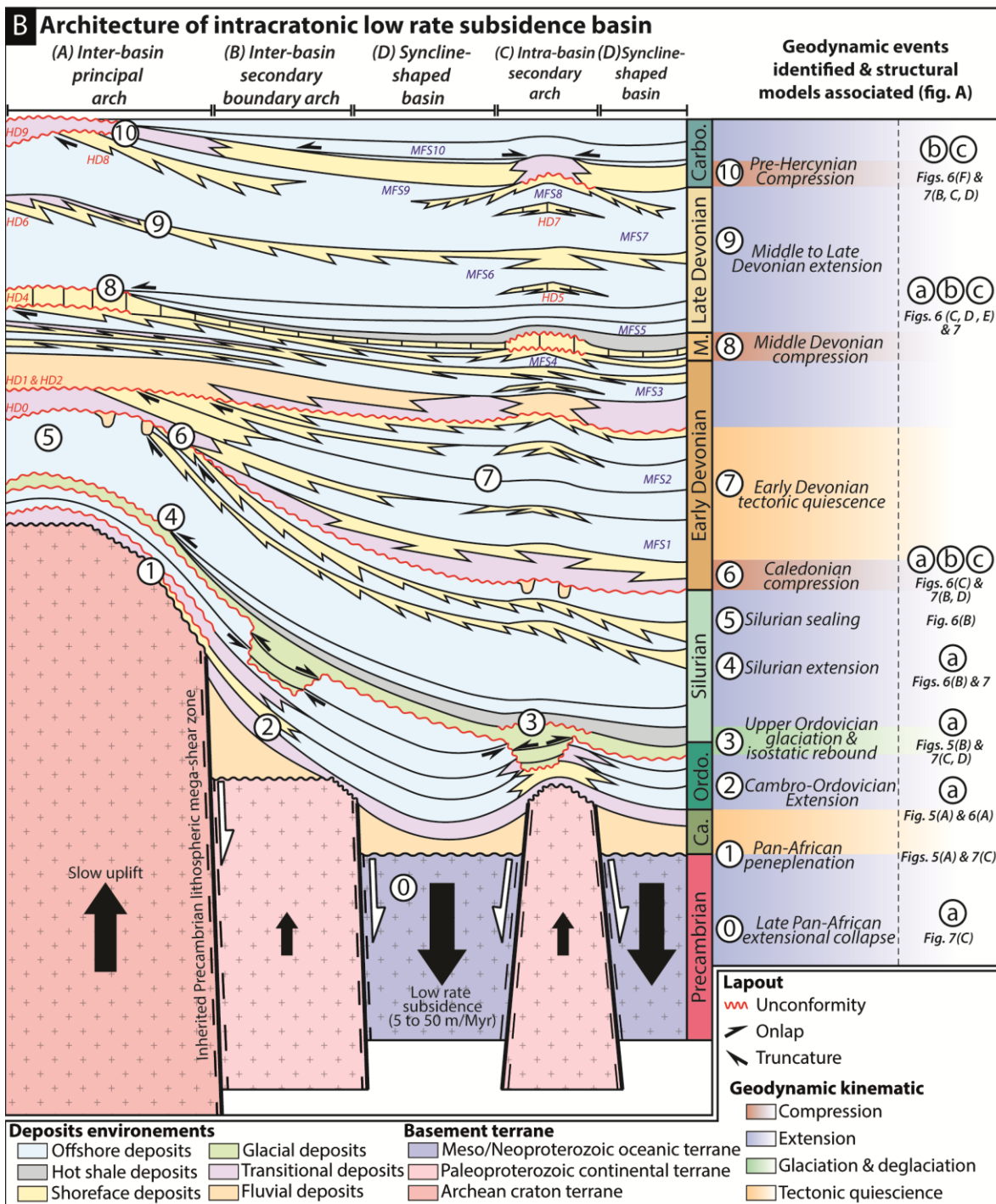
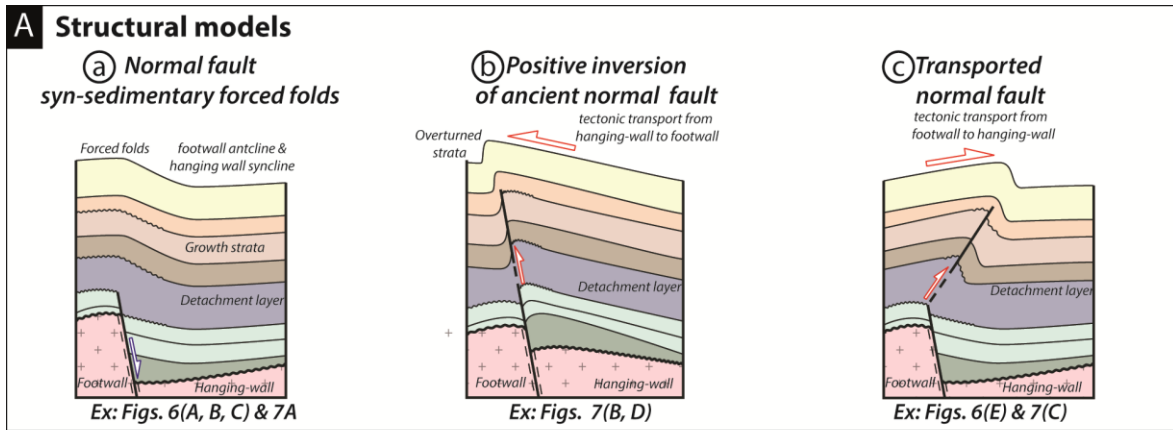


Figure [17](#) ~~13~~: (A) Different structural model styles identified from the analysis of seismic profiles and from interpretation of the satellite images; (B) Conceptual model of the architecture of intracratonic low rate subsidence basin and synthesis of the tectonic kinematics during the Paleozoic. Note that the differential subsidence between arches and basins is controlled by terrane heterogeneity (i.e. thermo-chronologic age, rheology, etc.).

Supplementary data [1](#) ~~4~~: Georeferenced geochronological dating data compilation of the study area.